6-2-2015 12:00 AM

Investigating the role of hydrogen sulfide in the survival, growth and angiogenic potential of clear cell renal cell carcinoma cell lines and xenografts

Eric Sonke, *The University of Western Ontario*

Supervisor: Dr. Alp Sener, *The University of Western Ontario*

A thesis submitted in partial fulfillment of the requirements for the Master of Science degree in Anatomy and Cell Biology

INVESTIGATING THE ROLE OF HYDROGEN SULFIDE IN THE SURVIVAL, GROWTH AND ANGIOGENIC POTENTIAL OF CLEAR CELL RENAL CELL CARCINOMA CELL LINES AND XENOGRAFTS

(Thesis format: Monograph)

by

Eric Sonke

Graduate Program in Anatomy and Cell Biology

A thesis submitted in partial fulfillment
of the requirements for the degree of
Master of Science

The School of Graduate and Postdoctoral Studies
The University of Western Ontario
London, Ontario, Canada

Abstract

Clear cell renal cell carcinoma (ccRCC) is characterized by Von Hippel-Lindau (VHL)-deficiency, resulting in *pseudohypoxic*, angiogenic and glycolytic tumours. Hydrogen sulfide (H_2S) is an endogenously-produced gasotransmitter that accumulates under hypoxia and has been shown to be pro-angiogenic and cytoprotective in cancer. It was hypothesized that H_2S levels are elevated in VHL-deficient ccRCC, contributing to survival, metabolism, and angiogenesis. Using H_2S-specific probes, it was found that H_2S levels were higher in VHL-deficient ccRCC cell lines compared to cells with wild-type VHL. Inhibition of H_2S-producing enzymes could reduce the proliferation, metabolism and survival of ccRCC cell lines, as determined by live-cell imaging, XTT/ATP assay, and flow cytometry, respectively. Using the chorioallantoic membrane angiogenesis model, it was found that systemic inhibition of endogenous H_2S production was able to decrease vascularization of VHL-deficient ccRCC xenografts. Endogenous H_2S production is an attractive new target in ccRCC due to its involvement in multiple aspects of disease.

Keywords

Clear cell renal cell carcinoma; hydrogen sulfide; cell hypoxia; angiogenesis; cell metabolism, cell proliferation, cell survival, oxidative stress

Co-Authorship Statement

The following persons contributed significantly towards the experimental design, experimental preparation, data acquisition, and analysis of experimental data contained within this thesis and recently-submitted manuscript:

Megan Verrydt: experimental design (CAM assays) and data acquisition (viability assays)

Carl O. Postenka: sample processing (CAM assays)

Siddika Pardhan: experimental preparation (CAM assays)

Chantalle J. Willie: experimental preparation (CAM assays)

Clarisse R. Mazzola: experimental design (CAM assays)

Ian Lobb: experimental design (viability assays)

Nicholas E. Power: revision

Ann F. Chambers: experimental design (CAM assays) and revision

Hon S. Leong: experimental design (CAM assays) and revision

Alp Sener: experimental design and revision

Acknowledgments

In addition to the aforementioned co-authors, I would like to thank lab technicians Dr. Manujendra Saha and Amy Mok, as well as all of the past and present students from the Sener lab for their everyday support and expertise during my graduate and undergraduate studies. I would also like to thank my committee members Dr. Alison Allan, Dr. Nicholas Power and Dr. Lakshman Gunaratnam for their scientific expertise, constructive criticism and translational approach that shaped this project. This work would also not be possible without the aid of Xizhong Zhang, Alex Pavlovsky and Ola Ismail from the Matthew Mailing Centre for Transplant Studies. Likewise, I would like to thank scientists and personnel in the labs of Dr. Ann Chambers and Dr. Hon Leong at the London Regional Cancer Program who provided me with extensive mentorship and training. I would also like to thank Dr. Anthony Jevnikar, Dr. Michael Pluth, Dr. Lakshman Gunaratnam and Dr. John McCormick for usage of equipment and/or provision of reagents. I would like to thank Dr. Jean-Baptiste Lattouf and Dr. Aaron Haig who were instrumental in the processing of human samples. Of course, without the funding provided by the department of Anatomy and Cell Biology and the Lawson Health Research Institute this work would not be possible. Finally, I would like to thank my supervisor Dr. Alp Sener for his un-ending optimism, encouragement, guidance and scientific mentorship. Your passion, creativity and inquisitive nature are a daily source of inspiration for myself and others.

Table of Contents

List of Figures

List of Appendices

List of Abbreviations

786-O VHL+	786-O Von Hippel-Lindau knock-in
Akt	protein kinase B
CAM	chorioallantoic membrane
CBS	cystathionine β-synthase
ccRCC	clear cell renal cell carcinoma
cGMP	cyclic guanosine monophosphate
CO	carbon monoxide
CSE	cystathionine γ-lyase
EGFP	extreme green fluorescent protein
EGFR	epidermal growth factor receptor
eNOS	endothelial nitric oxide synthase
ETC	electron transport chain
GAPDH	glyceraldehyde 3-phosphatase
GC	guanylyl cyclase
GFR	glomerular filtration rate
Glut-1	glucose transporter 1
H_2S	hydrogen sulfide
HA	hydroxylamine
Hcy	homocysteine
HIF	hypoxia-inducible factor
HRE	hypoxia response element
IFN-α	interferon alpha
IL-2	interleukin 2
K_{ATP}	ATP-dependent K^+
Keap1	kelch-like ECH-associated protein-associated protein-1
LC	L-cysteine
LCA	*lens culinaris agglutinin*
LDH	lactate dehydrogenase
mAb	monoclonal antibody
MAX	MYC-associated factor X
MMP	matrix metalloproteinase
MPST	3-mercaptopyruvate sulfurtransferase

mRCC	metastatic renal cell carcinoma
mTOR	mammalian target of rapamycin
mTORC	mammalian target of rapamycin complex
MXI1	MAX-interacting protein 1
NAD	nicotinamide adenine dinucleotide
NADPH	nicotinamide adenine dinucleotide phosphate
Nampt	nicotinamide phosphoribosyltransferase
NF-κB	nuclear factor kappa B
NKA	Na^+/K^+ ATPase
NKCC	$Na^+/K^+/2Cl^-$ co-transporter
NO	nitric oxide
Nrf2	NF-E2 p45-related factor 2
OCT	optimal cutting temperature
ORR	objective response rate
OS	overall survival
p38	mitogen-activated protein kinase p38
PAG	propargyl glycine
PBS	phosphate buffered saline
PD	pyruvate dehydrogenase
PDE5	phosphodiesterase type 5
PDGF	platelet-derived growth factor
PDK	pyruvate dehydrogenase kinase
pf	post-fertilization
PFS	progression-free survival
PGC-1β	peroxisome proliferator-activated receptor gamma coactivator 1-beta
PHD	prolyl hydroxylase
PI3K	phosphoinositide 3-kinase
PK	pyruvate kinase
PKC	protein kinase C
PKG	protein kinase G
PN	partial nephrectomy
PPP	pentose phosphate pathway
Q	quinone

RAS	renin-angiotensin system
RBF	renal blood flow
RCC	renal cell carcinoma
RN	radical nephrectomy
RNS	reactive nitrogen species
ROS	reactive oxygen species
RTK	receptor tyrosine kinase
RTKI	receptor tyrosine kinase inhibitor
SMI	small molecule inhibitor
SOU	sulfide oxidation unit
SQR	sulfide quinone reductase
TCA	tricarboxylic acid
TGF-α	transforming growth factor alpha
TNF-α	tumour necrosis factor alpha
VEGF	vascular endothelial growth factor
VHL	Von Hippel-Lindau
VHL WT	Von Hippel-Lindau wild-type

1. Introduction

1.1 Renal Cell Carcinoma (RCC)

As with other cancers, kidney cancer can be categorized into multiple sub-types. The most prevalent form of kidney cancer is known as renal cell carcinoma (RCC) and accounts for 80-90% of kidney cancer cases and 2-3% of all cancer cases (1). RCC arises as a result of mutations to the epithelial cells of nephrons – the functional units of the kidney. Increasing incidence rates for RCC have been reported over the last few decades, and this has been attributed to popular usage of CT and ultrasound imaging for other conditions (2). Some studies suggest that increasing incidence of RCC risk factors like diabetes, hypertension and obesity may also be responsible for the increasing prevalence of RCC, though these conditions have not been established as true etiological factors of RCC (3-7). Despite the increase in incidental detection of RCC and timely removal of the primary tumour, the cancer-specific mortality rate of RCC remains high at 30-40% (2). This high mortality rate is due to the high likelihood – approximately 20-30% – that the disease has already metastasized at the time of detection (2). Unfortunately, metastatic RCC (mRCC) has proven to be highly resistant to both chemotherapy and radiation therapy, and this resistance contributes to the high mortality rates observed (8). While it is true that novel growth-targeting therapies offer improvements in overall survival (OS) and progression-free survival (PFS), these therapies do not offer a cure for the disease (1).

RCC can be further sub-divided into various histotypes based on tumour morphology, genetic signature, and clinical manifestation. The area of the nephron from which the tumour arises (proximal tubule, distal tubule, collecting duct, etc.) also plays a role in the classification of RCCs (9). Whether sporadic or inherited, genetic mutations in RCC often affect pathways involved in oxygen, nutrient, or energy sensing and for this reason RCC is often described as a metabolic disease (9,10). In today's clinical landscape of targeted therapies, identifying key targets within these metabolic pathways is essential (1,11). While most subtypes of RCC seem to subvert cellular metabolic pathways to their advantage, the specific pathways that are disrupted in each subtype, and indeed in each

patient, varies widely (12). Identifying pathways that are commonly disrupted in RCC and developing therapies that target these pathways has proven to be an effective treatment strategy in RCC in that they improved PFS when compared to chemotherapy and radiation therapy (12).

1.1.1 Clear Cell RCC and Von Hippel-Lindau

The most common histotype of RCC is the clear cell histotype (ccRCC) and accounts for 75-80 % of all RCC cases (2). The characteristic "clear" cytoplasm of these cancer cells is due to increased production and accumulation of deposits containing cholesterol esters, fatty acids, and glycogen which makes histological identification relatively easy. While the exact mechanisms that lead to accumulation of these lipid deposits are still being investigated, we do know that a crucial step in this process is inactivation of a key tumour suppressor – the Von Hippel-Lindau (VHL) tumour suppressor (13,14). VHL is an E3 ubiquitin ligase that is crucial in targeting certain cellular proteins for proteasomal degradation in response to changing cellular conditions, and is inactivated in the large majority (90%) of ccRCC tumours (1,15). When VHL is expressed in its wild-type form (VHL WT), it is involved in regulating a number of homeostatic pathways, including the metabolism and storage of macromolecules. Cells that lack a functional copy of VHL (VHL-deficient) lose control of multiple metabolic pathways, leading to decreased β-oxidation of fatty acids, increased synthesis of fatty acids and glycogen, and increased storage of fatty acids and esterified cholesterol (13,14). The end result is a cell with clear, lipid-filled cytoplasm.

While VHL inactivation and subsequent lipid accumulation may prove to be an etiological link between established risk factors of ccRCC and the disease itself, VHL deficiency plays other, more significant roles in cancer initiation and progression. The best understood function of VHL is as a master regulator of the hypoxic response, and key tumour suppressor for many cells in the body (16). In combination with hypoxia-inducible factors (HIFs) and prolyl hydroxylase (PHD), VHL ultimately controls the expression of genes that allow cells to cope with the harmful effects of hypoxia, and restore cellular oxygenation. HIFs are heterodimeric transcription factors composed of α (HIF-α) and β (HIF-β) subunits that promote the transcription of genes containing

hypoxia response elements (HREs). PHD is an enzyme that hydroxylates proline residues on various proteins, but only in the presence of an essential cofactor – oxygen. As mentioned previously, VHL is an E3 ubiquitin ligase that specifically recognizes and binds to proteins with hydroxylated proline residues and targets them for proteasomal degradation through ubiquitination. HIF-β subunits are not a substrate for hydroxylation by PHD, and therefore are consistently present under normoxic and hypoxic conditions. HIF-α subunits on the other hand are hydroxylated by PHD and targeted for degradation by VHL under normoxic conditions to ensure that hypoxia response genes are not expressed unnecessarily (17). However when oxygen is absent during periods of hypoxia, PHD cannot hydroxylate HIF-α residues, allowing them to escape recognition by VHL, form a functional heterodimer with HIF-β, translocate to the nucleus, and initiate the hypoxic response (16).

Genes containing HREs include vascular endothelial growth factor (VEGF), platelet-derived growth factor (PDGF), transforming growth factor alpha (TGF- α), glucose transporter-1 (GLUT-1), matrix metalloproteinases (MMPs), carbonic anhydrase IX, erythropoietin, cyclooxygenase-2, c-MYC, cyclin D1, and many more (18). Induction of many of these genes through the VHL/HIF pathway is a useful means of minimizing injury and re-establishing tissue oxygenation during periods of hypoxia that occur following disruptions in blood supply (19). However, when these genes are aberrantly expressed under normoxic conditions as a result of VHL inactivation, the resulting cells are hyperproliferative, invasive, angiogenic and cell death-resistant as a result of their perceived hypoxia, or *pseudohypoxia* (Figure 1) (14). It is this pseudohypoxia, as a result of VHL inactivation, that plays the largest role in the initiation and progression of ccRCC.

As a tumour suppressor, VHL only loses its function after both genetic copies of the gene have been lost as a result of deletion, silencing via methylation, or some other form of mutation (15). In other words, spontaneous ccRCC often only occurs when an already heterozygous cell loses its functional genetic copy of VHL following a "second hit," resulting in complete loss of protein function. Loss of VHL function is common in many cancers, but it was first discovered to have tumourigenic consequences in a rare

autosomal-dominant condition known as VHL Disease (20). The majority (80%) of patients afflicted with VHL disease inherit a mutant copy of VHL from one of their parents, and following mutation to the second copy begin to develop cysts and tumours of the kidney (ccRCC), pancreas, retina, and other areas of the central nervous system (16). It was from studying this rare hereditary disease that the tumour suppressive role of VHL in ccRCC and other cancers was elucidated (21).

Clearly VHL loss of function is an important step in neoplastic and malignant transformation. However this, by itself, is neither necessary nor sufficient for the formation of ccRCC tumours (22,23). Furthermore, there has been no conclusive evidence which suggests that VHL mutation status – regardless of its overall effect on VHL function – holds any value as a biomarker or prognostic indicator (16). It is now generally accepted that classification of ccRCC tumours as VHL-deficient versus VHL WT is not sufficient. VHL-deficient tumours can be further subdivided according to the degree to which they express the two major HIF-α isoforms (HIF-1α and HIF-2α). There are VHL-deficient tumours which aberrantly express increased levels of HIF-1α and HIF-2α (H1H2), and those which express increased levels of HIF-2α only (H2) (24). Several studies have highlighted that HIF-1α and HIF-2α have very different effects on gene transcription in ccRCC (25), and most suggest that VHL-deficient H2 tumours are more proliferative and angiogenic than their H1H2 counterparts (26,27).

The increased proliferation of H2 ccRCC cell lines and tumours is in part due to autocrine growth signaling that occurs through HIF-2α, TGF-α and the epidermal growth factor receptor (EGFR) that binds TGF-α (26,28,29). Furthermore, the activity of oncoproteins such as c-MYC and cyclin D1 are upregulated by HIF-2α (24,26), whereas the activity of pro-apoptotic genes such as BNip3 are upregulated by HIF-1α (26). Angiogenesis in pseudohypoxic ccRCC cells also appears to be driven by induction of VEGF through HIF-2α, and loss of HIF-1α may actually exacerbate this process due to a loss of feedback inhibition that is normally mediated by HIF-1α (26,27). Not only is the H2 phenotype more aggressive than the H1H2 phenotype, but it may actually be more common in VHL-deficient ccRCC tumours as a result of a greater likelihood of HIF-1α undergoing degradation than HIF-2α (18). It has even been suggested that H2 tumours

are derived from H1H2 tumours and that loss of HIF-1α is a key step in ccRCC tumour progression (9,30).

With HIF-α transcription factors identified as mediators of ccRCC progression, the development of therapies is now focused on inhibiting the pathways that the downstream effectors of HIF-1/2 α (VEGF, TGF-α, etc.) feed into. The development of this targeted therapy approach has improved PFS of patients with ccRCC and represents a small victory in cancer treatment (31). However, these therapies are not curative, and are only effective for a matter of months before the cancer becomes resistant to them.

1.1.2 Past and Present (cc)RCC Therapies

First-line treatment of localized RCC, regardless of histotype, is usually surgery seeing as it is the only curative therapeutic approach (32). When determining the extent of renal mass to be excised, a number of factors must be evaluated. The staging of the tumour according to size and presence/absence of local/distant metastases (TNM staging) is the first to be evaluated. Patients with T1 tumours (<7 cm, limited to kidney) are often good candidates for a partial nephrectomy (PN), a procedure in which only the tumour and immediate surrounding area of the kidney are removed (33). Experienced centers may even perform this PN laparoscopically instead of opting for traditional open surgery. PN is the preferred course of treatment where the tumour is affecting a solitary functional kidney or the patient is in overall poor condition. In these cases, sparing as much functional tissue as possible is a priority and active surveillance may be preferred to surgery. Removal of the entire kidney, or radical nephrectomy (RN), is recommended in cases of locally advanced tumour growth or unfavourable tumour location. RN is often performed laparoscopically for T2 tumours (7-10 cm, limited to kidney), however open surgery is recommended for T3 and T4 tumours which involve local and distant metastases (32).

There are additional, minimally invasive first-line therapies for patients with localized disease who may not be good surgical candidates. RCC tumours have been shown to respond to various ablation therapies such as percutaneous radiofrequency ablation, microwave ablation, laser ablation, cryoablation and high-intensity focused ultrasound

ablation. The local progression rates for these therapies are often higher than those of partial and radical nephrectomy, however they are useful for treatment of incidental lesions in the elderly, multiple bilateral tumours, recurring small renal masses, and patients at risk of losing all renal function following nephrectomy (32). In general, treatment of localized RCC with surgery is good, but it is not perfect. The 5-year survival rate of patients with stage I disease (T1, N0, M0) is >90%. However relapse occurs within 5 years of surgery for patients with stage II (T2, N0, M0) or III (T3, N0, M0; T1-3, N1, M0) disease (34). Aggravating this situation is the fact that we have yet to identify adjuvant therapies that might manage this risk of relapse (35,36). Managing intermediate/high-risk RCC in its early stages is just as important as targeting stage IV mRCC, which presents its own set of challenges (36).

When possible, removal of metastases through surgery (metastectomy) can improve prognosis if all metastatic lesions are completely removed (37). However, systemic therapy is often required in cases where metastases are unresectable and/or burden of disease is too great (32). Chemotherapy and radiation therapy have, unfortunately, proven to be ineffective for treatment of mRCC, regardless of histotype. Poor response rates – ranging from 0-14% – to a wide range of cytotoxic agents have been well-documented and are attributed to expression of multi-drug resistance gene 1 and its protein product P-glycoprotein (8). The molecular mechanisms conferring resistance to radiation therapy are less well understood, however there have been links drawn to increased expression of HIF-2α and survivin (38,39). While investigations into these therapeutic immunities were being made, it was found that immune-based therapies were a viable treatment option for mRCC (2).

Alongside melanoma, RCC is considered to be one of the most immunogenic of all human malignancies. This is based on high tumoural infiltration of cytotoxic T-cells and other immune cells that can recognize tumour-associated antigens, the occurrence of RCC in patients receiving immunosuppression, and rare observation of spontaneous metastatic regression (40). Of the wide array of immunotherapies investigated, cytokine-based therapies such as high-dose interleukin-2 (IL-2) and interferon-alpha (IFN-α) have proven to be most effective and were recommended for treatment of mRCC prior to the

advent of targeted therapies. Some argue that such therapies are indeed still relevant for treatment of mRCC given their durable responses in a subset of patients, which is an area where newer therapies fall short (41,42). However, finding predictive biomarkers that can identify this subset of patients is a priority given the fact that associated toxicities of cytokine therapy are generally higher grade when compared to targeted therapies (42). First-line treatment of low-risk mRCC with IFN-α may also be just as effective as the currently recommended first-line targeted therapy sunitinib, but at significantly lower cost it could improve economic efficiency (41). Combination treatments consisting of cytokine/targeted therapy are also being investigated and present the possibility of durable responses in a larger proportion of patients (36,41,42).

From increased understanding of the molecular pathways that are active in RCC, specifically ccRCC, have emerged therapies that hone in on these pathways. These targeted therapies come in two forms: small molecule inhibitors (SMIs), and monoclonal antibodies (mAbs). Since 2007, 8 targeted therapies – sorafenib, sunitinib, temsirolimus, bevacizumab, everolimus, pazopanib, axitinib and tivozanib – have been approved for mRCC treatment (1,11,12). Of these drugs, only bevacizumab is a mAb and it is targeted against VEGF. The remaining 7 are SMIs that fall into two classes, receptor tyrosine kinase (RTK) inhibitors (RTKIs) and mammalian target of rapamycin (mTOR) inhibitors.

The RTKIs that are approved and/or in clinical trials for ccRCC – sunitinib, sorafenib, pazopanib, axitinib and tivozanib – primarily act on endothelial cell VEGF and PDGF receptors, inhibiting signal transduction initiated by tumour cell-secreted VEGF and PDGF (1). The mAb bevacizumab is specific for VEGF and prevents VEGF from interacting with its receptor on endothelial cells, thus inhibiting signaling between the tumour and blood vessels in a similar fashion (1). In this way, RTKIs and bevacizumab target both current metastases – by preventing the initial attraction of blood vessels (neovascularization) to secondary tumours – and future metastases – by preventing the growth of new blood vessels towards the primary tumour (angiogenesis) that allow tumour cells to travel throughout the body (1). While RTKIs can induce necrotic cell death in larger tumours as a result of decreased microvascular density (MVD), RTKIs display limited cytotoxicity when administered to ccRCC cells *in vitro* (43). However,

some off-target effects of RTKIs acting on tumour cells directly have been documented. For example, some of sorafenib's efficacy may stem from off-target inhibition of cyclin D1, cyclin B1 and survivin (44). Likewise, sunitinib has been observed to enhance the anti-tumoural immune response by recruiting regulatory T-cells (45). In general though, RTKIs and bevacizumab target mRCC by preventing vascularization of the primary tumour and its metastases, with the intention of enhancing cell death, reducing metabolic output, and preventing future metastases.

Unlike RTKIs, mTOR inhibitors are more direct in their treatment of ccRCC in that they target a signaling pathway that is overactive in the cancer cells themselves. mTOR can exist as a member of two functionally distinct complexes, mTOR complex 1 (mTORC1) and mTOR complex 2 (mTORC2). Both mTORC1 and mTORC2 regulate cell proliferation, cell survival, nutrient sensing, energy sensing, overall protein translation and angiogenesis, though their effects on these processes are not synonymous (1,46). The mTOR inhibitors currently approved for ccRCC – temsirolimus and everolimus – both prevent the formation of mTORC1, which results in decreased translation of HIF-1α, cyclin D1 and c-MYC (1). However as discussed previously, it is thought that HIF-2α is responsible for most of the tumourigenic signaling in ccRCC, and its translation is primarily mediated by mTORC2 (47). Furthermore, inhibition of mTORC1 alone has been shown to induce a paradoxical increase in the formation of mTORC2. Therefore, while mTORC1 inhibitors may have some effect on cell proliferation and survival, they could actually be exacerbating the angiogenic response through increased activity of mTORC2, increased expression of HIF-2α and subsequent secretion of VEGF (48). For this reason, SMIs that simultaneously target mTORC1/2 as well as the associated growth signaling kinases phosphoinositide 3-kinase (PI3K) and protein kinase B (Akt) are currently in development, though they have yet to reach clinical trials for management of mRCC (1,48).

While RTKIs, mAbs that target VEGF, and mTOR inhibitors have all shown to improve PFS and objective response rates (ORR) when compared to cytokine-based therapies, many have noted that durable, complete responses remain rare. Furthermore, while most assume that all of the approved targeted agents offer improved OS, improvements in OS

have only been objectively shown for some of the targeted agents, (1,11,12,31,34). The adverse events associated with these targeted therapies, especially next generation RTKIs like pazopanib and tivozanib, are also considered to be less severe than those associated with cytokine-based therapies (12,42). For these reasons, RTKIs are now the current first-line standard of care for patients with metastatic ccRCC and a favourable risk categorization (34). However, given the relatively recent approval of these drugs for treatment of mRCC, there is a significant lack of prognostic information to aid clinicians in deciding which drugs are most likely to work in which patients, and the order in which they should be administered (12). In fact, with the exception of bevacizumab + IFN-α, there is evidence to suggest that combined therapies – especially those combining multiple targeted therapies – are associated with serious adverse events (11).

Significant investment has been made into developing and refining RTKI and mTOR inhibitors in order to increase their specificity, thus increasing potency and decreasing the likelihood of adverse events (12). However, we already know that though RTKIs developed for ccRCC are anti-angiogenic, they are not cytotoxic in and of themselves (unless you consider their off-target effects). Likewise, though mTOR inhibitors are cytotoxic, they are not anti-angiogenic (they may actually be pro-angiogenic). Given the hazards associated with combined therapy, it seems that currently available treatment options are not capable of simultaneously targeting cell survival and angiogenesis, which may prove to be necessary in improving overall survival in a large proportion of patients (11). In summary, while targeted therapies have shown to be effective, investigation into new targets that play a role in both survival and angiogenesis is something that should be considered.

1.1.3 ccRCC Metabolism – The Warburg Effect

VHL inactivation and HIF-α stabilization occur early in the development of ccRCC, however these events alone do not lead to ccRCC. In fact 20% of VHL-knockout mice develop renal cysts that never progress to ccRCC (23). Additional events such as activation of oncogenic signaling pathways, inactivation of DNA repair mechanisms, and changes in cellular metabolism are required before small renal masses can be considered

cancerous. It is these additional events that further facilitate tumour progression, and might be better targets for therapy (14).

The change in metabolism that occurs in ccRCC, and many other cancers, is known as the "Warburg Effect" and involves a shift from aerobic respiration pathways to anaerobic respiration pathways, even when oxygen is abundant (49-51). Whereas aerobic respiration generates ATP through the tricarboxylic acid (TCA) cycle and the electron transport chain (ETC), anaerobic respiration generates ATP through glycolysis. The switch to aerobic glycolysis occurs in almost all RCC histotypes as a result of HIF-1α accumulation. While HIF-1α stabilization is due to VHL inactivation in ccRCC, its stabilization in other histotypes is due to mutation of key metabolic enzymes that ultimately result in inhibition of PHD (10,14). Regardless of the mechanism, accumulation of HIF-1α subsequently results in the upregulation of key enzymes involved in glycolysis. HIF-1α stabilization ultimately uncouples glycolysis from the TCA cycle via upregulation of pyruvate dehydrogenase kinase (PDK). PDK inactivates pyruvate dehydrogenase (PD) through phosphorylation, thus preventing the end product of glycolysis, pyruvate, from heading towards aerobic metabolic pathways (14,51). Instead of heading towards the TCA cycle, pyruvate is converted into lactate via lactate dehydrogenase (LDH) – another HIF-1α target – which allows for the regeneration of oxidized nicotinamide adenine dinucleotide (NAD^+) from its reduced form (NADH) (14,52). This alongside upregulation of GLUT-1 – yet another HIF-1α target – ensures that glycolysis substrates are in ample supply (14).

From the perspective of ATP production, shifting metabolites away from oxidative phosphorylation – ATP produced by the ETC – and towards substrate-level phosphorylation – ATP produced by glycolysis – is energetically unfavourable when oxygen is available. This has led cancer biologists to question the selective advantage that the Warburg Effect provides RCC and other cancers. One selective advantage that has been suggested is the decreased production of reactive oxygen species (ROS) that comes with decreased oxidative phosphorylation (53). In addition to uncoupling glycolysis from the TCA cycle by upregulating PDK, HIF-1α accumulation also leads to upregulation of the enzyme pyruvate kinase (PK) that facilitates the final step of

glycolysis – conversion of phosphoenolpyruvate into pyruvate. PK comes in two isoforms, PKM1 and PKM2, which have variable activities. ccRCC tumours often express the slower-acting PKM2 isoform as a result of c-MYC-mediated alternative splicing (54). As a result of this delay at the end of glycolysis, metabolites produced earlier in the glycolytic pathway accumulate and are available for other processes. One such process is the pentose phosphate pathway (PPP) which produces nicotinamide adenine dinucleotide phosphate (NADPH) – a molecule that helps cells cope with oxidative stress through various mechanisms – and molecules like ribose 5-phosphate and erythrose 4-phosphate – that are required for the synthesis of proteins and nucleic acids (53). Therefore despite reducing overall ATP production, aerobic glycolysis ensures that the enhanced growth of RCC tumours occurs in a cellular environment in which; i) oxidative stress is regulated and ii) there are sufficient materials for production of biomass (53).

HIF-1/2α accumulation also appears to suppress ROS production by inhibiting mitochondrial biogenesis, mitochondrial respiration and overall O_2 consumption (55). As mentioned earlier, ccRCC tumours often express elevated levels of c-MYC. c-MYC can heterodimerize with MYC-associated factor X (MAX) to form a transcriptional activator of peroxisome proliferator-activated receptor gamma coactivator 1-beta (PGC-1β) – a gene that promotes mitochondrial biogenesis (55). On the other hand, MAX can heterodimerize with MAX-interacting protein 1 (MXI1) to form a transcriptional repressor of PGC-1β, thus suppressing mitochondrial biogenesis. MXI1 happens to be a target of HIF-1/2α and is overexpressed in ccRCC (56), which results in greater formation of MXI1:MAX than c-MYC:MAX, overall repression of mitochondrial biogenesis, and overall decreased O_2 consumption (55). There is also evidence that HIF-1α-mediated upregulation of LDH inhibits mitochondrial respiration by competing for the same pool of NADH that is required for maintenance of the mitochondrial membrane potential and oxidative phosphorylation (52). Not only is LDH more abundant, but its cytoplasmic localization and faster kinetics ensure that it is able to outcompete mitochondrial cytochrome oxidases for the NADH being produced by glycolysis (52). The end result is lower ETC activity, lower O_2 consumption, and lower overall ROS production.

As the energetically preferred form of cellular metabolism, oxidative phosphorylation comes at the cost of increased ROS production. When the earth's atmosphere changed from a sulfide-rich environment to an oxygen-rich environment, bacterial and archaeal species were suddenly faced with a new molecule from which they were obligated to harness their energy. Each species either slowly acquired this new metabolic phenotype via advantageous genetic mutations over many generations, or perished. This concept, known as natural selection, is the driving force behind the evolution of species over time. However natural selection can apply to cells – malignant and benign – not just species as Darwin originally postulated (57). Cells are able to sense changes in their environment and react in many ways, just like organisms. Some of these mechanisms have been known for decades, some have only just come to light, and even more are still waiting to be discovered.

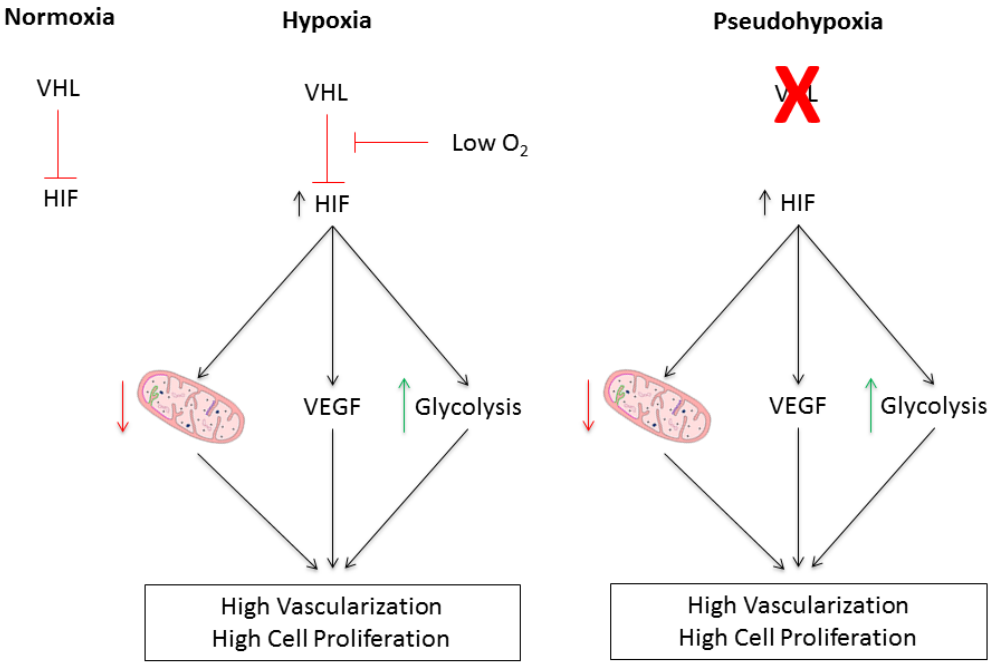

Figure 1. VHL/HIF signalling under normoxic, hypoxic, and pseudohypoxic conditions in ccRCC.

1.2 Hydrogen Sulfide: The Third Gasotransmitter

Gasotransmitters are small, gaseous, membrane-permeable molecules that are produced endogenously and in a dedicated fashion within mammalian cells in order to be perceived and invoke a response (58). Two gaseous molecules – carbon monoxide (CO) and nitric oxide (NO) – are widely accepted to fit this definition and their effects within the body have been recognized since the 1960s and 1980s respectively (59,60). The third and most recently discovered gasotransmitter is hydrogen sulfide (H_2S), though its classification as a bona fide gasotransmitter is still up for debate (61). While there is no doubt that H_2S is a small, membrane-permeable molecule that is produced in a dedicated fashion in nearly all mammalian cells, there is some disagreement over whether changing levels of H_2S can be sensed, or whether H_2S itself is the *sensor* (61,62). Regardless of how the semantics play out, it cannot be denied that H_2S production in mammalian cells plays important roles in normal physiology and pathophysiology (58).

It has long been known that at high enough concentrations H_2S is a mitochondrial poison that inhibits Complex IV of the ETC and eliminates aerobic respiration (63). As a result, nobody thought that H_2S could possibly be playing a meaningful role in humans, despite the fact that there was knowledge of mammalian enzymes that produce H_2S (64). The first physiological function of H_2S identified in mammals was its role as a neurotransmitter in the brain (65). Soon after, H_2S was shown to participate in synergistic smooth muscle relaxation alongside NO (66). To this day, the functions of H_2S are best described in the context of the central nervous system (67,68) and the cardiovascular system (69-71), although additional functions have been identified in the digestive system (72,73), musculo-skeletal system (74), endocrine system (75-77), excretory system (78-80), respiratory system (81,82) and reproductive system (83). Not only does endogenous H_2S production play a role in the normal functioning of these systems, but disruption of baseline H_2S production has been implicated in diseases such as hypertension, Alzheimer's Disease, diabetes mellitus, ulcerative colitis and end-stage renal disease (58,84,85). Furthermore, the enzymes responsible for endogenous H_2S production are expressed ubiquitously in human cells and H_2S is found in the blood at nanomolar to micromolar concentrations (84).

1.2.1 H_2S Production in the Kidneys: The Transsulfuration Pathway and Oxygen Sensing

Scientists were able to measure endogenous H_2S production *in vivo* before it was known to be physiologically relevant. The first documented measurements of tissue-derived H_2S were from rat liver and kidney and were simply used as a way to characterize the relative activities of the enzymes involved in the desulfhydration of L-cysteine (LC) (64). The three enzymes that facilitate this process are cystathionine γ-lyase (CSE), cystathionine β-synthase (CBS) and 3-mercaptopyruvate sulfurtransferase (MPST). At the time of these observations, it was known that the liver and kidneys were the major site for the desulfhydration of LC, although the ultimate purpose of this process was not entirely clear (64). We now know that these enzymes are important in the kidney because in addition to facilitating the desulfhydration of LC, they also convert the toxic metabolite homocysteine (Hcy) into LC (86,87). Together, the conversion of Hcy into LC, and subsequent processing of LC into sulfane sulfur (S^0), sulfites (SO_3^{2-}), sulfates (SO_4^{2-}) and sulfides (S^{2-}, HS^-, H_2S) is known as the transsulfuration pathway.

It was previously thought that the production of H_2S by CBS, CSE and MPST in the kidney was simply a byproduct of the transsulfuration pathway, necessary only for the purposes of chemical stoichiometry. It has recently been shown that H_2S derived from CSE and CBS is involved in regulating baseline hemodynamics and properties of renal tubules. Notably, renal H_2S concentrations were found to correlate with renal blood flow (RBF), glomerular filtration rate (GFR) and urinary excretion of Na^+ and K^+ – termed natriuresis and kaliuresis respectively (88). While increased RBF and GFR are likely due to the well-known vasodilatory effects of H_2S, increased natriuresis and kaliuresis are attributed to the inhibitory effect that H_2S has on the Na^+/K^+ ATPase (NKA) and the $Na^+/K^+/2Cl^-$ Co-transporter (NKCC) that maintain Na^+ transport across renal epithelial cells (88). There also appears to be a relationship between baseline H_2S production, production of ROS, and regulation of systemic blood pressure through the renin-angiotensin system (RAS) that is regulated by mesangial cells (89,90). Although CBS and CSE are noticeably lacking from glomerular epithelial cells, H_2S produced in nearby proximal tubule epithelial cells may act on glomerular epithelial cells in a paracrine

fashion to influence global protein synthesis through AMP-activated protein kinase and mTORC1 (91-93). Similar paracrine functioning of H_2S has been implicated in the vasodilation of proximal tubule capillaries, which also lack CBS and CSE (91).

One postulated function of H_2S within the kidney is oxygen sensing (94). This recently proposed hypothesis builds on empirical evidence that demonstrates that the relative proportion of sulfur in its oxidized forms (SO_x) and reduced forms (H_xS) depends on O_2 availability (81). When O_2 is available under normoxia, the oxidized forms of sulfur are favoured. Conversely, when O_2 is scarce under hypoxia, the reduced forms of sulfur, such as H_2S, are favoured. This is no doubt an oversimplified model, nonetheless there is significant evidence demonstrating that oxidation of H_2S is an effective cellular mechanism of sensing decreases in O_2 in a wide variety of tissues (62,95). Beltowski proposes that this acute mechanism may be important in regulating oxygenation to the renal medulla – an area of the kidney that requires tight regulation of blood flow in order to achieve the balance between hyperosmolality and O_2 supply that is required for the concentration of urine. Maintenance of this steep concentration gradient in the medulla requires high expression of NKCC channels and comes at the cost of significant O_2 consumption (60% of total renal O_2 consumption) (94). To ensure that maintenance of the gradient does not starve medullary cells of O_2, it is thought that high CBS expression in these cells results in accumulation of H_2S under hypoxia, inhibition of NKCC and NKA to reduce O_2 demand, and vasodilation of descending vasa recta to increase O_2 supply (93,94).

There is much that remains to be investigated regarding the role that endogenous H_2S production plays in maintaining normal renal function, however it is clear that its presence cannot simply be described as a byproduct of transsulfuration.

1.2.2 H_2S Production, Reactivity and Signalling

Gasotransmitters are by no means traditional signalling molecules. Unlike hormones and neurotransmitters, gasotransmitters are not suitable for long- or even short-term storage. There are no dedicated receptors for gasotransmitters, nor is there a need for channels to facilitate the movement of gasotransmitters across cell membranes due to their

hydrophobicity. As such, once gasotransmitters are enzymatically produced, they are immediately able to react with various functional groups in their nearby surroundings. Given the lack of control that the cell has on these molecules following their synthesis, it is imperative that their production is tightly regulated at the level of enzyme expression and activity (96).

H_2S is synthesized by three enzymes, two of which are localized primarily to the cytoplasm (CBS and CSE), the other of which is localized primarily to the mitochondria (MPST), although CBS and CSE have been observed in the nucleus and MPST in the cytoplasm (97). CBS is primarily regulated post-translationally through various mechanisms, although its transcription has been shown to be regulated by numerous transcription factors, including HIF-1/2α (98,99). CBS contains a redox-sensitive heme co-factor which can regulate enzyme activity in response to other gasotransmitters as well as oxidative stress. While oxidative stress activates CBS, presence of NO and/or CO inhibits CBS (100). CBS can also be allosterically activated by S-adenosylmethionine, which is a precursor of CBS's major substrate homocysteine (96). Regulation of MPST is also primarily achieved through post-translational mechanisms. Various intra- and inter-molecular disulfide bridges can form between cysteine residues under oxidative conditions, inactivating the enzyme. The presence of certain reducing substrates may regulate MPST activity by helping to break these inhibitory disulfide bonds under conditions of oxidative stress (101). Conversely, little is known regarding post-translational control of CSE activity, although its transcription may be inhibited by n-MYC (98).

Once produced, H_2S exists in an equilibrium with its anionic form (HS^-) and is also capable of forming reactive polymerized structures known as polysulfides, the effects of which may be restricted to the cells in which they are produced (67,96). While some believe that the effects of H_2S may actually be mediated by these other reactive sulfur species, it is generally accepted that H_2S exerts its effects by modifying protein activity post-translationally by reacting with thiol groups of cysteine residues (102). This reaction – known as S-sulfhydration – results in the formation of a sulfhydryl group (R-S-S-H) that alters protein structure and function. From a chemistry standpoint, S-

sulfhydration is very similar to the reaction by which NO interacts with cysteine residues – known as S-nitrosylation – however the biological effects of these two gasotransmitter-mediated post-translational modifications are very different (96,103). Whereas S-nitrosylation often results in the inhibition of target proteins, S-sulfhydration can be both inhibitory and stimulatory. Often, a protein's activity depends on whether key cysteine residues have been S-nitrosylated (inactive) or S-sulfhydrated (active) (96). This can be said for glyceraldehyde 3-phosphatase (GAPDH), a key regulator of glycolysis. S-Sulfhydration of GAPDH at Cys150 results in a 700% increase in its glycolytic activity whereas S-nitrosylation of this same residue inhibits the enzyme's glycolytic function (102). Competition between H_2S, NO and ROS for cysteine residues is likely a way by which cells buffer the effects of any one of these gaseous molecules, ensuring that a response is triggered only when levels of one of these molecules significantly outweighs the others (61).

In addition to altering the activity of phosphatases like GAPDH, H_2S also affects the activity of kinases, ion channels and transcription factors that are involved in regulating cell survival, cell proliferation, membrane polarization, angiogenesis and inflammation (104). S-sulfhydration of ATP-dependent K^+ (K_{ATP}) channels is a stimulant of vasodilation in the cardiovascular system that may be more potent than NO-mediated vasodilation (105). H_2S has also been shown to promote the anti-apoptotic signaling cascade initiated by tumour necrosis factor alpha (TNF-α) through S-sulfhydration of the p65 subunit of the transcription factor nuclear factor kappa B (NF-κB) (106). Finally, H_2S can activate various kinases that promote proliferation and angiogenesis – such as Akt, protein kinase C (PKC), mitogen-activated protein kinase p38 (p38) and extracellular signal-related protein kinase (ERK 1/2) – although S-sulfhydration of kinases is rarely documented in the literature (104).

1.2.3 H_2S: Vasodilator and Angiogenic Factor

The synergistic effects of H_2S and NO in the cardiovascular system have been known for quite some time (66). As previously mentioned, both of these gasotransmitters are potent vasodilators, and their effects may be mutually dependent on one another. Recent work has demonstrated that H_2S and NO are also mutually-dependent stimulants of

angiogenesis (107). Both vasodilation and angiogenesis are important physiological responses that occur in response to disruption of normal blood supply following various ischemic injuries. Whereas vasodilation involves increasing blood flow via relaxation of smooth muscle cells that surround blood vessels, angiogenesis increases blood flow via the growth and recruitment of new vascular networks, which requires the proliferation and migration of endothelial cells. At first glance these responses appear to be quite distinct, however closer inspection reveals that H_2S and NO coordinate these responses using the same pathway (107).

Activation of protein kinase G (PKG) is the junction at which gasotransmitter production and the induction of angiogenesis/vasodilation meet. In order for PKG to phosphorylate its target proteins, the co-factor cyclic guanosine monophosphate (cGMP) is required. Production of cGMP is accomplished via guanylyl cyclase (GC), and degradation of cGMP is accomplished via phosphodiesterase type 5 (PDE5). cGMP levels rise in the presence of NO and H_2S because NO activates GC – increasing cGMP production – and H_2S tonically inhibits PDE5 – decreasing cGMP degradation (107). Knock-out/inhibition of either one of the major endothelial enzymes responsible for NO and H_2S synthesis – endothelial nitric oxide synthase (eNOS) and CSE respectively – results in complete loss of the angiogenic response to VEGF and the vasodilatory response to cholinergic stimulation (107,108). This suggests that baseline production of H_2S and NO in endothelial cells is a necessary component of these cardiovascular responses.

Focusing on the angiogenic response, several groups have shown that exogenous H_2S can induce endothelial cell proliferation, tube formation and migration via PKG-mediated phosphorylation of ERK 1/2 and p38 (107-109). What is more interesting, is that VEGF-mediated angiogenesis appears to require endogenous H_2S production, suggesting that VEGF exerts its angiogenic effects through H_2S (108). In addition to inhibiting cGMP degradation by PDE5, it is thought that increasing levels of H_2S may increase cGMP via Akt-mediated activation of eNOS (107). This is based on evidence that Akt is activated in response to exogenous/endogenous H_2S production, albeit the mechanism is not currently known (107-109). The exact mechanisms that link VEGF, H_2S and NO are still being worked out, however a relationship surely exists.

1.2.4 H_2S: Antioxidative and Cytoprotective

When referring to oxidative damage, one is referring to the damage that cells incur as a result of generating ATP through oxidative phosphorylation. As the ultimate acceptor of electrons utilized in the ETC, O_2 must be present in abundance to ensure that electrons are quenched in pairs and not in isolation. When molecules with stable electronic configuration happen to accept a single electron, the result is an unstable free radical that can disrupt cellular function by inappropriately reacting with and damaging DNA, proteins and lipids. Free radicals that are most commonly formed in cells usually contain oxygen – referred to as ROS – or nitrogen – referred to as reactive nitrogen species (RNS). While the presence of moderate levels of ROS/RNS is normal and even necessary for appropriate cell signaling, excessive production of ROS/RNS has been implicated in several diseases, many of them age-associated. While mitochondrial dysfunction and other kinds of cell stress result in oxidative damage as a result of increased ROS/RNS production, oxidative damage can also occur as a result of decreased degradation of ROS/RNS by antioxidative mechanisms (110).

Several studies have shown that exogenous administration and/or endogenous production of H_2S can attenuate injury and cellular senescence caused by oxidative stress (111-115). It was originally believed that H_2S mediates these antioxidative effects by reacting directly with ROS and RNS. However, due to the relatively low abundance of H_2S compared to other cellular reductants like glutathione, as well as the low rate constants for H_2S-mediated oxidation, it seems likely that this is not the case (111). To explain the antioxidative properties of H_2S, it has been postulated that they could simply be the result of reversible Complex IV inhibition, decreasing metabolic rate and overall ROS production (116). H_2S has also been shown to react with electrophiles that are generated during oxidative damage and lead cells down cell death/senescence pathways. In this way H_2S blunts the cell's response to oxidative stress, promoting damage recovery as opposed to cell death (117). Along the same line, H_2S can abrogate apoptosis by counteracting declines in mitochondrial membrane potential and preventing caspase activation (112).

Alternatively, exogenous H_2S can induce the antioxidant response through regulation of the master transcription factor NF-E2 p45-related factor 2 (Nrf2). Under normal REDOX conditions, Nrf2 is degraded by kelch-like ECH-associated protein-associated protein-1 (Keap1), however under oxidative stress H_2S inactivates Keap1 through S-sulfhydration, allowing Nrf2 to accumulate and induce expression of antioxidative proteins (118). Interestingly, CBS and CSE are amongst the antioxidative proteins that are induced by Nrf-2, creating a positive feedback loop in which H_2S production plays a central role (118). This positive feedback loop could explain how H_2S can pre-condition cells to various forms of injury that involve oxidative stress (119). Regardless of the mechanism, H_2S is clearly playing an important role in responding to oxidative stress.

1.2.5 H_2S: Metabolic Substrate and Regulator

Given its toxic reputation, it is rather hard to believe that H_2S could be contributing to mammalian cellular metabolism in any meaningful way. The existence of prokaryotes that oxidize sulfides for energy production has been known for decades. However, these anaerobic organisms – which usually inhabit sulfide-rich environments like the deep ocean or volcanic springs similar to primordial earth– cannot rely on oxidative phosphorylation for ATP production like humans and other aerobic organisms do. However, when one considers the endosymbiotic relationship that links eukaryotic mitochondria with ancient sulfide-oxidizing prokaryotes, perhaps it is not surprising that eukaryotes retained a sulfide oxidation pathway (120). Conversion of H_2S into persulfide (S_2^{2-}), sulfite (SO_3^{2-}), thiosulfate ($S_2O_3^{2-}$) and sulfate (SO_4^{2-}) occurs under aerobic conditions and is important in ensuring that H_2S does not inhibit the heme co-factors of Complex IV of the ETC, halting oxidative phosphorylation and ATP synthesis (121). In fact, given the high flux of sulfur into H_2S we know that most of the H_2S being produced under normoxic conditions is removed via mitochondrial oxidation in order to account for the relatively low concentration of H_2S in mammalian tissues (111). This is especially true for epithelial cells of the kidney and colon which are exposed to high levels of H_2S produced by the transsulfuration pathway and H_2S-producing bacteria respectively (122). While these physiological adaptations are impressive in their own right, what is truly impressive is that these, and other cells of the body, are capable of funneling the electrons

liberated by sulfide oxidation into the ETC to contribute to ATP production. This makes H_2S the first inorganic substrate for oxidative phosphorylation identified in mammalian cells (121).

The first step of sulfide oxidation in mammalian cells is the transfer of electrons from H_2S to coenzyme quinone (Q), which is catalyzed by sulfide quinone reductase (SQR) (122). When compared to the canonical players involved in the ETC, H_2S is analogous to NADH in that they are both the primary donors of electrons, and SQR is analogous to Complex I in that they both feed into coenzyme Q (120). Following loss of its electrons, H_2S is processed by a sulfide-oxidizing unit (SOU) consisting of a dioxygenase and sulfurtransferase through a mechanism that requires one molecule of O_2. In this way, oxidation of 1 mole of H_2S requires 1.5 moles of O_2 (1 mole for SOU and 0.5 moles for Complex IV), which is considerably more than the 0.5 moles of O_2 required for oxidation of NADH. Therefore, oxidation of sulfide in eukaryotes is an oxygen-dependent process, which is why H_2S levels rise under hypoxia (62). The differences in stoichiometry also highlight that oxidation of H_2S is energetically less favourable than oxidation of NADH in that it only supplies half of the electrons. Furthermore, catabolism of L-cysteine into pyruvate would yield ten times the number of electrons available for oxidative phosphorylation when compared to catabolism of L-cysteine into H_2S. This prompts the question "Why would eukaryotic cells saturate the activity of coenzyme Q with H_2S/SQR when electron transport through NADH/Complex I is much more efficient?" (120).

The reasons for this are three-fold, and together they emphasize the role of H_2S as an 'emergency substrate.' First and foremost, H_2S is membrane-permeable so gaining access to the mitochondria does not require additional energy expenditure for transport and also occurs rapidly. Second, production of H_2S from L-cysteine does not require energy investment as is the case for metabolism of carbon sources which requires initial activation before reducing agents like NADH can be produced. Finally, the SOU has a high affinity for H_2S when present at physiological concentrations which ensures that nearly all of it is used for production of ATP (120). The role of H_2S as an emergency metabolic substrate following various stresses has been demonstrated in smooth muscle cells and hepatocytes (123,124).

Tackling this issue from another angle, it has also been suggested that by competing with electron donors from carbon-based metabolism, H_2S may play a role in fine-tuning oxygen consumption. It has been shown that moderate levels of H_2S (100 nM – 10 μM) can stimulate oxygen consumption in the presence of various carbon-based metabolic substrates *in vitro*, whereas higher levels of H_2S (>10 μM) overwhelm the SOU, inhibit Complex IV and decrease oxygen consumption (125). Increasing oxygen consumption through the SOU can be useful in reducing oxidative stress associated with oxidative phosphorylation and may be a key link between cellular REDOX potential and cellular metabolism. With increased aerobic respiration comes increased risk of oxidative stress, however moderate H_2S production may allow cells to achieve the same metabolic output with less oxidative damage. Production of H_2S also increases glycolysis through S-sulfhydration of GAPDH, as previously mentioned.

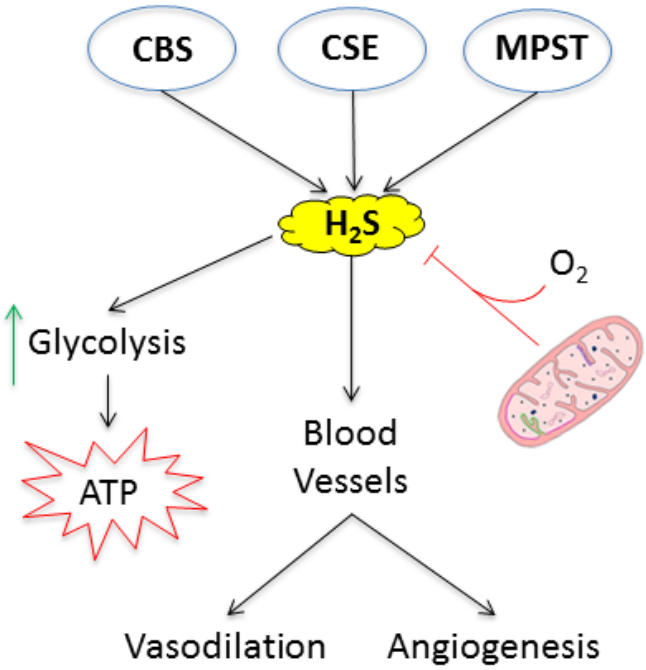

Figure 2. Cellular H_2S metabolism and signalling.

1.3 H_2S and Cancer

Given its many properties, the therapeutic potential of H_2S has been investigated in many disease states, including cancer. In many of these disease states endogenous H_2S production seems to have been suppressed or lost, in which case exogenous administration of H_2S has been investigated as a treatment option. In these cases, determining the proper dose, method of administration, and even rate of release through the use of slow-release H_2S-donour molecules are major challenges due to the small range of concentrations at which H_2S is effective before it becomes toxic (85). These same issues have led to conflicting results on the role that H_2S plays in various cancers.

1.3.1 Exogenous H_2S as a Cancer Treatment?

It has been shown that exogenous H_2S treatment can restrict gastric cancer growth and survival, although the dose used *in vitro* was not shown to be non-toxic to non-malignant cells and the mechanism of action *in vivo* was not identified (126). Exogenous H_2S treatment has also been shown to target the growth and survival of oral cancer, breast cancer and hepatoma cell lines over non-malignant cell lines of similar origin. However the pro-apoptotic effects of H_2S in these instances are reliant on the presence/absence of certain proteins (127,128). If one believes that proliferating cancer cells are affected by natural selection in the same way that all organisms are, then one would expect that endogenous H_2S production would be down-regulated if H_2S is indeed anti-tumoural. However, decreased expression of H_2S-producing enzymes – and decreased endogenous H_2S production – has only been shown in aggressive prostate cancer cell lines (129). In fact, the opposite seems to be true when evaluating endogenous H_2S production in most cancer cell lines, and inhibition of this enhanced H_2S production targets cell growth, survival, metabolic output, migration, angiogenic potential and therapy-resistance.

1.3.2 Role of Endogenous H_2S Production in Cancer

Much attention has been paid to the role that endogenous H_2S production plays in the progression of colon cancer, given that the colon is rich in bacterial H_2S that is continuously being oxidized in the mitochondria of colonocytes (122). It was first shown that exogenous H_2S treatment could enhance cell cycle entry in several colon cancer cell

lines by increasing Akt activation and decreasing expression of the cell cycle inhibitor p21 (130). More recently, it was shown that several malignant traits of colon cancer were due to enhanced expression of CBS in human tumours and malignant cell lines when compared to non-malignant samples (131). In addition to facilitating proliferation *in vitro*, increased endogenous H_2S production was contributing to cell migration and cell bioenergetics. When cell lines were xenografted *in vivo*, silencing/inhibition of CBS could attenuate tumour growth and blood supply (131). CSE has also been implicated in facilitating colon cancer growth, migration and vascularization, and its expression appears to be transcriptionally up-regulated in cell lines characterized by aberrant Wnt signalling (132).

CBS was also found to be upregulated in human epithelial ovarian cancer cell lines and tissue samples when compared to normal epithelial cells, and inhibition/knock-down of CBS restricted cell growth, cell viability and cellular metabolism *in vitro*. When xenoplanted into mice, silencing of CBS was also able to reduce xenograft neovascularization and sensitized tumours to platinum-based chemotherapy which cells had previously been resistant towards (133). Whether H_2S itself was able to protect against the oxidative stress induced by the chemotherapy was not investigated, however it has been shown that induction of CBS/CSE and elevated H_2S production under hypoxia contributes to hypoxia-induced radiation therapy resistance in hepatoma cells (134). It has also been suggested that bystander effects – tumour cell death surrounding the irradiated area of the tumour – in hepatocellular carcinoma may also be the result of decreased endogenous H_2S synthesis (135). Together, these studies suggest that inhibition of endogenous H_2S production could prove to be an effective adjuvant therapy in tumours such as ccRCC that are hypoxic and/or resistant to chemotherapy/radiation therapy.

An important aspect of natural selection is the presence of a selective pressure. From the point of view of cancer cells, naturally occurring selective pressures include hypoxia, nutrient deprivation, and oxidative stress. However, by targeting cancer cells with specific therapies we can introduce additional selective pressures that cancer cells may or may not adapt to. Only a subset of cells will survive these pressures, proliferate and lead

to changes in the cellular make-up and behaviour of tumours over time, a process referred to as tumour progression (136). Recent studies have shown that breast, liver and colon cancer cell lines are able to recover from cell damage induced by nutrient deprivation, hypoxia, oxidative stress and chemotherapeutics through a mechanism involving H_2S (137,138). Essentially, damage-recovered cells exhibit increased endogenous H_2S production which upregulates nicotinamide phosphoribosyltransferase (Nampt), an enzyme involved in salvaging NAD^+ and driving aerobic glycolysis. Damage-recovered cells therefore display reduced mitochondrial bioenergetics, increased aerobic glycolysis, increased resistance to oxidative stress, and increased proliferation as a result of this H_2S-Nampt pathway (138). This same pathway has also been shown to be associated with the stem-like phenotype of cancer cells that survive such damage (139).

1.3.3 Role of H_2S in kidney cancer

Renal malignancies, specifically ccRCC tumours, have been described as metabolic diseases that display dysfunctional oxygen-, nutrient-, and energy-sensing pathways (9). Functional loss of the tumour suppressor VHL is responsible for this dysfunction in that it results in the accumulation of HIF-1/2α, rendering ccRCC tumours *pseudohypoxic* (14). This pseudohypoxia results in an overall shift in metabolism that results in the activation of aerobic glycolysis, suppression of mitochondrial bioenergetics, and flux of glycolytic metabolites towards production of reducing agents and biomass – otherwise known as the Warburg Effect (53). Finally, pseudohypoxic ccRCC tumours are highly angiogenic due to their high secretion of VEGF, which increases their access to vasculature and the rest of the body (18).

H_2S is an endogenously-produced molecule that functions as an oxygen sensor (62), angiogenic factor (108), metabolic substrate (122), and cytoprotectant (111). In renal epithelial cells, H_2S is produced in abundance by enzymes that are involved in the detoxification of homocysteine (64) and this excessive H_2S is readily oxidized by mitochondria under normoxia, contributing to ATP production (122). In the context of other cancers, it is known that elevated levels of H_2S can enhance ATP production and reduce oxidative stress via mitochondrial oxidation (131,133) or enhanced aerobic glycolysis (137,138). Finally, endogenous H_2S production appears to confer resistance to

natural pressures felt by cancer cells as well as clinically-administered pressures like chemotherapy and radiation therapy (134,139).

Taken together, there is considerable evidence to suggest that endogenous H_2S production plays an important role in the progression of kidney cancer, and inhibiting its production may be a legitimate course of treatment. Specifically, pseudohypoxic ccRCC tumours may produce particularly high levels of H_2S as a result of decreased removal of H_2S via oxidation and increased expression of CBS via HIF-1/2α (99).

1.4 Hypothesis and Objectives

1.4.1 Hypothesis

It is hypothesized that endogenous production of H_2S is upregulated in VHL-deficient ccRCC cell lines and tumours, and contributes to their survival, growth and angiogenic potential.

1.4.2 Objective I: Is Endogenous H_2S Production Enhanced in VHL-deficient ccRCC Cell Lines?

Our first objective was to determine whether endogenous production of H_2S is enhanced in VHL-deficient ccRCC cell lines. To investigate this, five cell lines were used. The non-malignant, human, renal epithelial cell line HK-2 served as the control for four different ccRCC cell lines: the VHL WT ccRCC cell line Caki-1, two VHL-deficient ccRCC cell lines 769-P and 786-O, and a 786-O cell line with VHL function restored using an exogenous lentiviral vector containing a single wild-type allele of the gene (786-O VHL+).

As a result of its gaseous nature, quantification of cellular H_2S production has proven difficult and has been a significant hurdle in this field of research. Recently published articles documenting endogenous H_2S production often use the Methylene Blue Assay which has been practiced since the 1970s but is known to produce false-positive results by reacting non-specifically with thiols. To avoid such false positive results, we used a cell-permeable, H_2S-specific, fluorescent probe in combination with live-cell imaging to track endogenous H_2S production in our cell cultures in real-time. Cells in the presence/absence of the probe were imaged at the beginning of experiments as a control to demonstrate that differences in fluorescent signal were the result of differences in H_2S production, and not differences in background fluorescence. Use of this probe was impractical in the 786-O VHL+ cell line due to high background fluorescence, and so the Methylene Blue Assay was used instead in its stead, with heat-killed cells serving as a control against false-positive results.

Since the probe only quantifies net H_2S production, it alone cannot distinguish between cell cultures that have a high concentration of H_2S due to enhanced production, and cell cultures that have a high concentration of H_2S due to dysfunctional clearance. To more adequately address whether VHL-deficient ccRCC cell lines display enhanced *production* of H_2S, western blot analysis of baseline CBS, CSE and MPST expression was performed. Hypoxic induction of CBS/CSE/MPST expression was also investigated using western blot analysis to try and establish links between expression of H_2S-producing enzymes, VHL functional status, and HIF-1/2α expression.

1.4.3 Objective II: Does Endogenous H_2S Production Contribute to the Proliferation, Metabolism and Survival of ccRCC Cell Lines?

Our second objective was to determine whether endogenous production of H_2S contributes to the proliferation, metabolism and survival of ccRCC cell lines. In order to determine whether endogenous H_2S production can be inhibited in our cell lines we treated them with the validated CBS/CSE inhibitors hydroxylamine (HA) and propargyl glycine (PAG) (140) and monitored changes in H_2S production using the fluorescent probe described in Objective I. Treating cells with the substrate for endogenous H_2S production (LC) allowed us to evaluate whether endogenous H_2S production can be stimulated above baseline levels, or whether it is at capacity. Combination treatment of cells with HA and LC will allow us to determine if we can partially rescue H_2S production with LC when the inhibitor is present. Cells were left untreated as a control, seeing as HA, PAG and LC were all dissolved in phosphate-buffered saline (PBS).

Using these treatments under both normoxic (21% O_2) and hypoxic (1% O_2) growth conditions, we evaluated how changing endogenous production of H_2S influenced cell growth, cell survival, and cell metabolism *in vitro*. Changes in cell growth were quantified by measuring changes in confluency over time. Cell viability was quantified via flow cytometry identification of the apoptotic and necrotic markers Annexin-V and 7-AAD, respectively. Finally, cell metabolism was quantified using a combination of the XTT Assay – which quantitates electron turnover by spectrophotometric changes – and an ATP quantitation kit – which measures cellular ATP concentration using a luciferin-

luciferase system. The role that VHL mutation status plays in conferring resistance/susceptibility to such treatments was further investigated here.

1.4.4 Objective III: Does Endogenous H_2S Production Contribute to Neovascularization of ccRCC Xenografts?

Our third objective was to determine whether endogenous production of H_2S contributes to the neovascularization of ccRCC xenografts. In order to investigate this, ccRCC cell lines were xenografted into the chorioallantoic membranes (CAMs) of developing chicken embryos. This immune-deficient xenograft model is ideal for studying the neovascularization of human tumours in real-time (141), and has also been used to study the effects of H_2S on angiogenesis (108). Treatments were administered systemically to determine whether changes in endogenous H_2S production can influence the recruitment of blood vessels to ccRCC tumours. PBS was injected intravascularly as a control. The effect of treatments on tumour size was also investigated, as well as the efficacy of treatments in relation to VHL mutation status.

1.4.5 Objective IV: Is Endogenous H_2S Production Enhanced in human RCC tumours?

Our fourth and final objective was to determine whether expression of the H_2S-producing enzymes CBS and CSE is upregulated in human RCC tumours. In order to investigate this, immunohistochemical staining of CBS and CSE was performed on samples derived from 49 patients with renal masses. Tissue was also harvested from non-neoplastic areas of the affected kidney to serve as an internal control. Expression of each protein in ccRCC tissue was pathologically scored and compared to expression in normal renal tissue from the same patient, as well as expression in non-malignant and non-ccRCC renal masses. Correlations to Fuhrman grade – a pathological indicator of disease severity – and tumour size were also performed.

2. Materials and Methods

2.1 Cell Culture

All cells were cultured under normal growth conditions (37 °C, 5% CO_2, 21% O_2) in growth media (Gibco®, Burlington, ON) supplemented with 10% fetal bovine serum and 1% penicillin/streptomycin. Subculturing of cells was performed weekly with use of 0.05% trypsin EDTA (Gibco®). The human renal epithelial cell line HK-2 was generously donated by Dr. Lakshman Gunaratnam (Western University, London, ON) and cultured in Keratinocyte Serum Free Medium supplemented with human recombinant Epidermal Growth Factor 1-53 and Bovine Pituitary Extract. The VHL WT ccRCC cell line Caki-1 was generously donated by Dr. Alison Allan (Western University, London, ON) and cultured in McCoy's 5A growth medium. The VHL-deficient ccRCC cell lines 769-P and 786-O were also donated by Dr. L. Gunaratnam and cultured in Dulbecco's Modified Eagle Medium. The ccRCC 786-O VHL+ cell line was generously donated by Dr. James Brugarolas (UT Southwestern, Dallas, TX) and grown in Dulbecco's Modified Eagle Medium.

2.2 Treatments

Inhibitors of endogenous H_2S synthesis (HA and PAG) and the substrate for endogenous H_2S production (LC), were prepared as 100 mM stock solutions in PBS. Effective doses ranged from 0.5 mM to 5 mM, depending on the assay, and were used to treat cells seeded in 96-well, 24-well, 12-well or 6-well plates. Cells were treated for 6-48 hours in either normoxic growth conditions (37 °C, 5% CO_2, 21% O_2) or hypoxic growth conditions (37 °C, 5% CO_2, 1% O_2) using a HypOxystation® H85 hypoxia chamber ($HYPO_2XYGEN$, Frederick, MD).

2.3 Measurement of Endogenous H_2S Production

2.3.1 Live Cell Imaging with Fluorescent Probe

A cell-permeable, H_2S-specific, fluorescent probe was used in combination with live-cell imaging to track endogenous H_2S production in our cell cultures in real-time. The H_2S-specific probe was generously donated by Dr. Michael Pluth (University of Oregon, Eugene, OR) and is the second-generation product of probes previously developed in the Pluth lab. The probe is an azide-functionalized fluorophore that reacts specifically with H_2S to produce a green fluorescent signal (142). The live-cell imaging platform used here was the IncuCyte ZOOM (Essen BioScience, Ann Arbour, MI) and its use was graciously afforded by Dr. Anthony Jevnikar (Western University, London, ON). Cells were seeded into 96-well plates (2×10^4 cells per well) and allowed to adhere overnight. Treatments and H_2S-specific probe were added to wells simultaneously and green channel fluorescent images of each well were captured every 30 minutes for 15 hours (4X objective, 440 nm excitation/520 nm emission). Using IncuCyte internal software, thresholding was performed on wells in which no H_2S-specific probe had been added in order to eliminate background cellular fluorescence. The total number of cells fluorescing above the established threshold was quantified, yielding a Total Probe Count. IncuCyte internal software was also able to quantify percentage cell confluency after additional thresholding, and this was used to normalize the Total Probe Count.

2.3.2 Methylene Blue Assay

Cells were seeded into 6-well plates and allowed to reach 90% confluency. Growth media was aspirated and cells were washed twice with PBS before the addition of 50 µL of lysis buffer. Immediately, a solution of zinc acetate (12% NaOH) was added to each sample to 'capture' H_2S released by lysis. Subsequent reaction with 20 mM N,N-dimethyl-p-phenylenediamine in 7.2 M HCl and 30 mM $FeCl_3$ in 1.2 M HCl allowed for a colour change to occur over 10 minutes which was spectrophotometrically quantified at 670 nm. Standard H_2S solutions were prepared by dissolving Na_2S in lysis buffer and were processed in parallel. Heat-killed cell pellets were also processed in parallel to serve as a negative control.

2.4 Protein Expression Analysis

2.4.1 Protein Isolation

Cells were plated into 60 mm dishes and allowed to reach 90-100% confluency. Cells were either kept in normoxia or exposed to hypoxia for 6-24 hours. Following treatment, media was aspirated, cells were washed twice with PBS before being lysed on ice for 15 minutes in RIPA buffer. Lysates were collected and centrifuged at 4 °C and 10,000 x g for 10 minutes before being aliquoted and stored at -80 °C.

2.4.2 SDS-PAGE and Western Blotting

Forty-fifty micrograms of each sample was run on 10-12%, Tris-glycine, SDS-polyacrylamide gels under thiol-reducing conditions at 60-120 V and transferred to PVDF membranes for 45 minutes at 80V. Membranes were blocked in TBS (5% BSA) and incubated overnight at 4°C with primary antibody (mouse-anti-human CBS (B-4): Santa Cruz Biotechnology Inc., sc-133154; rabbit-anti-human CTH (CSE): Sigma Aldrich, SAB2100501; mouse-anti-human MPST (D-8): Santa Cruz Biotechnology Inc., sc-374326; mouse-anti-human β-actin: Sigma Aldrich, A5441). Membranes were washed in TBS (1% Tween-20) for 3 x 10 minutes, incubated with HRP-conjugated secondary antibody (goat-anti-mouse IgG HRP conjugate: Life Technologies™, G-21040; goat-anti-rabbit IgG-HRP-conjugate: Jackson Immunoresearch Laboratories Inc., 111-035-003) for 1 hour at room temperature and washed for 3 x 10 minutes. Chemiluminescence was induced using Luminata™ Crescendo Western HRP Substrate (EMD Millipore, WBLUR0100A).

2.4.3 Imaging and Analysis

The majority of blots were imaged using the C-DiGit® Blot Scanner (LI-COR) and subsequently analyzed using Image Studio Lite version 4.0. Due to equipment malfunction, some blots were imaged using the FluorChem™ M System (ProteinSimple, Toronto, ON) and band density was determined using a combination of internal software (for most blots) and ImageJ Software (for blots with low signal).

2.5 Cell Proliferation Assay

Cells were seeded into 96-well plates (1 x 10^4 cells per well) and allowed to adhere overnight, resulting in roughly 50% confluency at the time of treatment. Treatments were added to wells and images (4X magnification) of each well were captured every 30 minutes for 12 hours using the IncuCyte ZOOM live-cell imaging platform (Essen BioScience, Ann Arbour, MI). Using IncuCyte internal software, thresholding was performed on wells in which cells received no treatment in order to optimize the quantitation of cell confluency. The percentage change in confluency for each individual well was then calculated.

2.6 Cell Viability Assay

Cells were seeded into 12-well plates and allowed to reach 70-90% confluency. Treatments were applied and cells were then placed in hypoxic or normoxic growth conditions for 48 hours. Following treatment, cells were trypsinized and washed with PBS in preparation for flow cytometry. Cells were stained with the necrosis marker 7-AAD (Biolegend®, 420404) and the apoptosis marker phycoerythrin-conjugated Annexin-V (Biolegend®, 640908) and analyzed using the Cytomics FC500 flow cytometer (Beckman Coulter, Mississauga, ON). Heat-killed samples singly stained for each marker and doubly stained for both markers served as positive controls for compensation analysis. Cells identified as viable were those negative for both Annexin-V and 7-AAD, as compared to the gated normoxic control samples.

2.7 XTT Cytotoxicity Assay

Pre-assay optimization was performed according to manufacturer protocol (ATCC, 30-1011K) which allowed for identification of ideal seeding density and ideal reagent incubation time. In 96-well plates, 786-O, 769-P and 786-O VHL+ cells were plated at 1 x 10^4 cells/mL, whereas Caki-1 and HK-2 cells were plated at 5 x 10^4 cells/mL. Following plating, cells were allowed to adhere overnight before addition of treatment and growth under either normoxia or hypoxia. Cells were treated for 44 hours before addition of XTT Reagent to growth media for the remainder of the 48 hour incubation. Plates were read by a spectrophotometer at 660 nm, for measurement of non-specific

absorbance, and again at 475 nm for measurement of metabolic activity. Wells were also blanked against growth media without cells or drug added. Data was then normalized to the normoxic control after converting all final readings to positive values.

2.8 ATP Quantitation Assay

Cells were seeded into 24-well plates (3×10^5 cells per well) and allowed to reach 90% confluency. Treatments were applied and cells were then placed in normoxic or hypoxic growth conditions for 6 hours. Growth media was aspirated, cells were washed twice with PBS and boiling ddH_2O was used to lyse cells. Cell lysate was transferred to Eppendorf tubes and centrifuged at 4 °C and 10,000 x g for 10 minutes. The concentration of ATP in each sample was then quantified using Molecular Probes' ATP Determination Kit (Invitrogen, A22066) which employs a luciferin/luciferase bioluminescence system. Samples were quantified relative to ATP standard solutions using the luminometer function on the Synergy H4 Hybrid Multi-Mode Microplate Reader (Biotek Instruments, Winooski, VT), use of which was generously afforded by Dr. John McCormick (Western University, London, ON). Luminometer readouts were blanked and converted to ATP concentrations using the curve generated by ATP standards. ATP concentrations were normalized to protein concentrations for each sample after protein concentration was quantified using a Bradford protein assay (Bio-Rad, 500-0006) and BSA standards.

2.9 Avian Xenograft Vascularization Model

2.9.1 Lentiviral Infection

Four RCC cell lines (Caki-1, 769-P, 786-O, and 786-O VHL+) were seeded and grown to 50-60% confluency. Cells were inoculated with ZsGreen lentiviral vector containing a gene for extreme green fluorescent protein (EGFP) and a puromycin resistance gene for pooled clone selection. Two days following infection, EGFP-expressing cells were selected for using 1-2 μg/mL of puromycin, depending on the cell line. Puromycin was removed from growth medium following 2 weeks of sub-culturing.

2.9.2 Avian Chorioallantoic Membrane Xenografting

Fertilized chicken eggs were incubated at 37°C in humidified, non-sterile conditions for three days before being cracked and deposited into individual plastic trays. Embryos were placed back in the incubator and were ready for introduction of cancer cells after another six days of incubation. On day 9 post-fertilization (pf), a filter paper disc 7 mm in diameter was placed onto the CAM near large oxygenated blood vessels and subsequently ripped off to remove the upper-most layers of the CAM. Ten microliters of a 1:1 suspension of EGFP-expressing cancer cells in BD Matrigel™ were then implanted on top of this exposed area, and tumours were given two days to establish themselves within the tissue.

2.9.3 Xenograft Treatment and Processing

At 2 days post-implantation, tumours that had successfully begun recruiting blood vessels were randomly sorted into four groups. Intravascular injections of 50 µL of either: i) 20 mM HA, ii) 10 mM LC, iii) 20 mM HA + 10 mM LC or iv) PBS vehicle control were administered daily on days 11 pf through 14 pf. On day 15 pf, embryos were intravascularly injected with 75 µL of 0.5 mg/mL rhodamine-labelled *lens culinaris agglutinin* (rhodamine-LCA; Vector Laboratories, RL-1042) to fluorescently label vasculature for subsequent analysis prior to harvesting tumours from the CAM. As a control, 4 PBS-treated tumours were harvested and analyzed without rhodamine-LCA injection. Tumours were washed in PBS then fixed in 10% neutral buffered formalin containing 30% sucrose for a minimum of 1 week. Tumours were then embedded in Optimal Cutting Temperature (OCT) compound and stored at -80°C until sectioning. Using a CM30505 Cryostat (Leica, Concord, ON), ten 10 µm sections were obtained from various depths of each tumour, with the plane of sectioning running parallel to the surface of the once-surrounding CAM.

2.9.4 Quantification of Tumour Size

Fluorescence stereoscope images of tumours were obtained at 20X magnification using the AX10 Zoom V.16 stereoscope (Zeiss, Toronto, ON) before tumours were harvested

from the CAM. The cross-sectional area of stereoscope tumour images was measured using the hand trace tool in ImageJ Software.

2.9.5 Quantitation of Vascularization

Sectioning (Carl Postenka) and imaging/quantitation (Eric Sonke) of tumours were performed by separate individuals and both were performed in a blinded fashion. Sections were imaged using the Fluoview FV1200 confocal laser scanning microscope (Olympus, Toronto, ON) and the number of rhodamine-LCA positive blood vessels in each section was visually quantified.

2.10 Human Tissue Microarray Analysis

Three tissue biopsies were taken from 49 patients who underwent surgical procedures at L'Université de Montréal for the removal of renal masses. Two biopsies were from diseased tissue and the third was from surrounding healthy tissue. Acquisition and processing of formalin-fixed, paraffin-embedded samples was performed by personnel of Dr. Jean-Baptiste Lattouf (L'Université de Montréal, Montréal, QC) and samples were probed for CBS (rabbit anti-human CBS, Novus Biologicals, NBP1-33518) and CSE (rabbit anti-human CSE, ProteinTech, 12217-1-AP). Digital images of stained tissue as well as patient information were sent from the Lattouf lab to the Sener lab. Blinded scoring of antibody staining was performed by Eric Sonke using a system advised by Dr. Aaron Haig (Western University, London, ON). Using a scale of 0-3, samples were scored on the degree of both diffuse and localized expression. Correlation analysis relating protein expression to Fuhrman grade and tumour size were also performed.

2.11 Statistical Analyses

All statistical analyses were performed using GraphPad Prism v6.05 software. Figures displaying representative data of one independent experiment show standard deviation of the mean. Figures displaying data of multiple independent experiments show standard error of the mean. Results from one-way ANOVA were further subjected to Tukey's multiple comparisons test due to unequal sample sizes between groups. Results from two-way ANOVA were further subjected to Sidak's multiple comparisons test (to

optimize power), Tukey's multiple comparisons test (in cases of unequal sample sizes) and Dunnett's multiple comparisons test (when comparing to an identified control).

3. Results

3.1 Objective I – Is Endogenous Production of H_2S Enhanced in VHL-deficient ccRCC Cell Lines?

3.1.1 Levels of H_2S are increased in VHL-deficient ccRCC cell lines

To address whether baseline H_2S production is increased in VHL-deficient ccRCC, endogenous levels of H_2S were measured in two VHL-deficient ccRCC cell lines (786-O and 769-P) and compared to a VHL WT ccRCC cell line (Caki-1) and a nonmalignant renal cell line (HK-2). Accumulation of intracellular H_2S was tracked over 15 hours using a fluorescent H_2S-specific probe in combination with live-cell imaging (Figure 3). It was found that significant accumulation of H_2S occurred in HK-2 cells ($p < 0.001$), 786-O cells ($p < 0.0001$) and 769-P cells ($p < 0.0001$) over 15 hours, though not in Caki-1 cells ($p > 0.05$; Figure 3A). When compared to HK-2 cells, the accumulation of H_2S in 786-O and 769-P cells after 15 hours was significantly greater ($p < 0.0001$), while the accumulation of H_2S in Caki-1 cells was significantly lower ($p < 0.05$) (Figure 3A, 1B). Accumulation of H_2S in the VHL-deficient ccRCC cell lines after 15 hours was also significantly greater ($p < 0.0001$) than in the VHL WT Caki-1 cells (Figure 3A).

In an attempt to implicate VHL deficiency in the accumulation of H_2S, a functional allele of VHL was reintroduced into 786-O cells to partially restore its function. Endogenous levels of H_2S were then measured using the methylene blue assay and compared to unmolested 786-O cells, HK-2 cells and heat-killed control cells (Figure 4). Re-introduction of VHL into 786-O cells was unable to bring levels of H_2S back down to baseline (Figure 4). Detectable levels of H_2S were observed in heat-killed cells, which highlights the non-specificity of this assay.

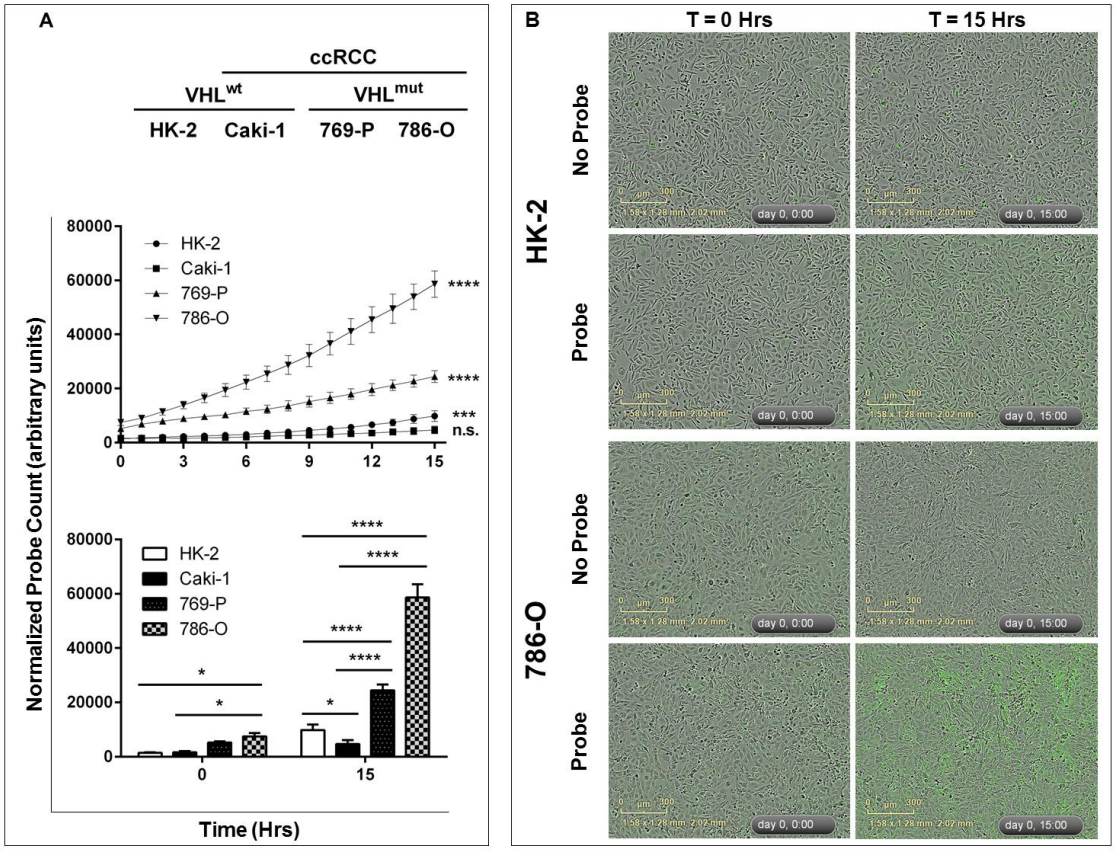

Figure 3. Baseline endogenous H_2S production is greater in VHL-deficient ccRCC cell lines than in VHL WT malignant and non-malignant renal cell lines. Cells were seeded into 96-well plates and allowed to reach 90-100% confluency. A cell-permeable probe that reacts specifically with H_2S to fluoresce green was then either added (probe), or not added (no probe), to growth media and cells were imaged every hour for 15 hours. Following imaging, the number of fluorescent "hits" was normalized to cell confluency for each well and each time point, resulting in a normalized probe count which was then averaged (n = 3, error bars represent standard deviation of the mean). Results are representative of 3 independent experiments (n = 9 total). One-way ANOVA with Tukey's multiple comparisons test was used to asses statistically significant differences between groups (* $p < 0.05$; ** $p < 0.01$; *** $p < 0.001$; **** $p < 0.0001$). **(A)** (i) VHL mutation status of nonmalignant renal cells (HK-2) and ccRCC cell lines (Caki-1, 769-P, 786-O). Statistically significant changes in endogenous H_2S production over time (between 0 hours and 15 hours) in each cell line. Statistically significant differences in endogenous H_2S production between cell lines. **(B)** Representative images of enhanced endogenous H_2S production in 786-O cells as compared to HK-2 cells.

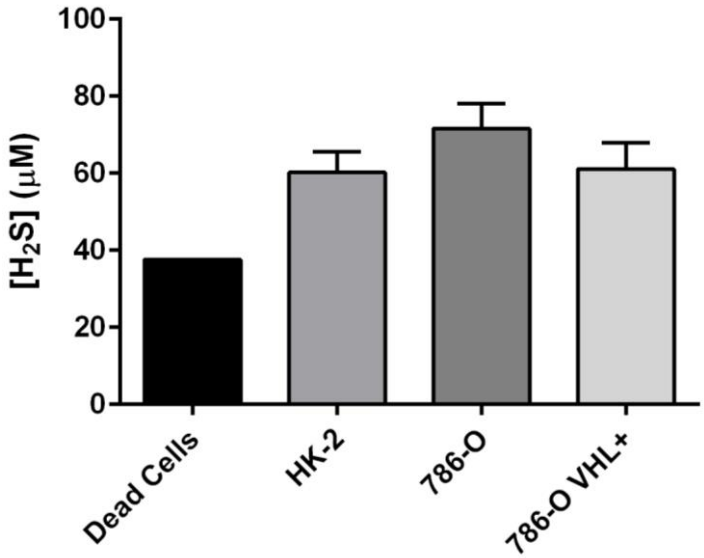

Figure 4. Effect of VHL knock-in on endogenous H_2S production in 786-O cells, as measured by methylene blue assay. The methylene blue assay was used to compare endogenous H_2S production in heat-killed cells (dead cells), non-malignant renal cells (HK-2), VHL-deficient ccRCC cells (786-O), and 786-O cells with VHL knocked-in through lentiviral transfection. One-way ANOVA with Tukey's multiple comparisons test revealed a lack of statistically significant differences between groups; n = 4 per cell line (n = 1 for dead cells).

3.1.2 VHL-deficient ccRCC cell lines do not display increased expression of CBS, CSE, or MPST

It was hypothesized that VHL inactivation leads to increased expression of the H_2S-producing enzymes CBS, CSE and/or MPST, which in turn leads to increased cellular levels of H_2S. To answer this question, western blot analysis of CBS, CSE and MPST was performed to determine baseline expression of these enzymes in HK-2, Caki-1, 786-O and 769-P cell lines (Figure 5). There were no significant differences in baseline normoxic expression of CBS, CSE, nor MPST (Figure 5). There was no clear trend to suggest that VHL inactivation leads to aberrant upregulation of endogenous H_2S-producing enzymes.

To determine whether expression of CBS, CSE and/or MPST is regulated by hypoxia through mechanisms not involving VHL/HIF-1/2α, the same cell lines were grown in hypoxia for 6, 12 and 24 hours and protein extracted for further western blot analysis (Figure 6). When compared to normoxic controls, expression of CBS, CSE, and MPST did not significantly increase under hypoxia in any of the cell lines (Figure 6).

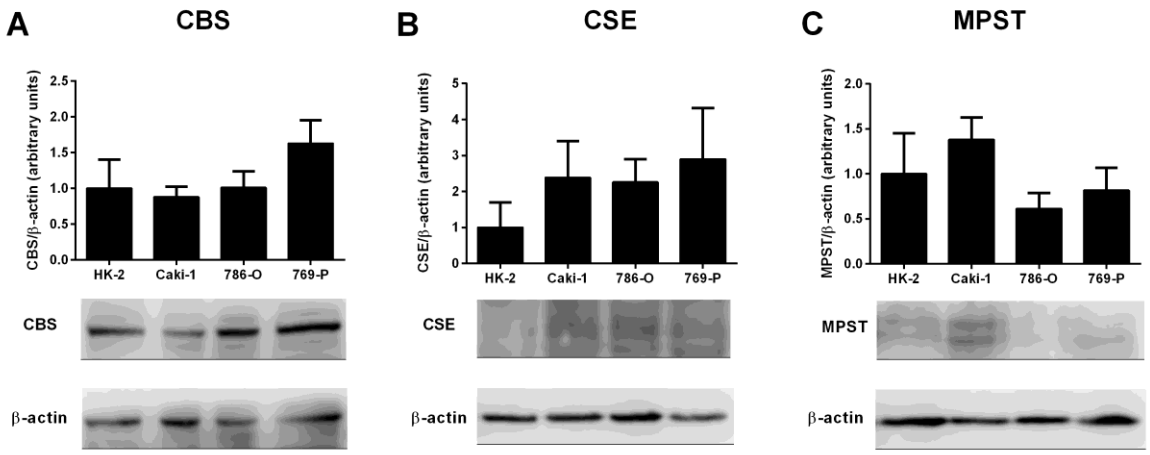

Figure 5. Baseline normoxic expression of H_2S-producing enzymes is unaltered in VHL-deficient ccRCC cell lines when compared to malignant and non-malignant VHL WT renal cell lines. Protein was isolated from 80-90% confluent cell cultures grown in normoxia (21% O_2) using RIPA buffer. SDS-PAGE was carried out on 40-50 μg of whole cell lysate using 10-12% poly-acrylamide gels and western blots were performed using PVDF membranes. Blots were probed for **(A)** CBS (63 kDa), **(B)** CSE (45 kDa) and **(C)** MPST (33 kDa) while β-actin (43 kDa) served as a loading control against which protein expression was normalized. Expression of CBS, CSE and MPST in renal cancer cell lines (Caki-1, 786-O, 769-P) was normalized to expression of these same enzymes in the non-malignant renal epithelial cell line HK-2. Error bars represent standard error of the mean (SEM), n = 3. Blots shown are representative of all three blots. One-way ANOVA and Tukey's multiple comparisons test revealed no statistically significant differences in CBS, CSE nor MPST expression between cell lines.

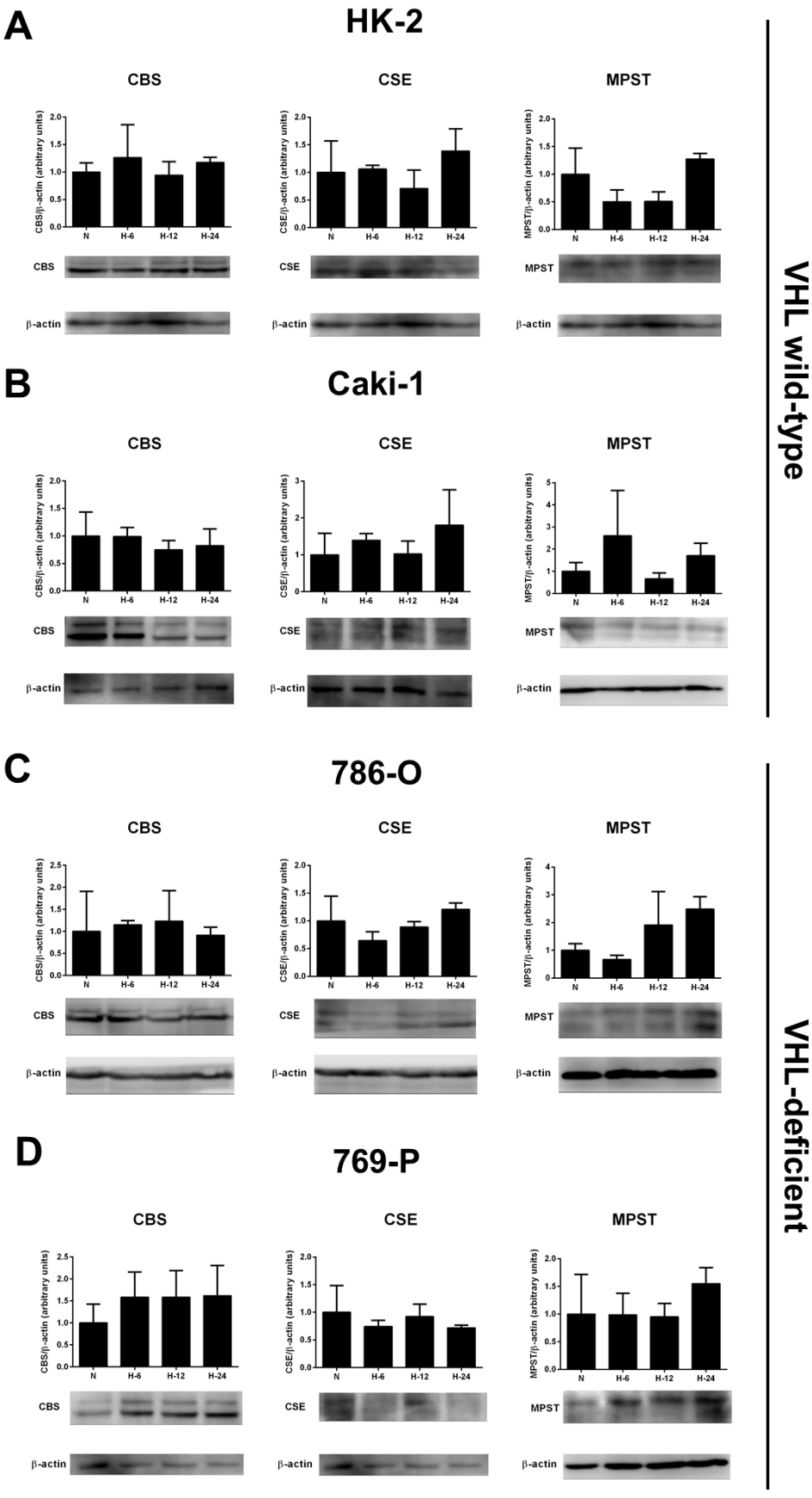
A
HK-2
CBS
CSE
MPST
CBS/β-actin (arbitrary units)
CSE/β-actin (arbitrary units)
MPST/β-actin (arbitrary units)
N
H-6
H-12
H-24
CBS
CSE
MPST
β-actin
B
Caki-1
C
786-O
D
769-P
VHL wild-type
VHL-deficient

Figure 6. Hypoxic induction of H_2S-producing enzymes in malignant, and non-malignant renal cell lines. Protein was isolated from 80-90% confluent cell cultures grown in normoxia (N; 21% O_2) or hypoxia (1% O_2) for 6, 12 or 24 hours (H-6, H-12, H-24) using RIPA buffer. SDS-PAGE was carried out on 40-50 μg of whole cell lysate using 10-12% poly-acrylamide gels and western blots were performed using PVDF membranes. Hypoxic induction of CBS (63 kDa), MPST (33 kDa) and CSE (45 kDa) was evaluated in **(A)** HK-2, **(B)** Caki-1, **(C)** 786-O and **(D)** 769-P cell lines. β-actin (43 kDa) served as a loading control against which protein expression was normalized. Error bars represent standard error of the mean (SEM), n = 3. Blots shown are representative of all three blots. One-way ANOVA and Tukey's multiple comparisons test revealed a lack of statistically significant differences in CBS, CSE and MPST expression between treatments in all cell lines.

To more thoroughly investigate the relationship between VHL function and hypoxic induction of CBS, CSE and MPST, western blot analysis comparing expression of CBS, CSE and MPST in 786-O and 786-O VHL+ cells under normoxia and hypoxia was performed (Figure 7). When VHL function was restored to 786-O cells, expression of CBS, CSE and MPST did not change (Figure 7). Interestingly, the hypoxic expression profile of CSE (ratio of high molecular weight band to low molecular weight band) was significantly altered following knock-in of VHL into 786-O cells (Figure 7B). Successful knock-in of functional VHL (VHL^{wt}) was also confirmed via western blot analysis (Figure 7C).

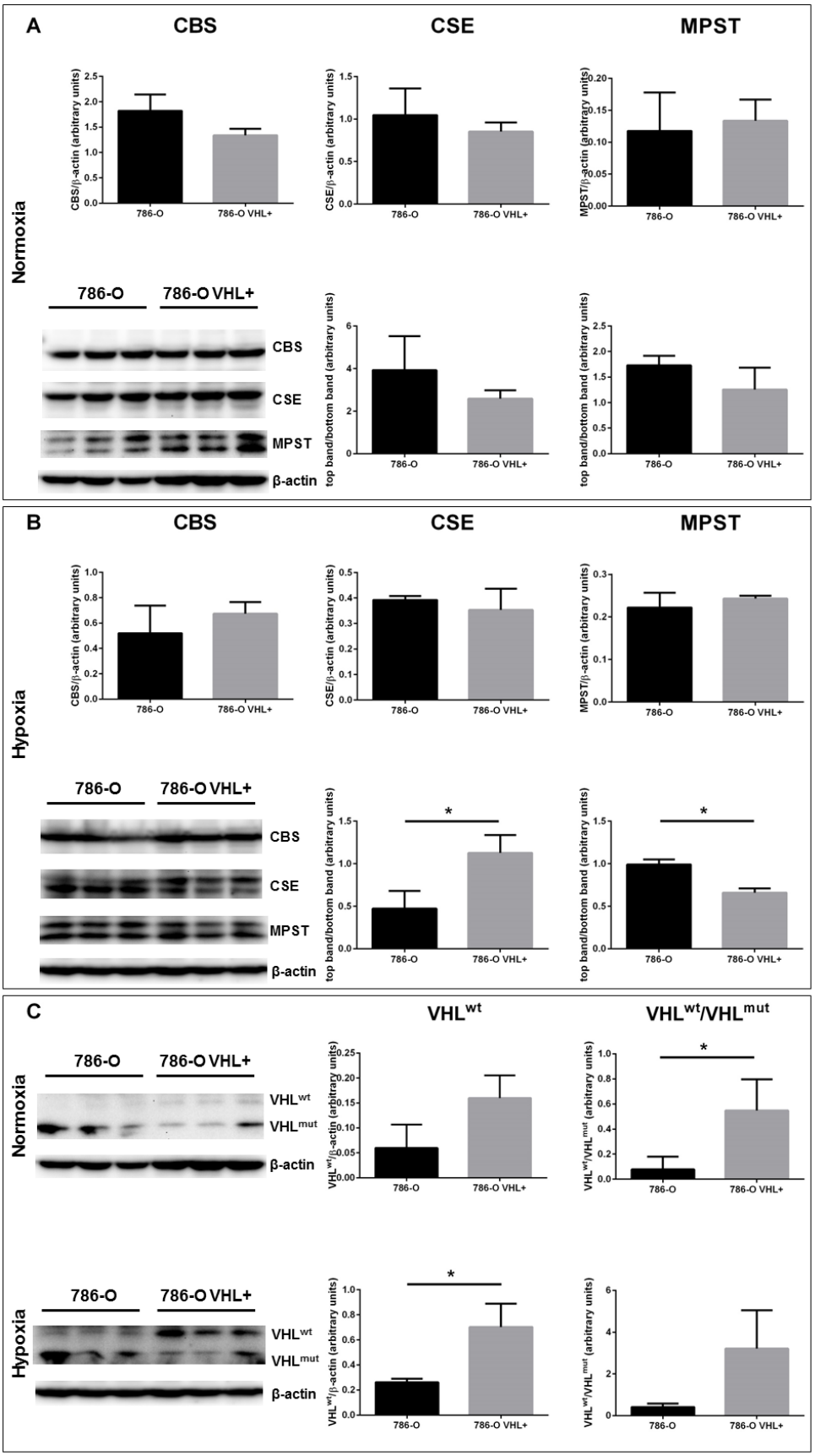
A
CBS
CSE
MPST
Normoxia
CBS/β-actin (arbitrary units)
CSE/β-actin (arbitrary units)
MPST/β-actin (arbitrary units)
786-O
786-O VHL+
top band/bottom band (arbitrary units)
CBS
CSE
MPST
β-actin
B
Hypoxia
*
C
VHLwt
VHLwt/VHLmut
VHLwt/β-actin (arbitrary units)
VHLwt/VHLmut (arbitrary units)
VHLmut

Figure 7. Normoxic expression and hypoxic induction of H_2S-producing enzymes in wild-type 786-O cells (786-O) and VHL knock-in 786-O cells (786-O VHL+). Protein was isolated from 80-90% confluent cell cultures grown in normoxia (21% O_2) or hypoxia (1% O_2) for 15 hours using RIPA buffer. SDS-PAGE was carried out on 40-50 μg of whole cell lysate using 10-12% poly-acrylamide gels and western blots were performed using PVDF membranes. Normoxic expression **(A)** or hypoxic induction **(B)** of CBS (63 kDa), MPST (33 kDa) and CSE (45 kDa) was evaluated in 786-O and 786-O VHL+ cell lines. Validation of VHL^{wt} (20 kDa) knock-in was performed under both normoxia and hypoxia **(C)**. Protein levels were expressed relative to β-actin (43 kDa), or as a ratio of top band: bottom band (CSE, MPST) or as a ratio of functional protein:non-functional protein (VHL) in instances where doublet bands are presented. Error bars represent standard error of the mean (SEM), n = 3. One-way ANOVA and Tukey's multiple comparisons test indicate statistically significant differences ($p < 0.05$) where indicated (*).

3.2 Objective II – Does Endogenous H_2S Production Contribute to the Proliferation, Metabolism and Survival of ccRCC Cell Lines?

3.2.1 Endogenous H_2S production can be targeted, though not stimulated, in VHL-deficient ccRCC cell lines

The dual CBS/CSE inhibitor HA, the CSE inhibitor PAG and the substrate for endogenous H_2S production LC were administered to HK-2, Caki-1, 786-O and 769-P cell lines to determine if they could influence baseline H_2S production (Figure 8). Using the fluorescent H_2S-specific probe it was found that accumulation of H_2S in HK-2 cells significantly ($p < 0.0001$) increased over time when LC (blue) was added to growth media (Figure 8A) and that this increase in H_2S was significantly greater than the increase observed in untreated cells (Figure 8B). LC was able to evoke a similar response in VHL WT Caki-1 cells (Figure 8A, B). However, in the VHL-deficient ccRCC cell lines, treatment with LC did not increase endogenous H_2S production to the same degree, as a result of increased baseline levels (Figure 8A, B).

As a result of their elevated baseline production of H_2S, VHL-deficient ccRCC cell lines were much more susceptible to inhibition with HA when compared to non-malignant HK-2 cells and VHL WT Caki-1 cells (Figure 8, red). There was no significant accumulation of H_2S in HK-2 cells over 15 hours when cultured in the presence of HA (Figure 8A) and levels of H_2S in HA-treated cells were significantly ($p < 0.05$) lower than in untreated cells (Figure 8B). The reductions in H_2S upon HA treatment were also significant in 769-P cells ($p < 0.0001$; Figure 8B) and 786-O cells ($p < 0.0001$; Figure 8Biv). Treatment of all cell lines with a combination of HA and LC could significantly increase production of H_2S when compared to treatment with HA alone (Figure 8, green). Treatment with the CSE inhibitor PAG did not significantly decrease endogenous H_2S production (data not shown).

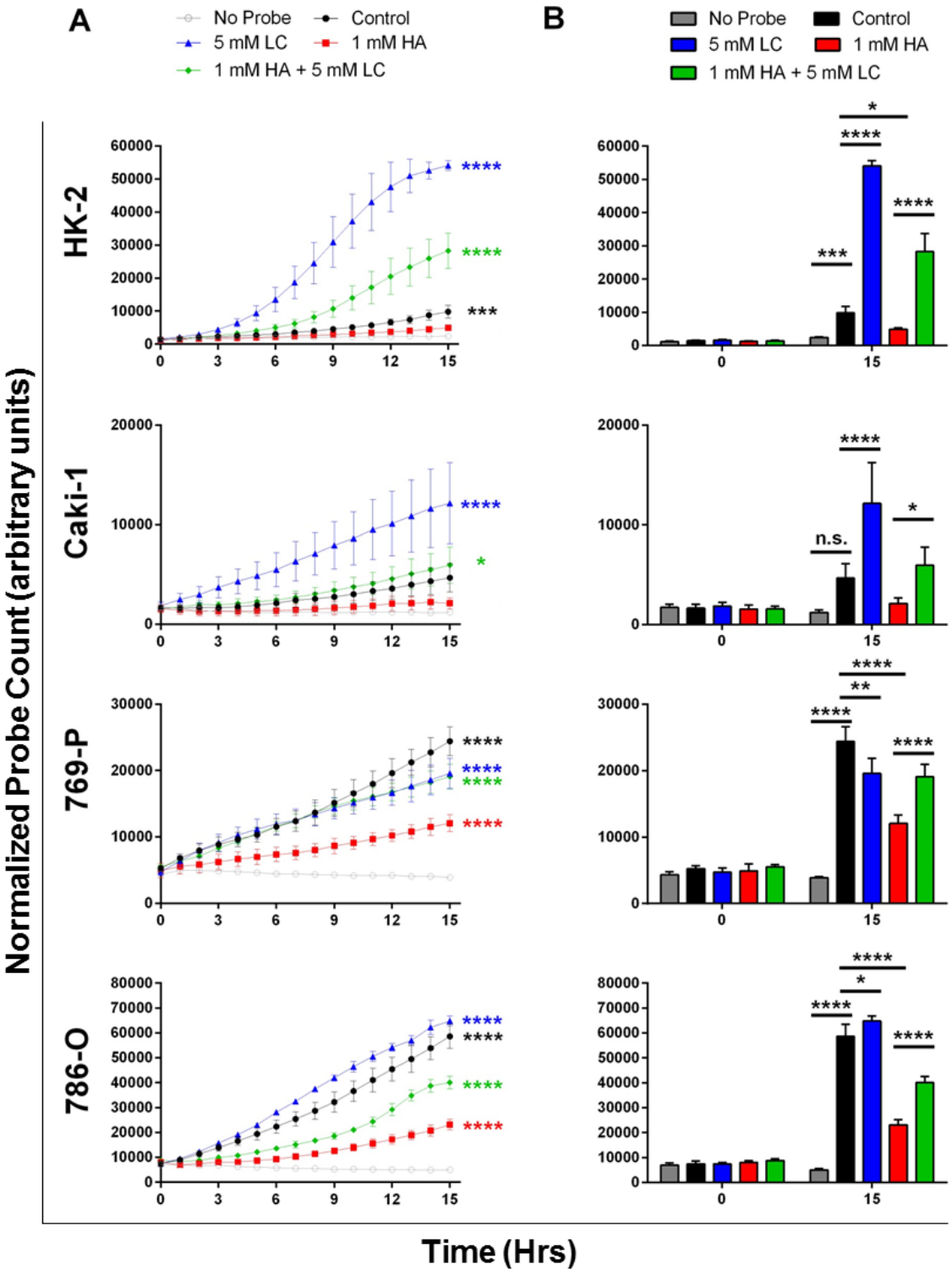
A
No Probe
Control
5 mM LC
1 mM HA
1 mM HA + 5 mM LC
B
No Probe
Control
5 mM LC
1 mM HA
1 mM HA + 5 mM LC
HK-2
Caki-1
769-P
786-O
Normalized Probe Count (arbitrary units)
Time (Hrs)
n.s.

Figure 8. Inhibition of endogenous H_2S production reduces elevated levels of H_2S in VHL-deficient ccRCC cell lines. Cells were seeded into 96-well plates and allowed to reach 90-100% confluency. A cell-permeable probe that reacts specifically with H_2S to fluoresce green was then added (or not added; ie. no probe), to growth media. At the same time, cells were treated with either PBS vehicle (control; black) an inhibitor of endogenous H_2S synthesis (hydroxylamine (HA); 1 mM; red), the substrate for endogenous H_2S synthesis (L-cysteine (LC); 5 mM; blue) or a combination of the two (1 mM HA + 5 mM LC; green). Cells were imaged every hour for 15 hours and background fluorescence was compensated for using thresholding. Following compensation, the number of fluorescent "hits" was normalized to cell confluency for each well and each time point, resulting in a normalized probe count which was then averaged (n = 3, error bars represent standard deviation of the mean). Results are representative of 3 independent experiments (n = 9 total). One-way ANOVA with Tukey's multiple comparisons test was used to asses statistically significant differences between groups (* $p < 0.05$; ** $p < 0.01$; *** $p < 0.001$; **** $p < 0.0001$). **(A)** Statistically significant changes in endogenous H_2S production over time (between 0 hours and 15 hours) were determined for each treatment in HK-2, Caki-1, 769-P and 786-O cells. **(B)** Statistically significant differences in endogenous H_2S production between treatments were determined in each cell line.

3.2.2 Endogenous H_2S production contributes to the proliferation of ccRCC cell lines

Cells were treated with HA and cell confluency was tracked over 15 hours using live-cell imaging to determine whether endogenous H_2S production plays a role in mediating cell growth (Figure 9). HA treatment did not significantly restrict the growth of HK-2 cells (Figure 9). Significant ($p < 0.05$) restriction of cell growth was observed in Caki-1 cells, 769-P cells and 786-O cells, though not in 786-O VHL+ cells (Figure 9). While higher concentrations of HA (1 mM) were cytotoxic to ccRCC cell lines, lower concentrations of HA (0.1 mM) actually slightly stimulated cell growth (data not shown). As such, there is a narrow range in which inhibition of endogenous H_2S production can restrict cell growth. There was no clear relationship between VHL inactivation, and reliance on H_2S for cell growth (Figure 9).

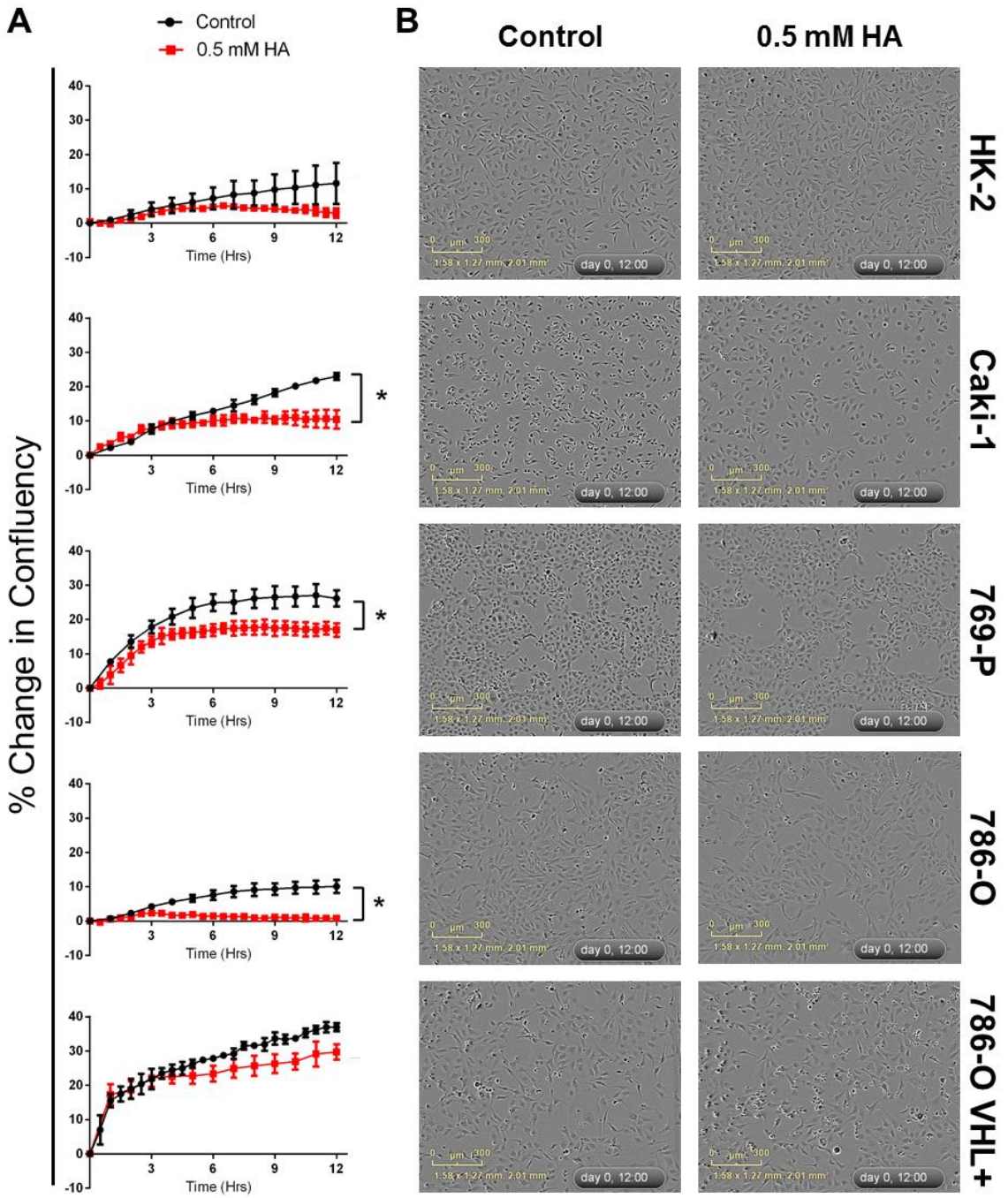
A
Control
0.5 mM HA
% Change in Confluency
Time (Hrs)
*
B
Control
0.5 mM HA
HK-2
Caki-1
769-P
786-O
786-O VHL+
day 0, 12:00

Figure 9. Inhibition of endogenous H_2S production attenuates proliferation of ccRCC cell lines. Cells were seeded into 96-well plates and allowed to reach 40-60% confluency. Cells were treated with either PBS vehicle (control; black) or an inhibitor of endogenous H_2S synthesis (hydroxylamine (HA); 0.5 mM; red). Cells were imaged every hour for 12 hours and phase confluency was measured. **(A)** Following imaging, percentage change in cell confluency was determined for each well and averaged for each time point (n = 3, error bars represent standard deviation of the mean). Results are representative of 2 independent experiments (n = 6 total). Multiple t-tests were used to asses statistically significant differences between groups at T = 12 hours (* $p < 0.05$). **(B)** Representative images depicting inhibition of cell proliferation following 12 hour treatment with HA.

3.2.3 Endogenous H_2S production contributes to the survival of ccRCC cell lines

Cells were treated with HA and PAG to determine whether loss of endogenous H_2S production impacts 48 hour cell survival under normoxic and hypoxic conditions, as determined by Annexin-V-PE and 7-AAD detection (Figure 10). Under normoxic conditions all ccRCC cell lines were found to be significantly ($p < 0.05$) more susceptible to treatment with HA than HK-2 cells (Figure 10A,C). Caki-1 and 786-O cell lines were also significantly ($p < 0.05$) more susceptible to treatment with HA than HK-2 cells under hypoxic conditions, however 769-P cells were not (Figure 10A). The reduction in hypoxic viability of HK-2 cells was significantly ($p < 0.05$) greater than the reduction in normoxic viability (Figure 10B), while the opposite was true of the ccRCC cell lines (Figure 10D). Inhibition of CSE alone, through use of the inhibitor PAG, proved to be less effective in reducing viability than inhibition of CBS and CSE through use of the inhibitor HA (Figure 10D). The only cell line to display significant declines in viability following PAG treatment was the ccRCC cell line 769-P (Figure 10D).

When treated with a combination of HA and LC, the VHL-deficient ccRCC cell lines 769-P and 786-O displayed significant ($p < 0.05$) restoration of viability when compared to treatment with HA alone (Figure 10E). The same could not be said of the VHL WT Caki-1 cell line.

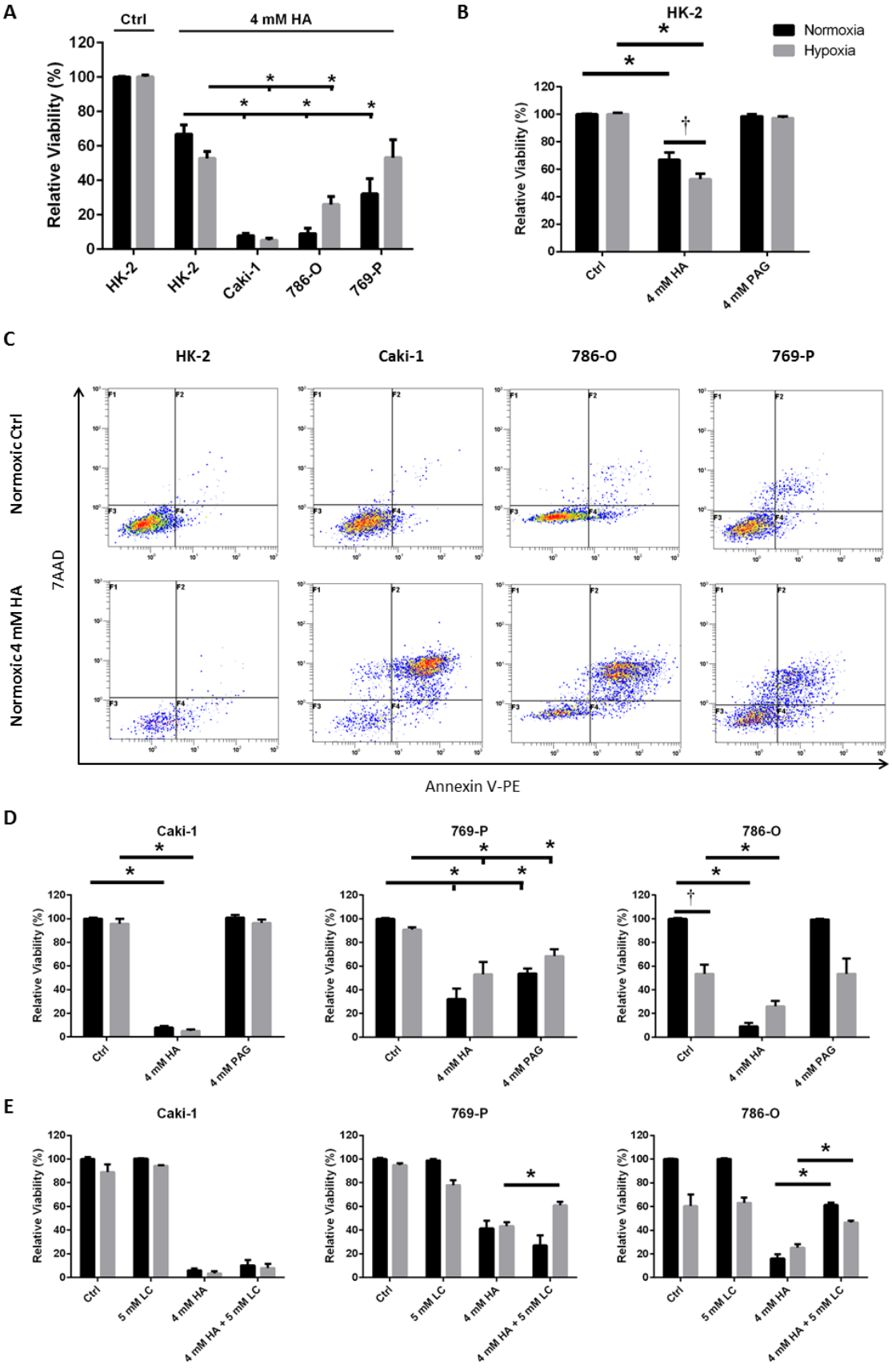
A
Ctrl
4 mM HA
Relative Viability (%)
HK-2
HK-2
Caki-1
786-O
769-P
B
HK-2
Normoxia
Hypoxia
Relative Viability (%)
Ctrl
4 mM HA
4 mM PAG
C
HK-2
Caki-1
786-O
769-P
Normoxic Ctrl
Normoxic 4 mM HA
7AAD
Annexin V-PE
D
Caki-1
769-P
786-O
Relative Viability (%)
Ctrl
4 mM HA
4 mM PAG
E
Caki-1
769-P
786-O
Relative Viability (%)
Ctrl
5 mM LC
4 mM HA
4 mM HA + 5 mM LC

Figure 10. Inhibition of endogenous H_2S production selectively kills ccRCC cells over non-malignant renal cells. Cells were treated for 48 hours with inhibitors of endogenous H_2S production hydroxylamine (HA) and propargyl glycine (PAG) and/or the substrate for endogenous H_2S production L-cysteine (LC) in normoxic (21% O_2) or hypoxic (1% O_2) growth conditions. Cell culture viability was determined via detection of Annexin-V-PE and 7AAD using flow cytometry and quantified relative to the untreated, normoxic cells within each experimental trial. Error bars represent standard error of the mean (SEM). Two-way ANOVA with Dunnett's multiple comparisons test was used to asses significant differences between groups (i.e. normoxic control vs. hypoxia control; †; $p < 0.05$). Two-way ANOVA with Sidak's multiple comparisons test was used to assess significant differences between treatments within groups (i.e. normoxic control vs. normoxic 4 mM HA; *; $p < 0.05$). **(A)** ccRCC cell lines are more susceptible to treatment with HA than non-malignant HK-2 cells, n = 6-9. **(B)** HK-2 cells are susceptible to treatment with HA, however hypoxic viability is impacted more-so than normoxic viability, n = 6. **(C)** Representative flow cytometry dot plots illustrating changes in normoxic viability of cell lines following treatment with 4 mM HA, as quantified in (A). **(D)** Differential susceptibility of ccRCC cell lines to treatment with HA and PAG (Caki-1, n = 6-8; 769-P, n = 6-12; 786-O, n = 6-10). **(E)** VHL-deficient ccRCC cell lines treated with HA and LC simultaneously display attenuated declines in viability (Caki-1, n = 3-6; 769-P, n = 3-8; 786-O, n = 4-6).

3.2.4 Endogenous H_2S production contributes to the metabolism of ccRCC cell lines

To determine if declines in viability upon inhibition of endogenous H_2S production were the result of deficits in metabolic activity, the XTT cytotoxicity assay was used to measure alterations in metabolic activity after 48 hour treatment (Figure 11). It was observed that the VHL-deficient cell lines 786-O and 769-P suffered significant declines in metabolic activity upon treatment with HA ($p < 0.05$) while the VHL wild-type cell lines HK-2, Caki-1 and 786-O VHL+ did not (Figure 11). As with the viability assays, combination treatment with HA and LC resulted in significant ($p < 0.05$) restoration of hypoxic metabolic activity compared to HA treatment alone in the VHL-deficient ccRCC cell lines 786-O and 769-P (Figure 11). Combination treatment with HA and LC also resulted in significant ($p < 0.05$) differences between normoxic and hypoxic viability in all ccRCC cell lines, but not HK-2 cells (Figure 11).

The XTT assay measures mitochondrial metabolism based on the activation of coenzyme Q by NADH and other electron donors. In order to quantitate how H_2S production may be contributing to forms of metabolism that do not rely on electron transport, total ATP was measured following 6 hour treatments administered under normoxia and hypoxia (Figure 12). Unexpectedly, hypoxic ATP production was significantly ($p < 0.05$) higher than normoxic ATP production for HK-2 cells (Figure 12). Inhibition with HA significantly ($p < 0.05$) decreased normoxic and hypoxic ATP production in all HK-2 cells, 786-O cells and 786-O VHL+ cells (Figure 12). Combined treatment with HA and LC could not restore ATP production in any of the cell lines, contrary to results of the XTT assay (Figure 12).

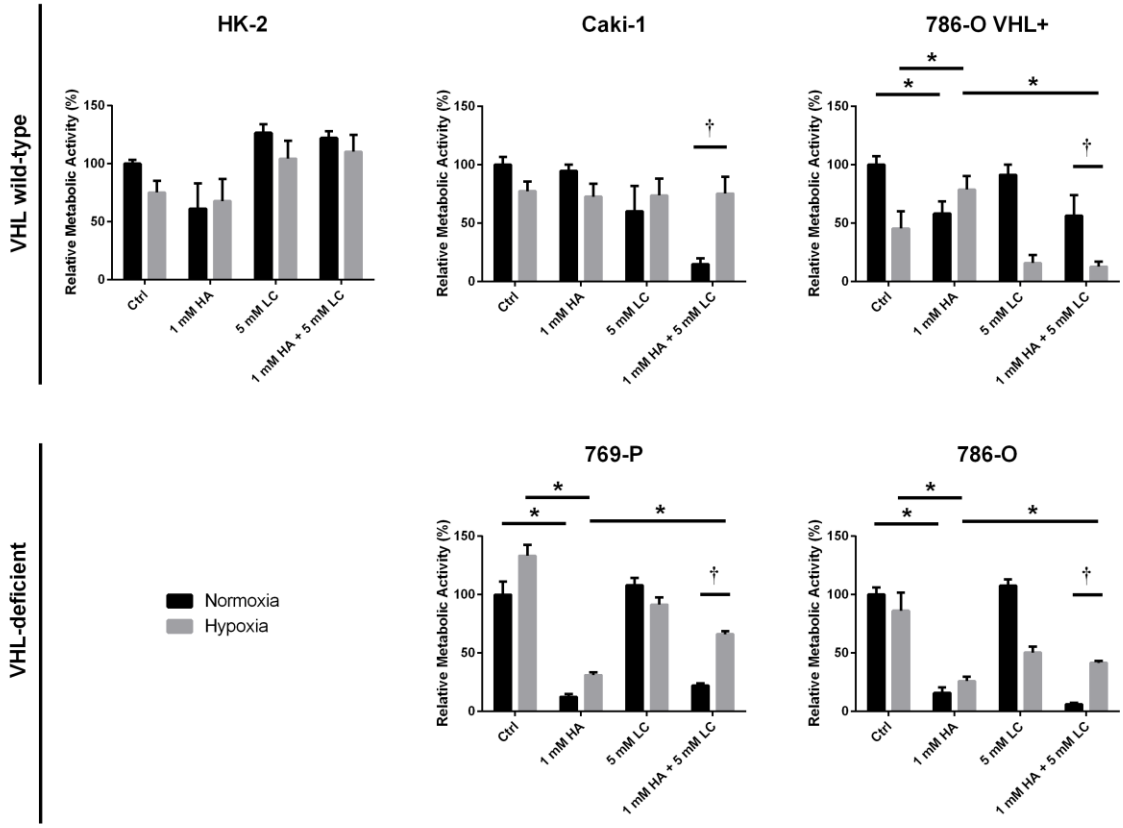

Figure 11. Inhibition of endogenous H_2S production reduces overall metabolic activity of ccRCC cell lines. Metabolic activity was assessed via the XTT assay following 48 hour treatment with hydroxylamine (HA), L-cysteine (LC) or a combination of both. Values are presented as relative to the untreated, normoxic cells within each experimental trial. Error bars represent standard error of the mean (SEM). HK-2 (n = 6), Caki-1 (n = 6), 786-O VHL+ (n = 6), 769-P (n = 5-6), 786-O (n = 5-6). Two-way ANOVA with Dunnett's multiple comparisons test was used to asses significant differences between groups (normoxic control vs. hypoxia control; †; $p < 0.05$). Two-way ANOVA with Sidak's multiple comparisons test was used to assess significant differences between treatments within groups (normoxic control vs. normoxic 4 mM HA; *; $p < 0.05$).

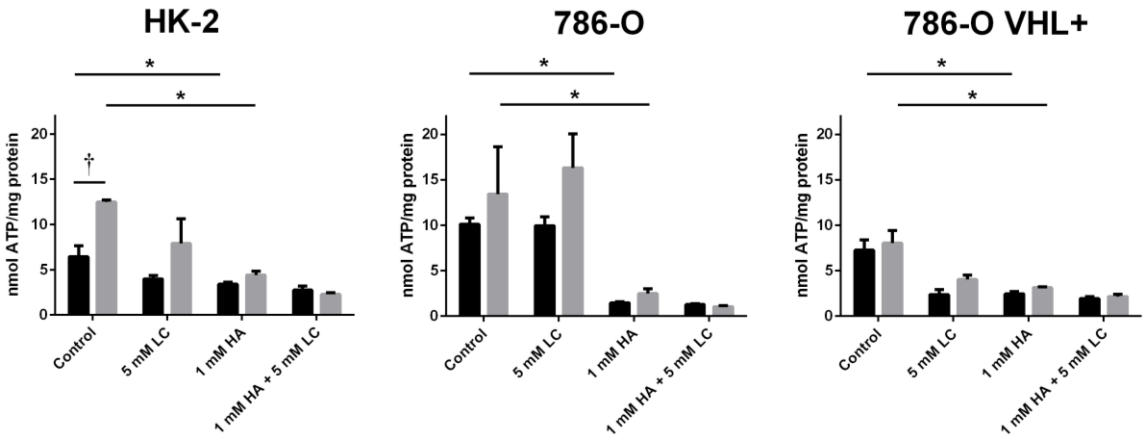

Figure 12. Inhibition of endogenous H_2S production reduces ATP production in malignant and non-malignant renal cell lines. Total cellular ATP was assessed using a luciferin/luciferase-based assay following 6 hour treatment with hydroxylamine (HA), L-cysteine (LC) or a combination of both. ATP concentration was normalized in each sample using protein concentration and then averaged (n = 3, error bars represent standard deviation of the mean). Results are representative of 2 independent experiments (n = 6 total). Two-way ANOVA with Dunnett's multiple comparisons test was used to asses significant differences between groups (normoxic control vs. hypoxia control; †; $p < 0.05$). Two-way ANOVA with Sidak's multiple comparisons test was used to assess significant differences between treatments within groups (normoxic control vs. normoxic 4 mM HA; *; $p < 0.05$).

3.3 Objective III – Does Endogenous H_2S Production Contribute to the Neovascularization of ccRCC Xenografts?

3.3.1 Inhibition of endogenous H_2S production restricts the neovascularization of ccRCC xenografts

H_2S is known to participate in paracrine angiogenic signalling and has been shown to play a role in the vascularization of other cancers. To investigate the effects of endogenous H_2S production on the vascularization of ccRCC tumours, the chick chorioallantoic membrane (CAM) was used as a vascular structure for xenograft implantation of ccRCC cell lines. Cell lines were manipulated to express EGFP and chick vasculature was labelled with rhodamine-labelled *lens culinaris agglutinin* (rhodamine-LCA) such that the number of intratumoural blood vessels could be quantified using fluorescent microscopy. Treatments were injected IV for four consecutive days following two days of initial tumour growth and then harvested, sectioned and imaged (Figure 13).

Treatment with HA was able to significantly ($p < 0.05$) decrease the vascularization of the VHL-deficient 786-O and 769-P xenografts while the same treatment had no effect on the vascularization of VHL wild-type Caki-1 xenografts (Figure 13). Treatment with LC was able to significantly ($p < 0.05$) increase the number of intratumoural blood vessels (Figure 13A) and also appeared to dilate blood vessels (Figure 13B). When 786-O and 769-P xenografts were treated with a combination of HA and LC simultaneously, the decline in vascularization observed with HA treatment alone was attenuated (Figure 13). Knock-in of VHL into the 786-O cell line not only decreased overall vascularization of untreated xenografts, but also appeared to eliminate the cells' sensitivity to HA and LC treatment (Figure 13).

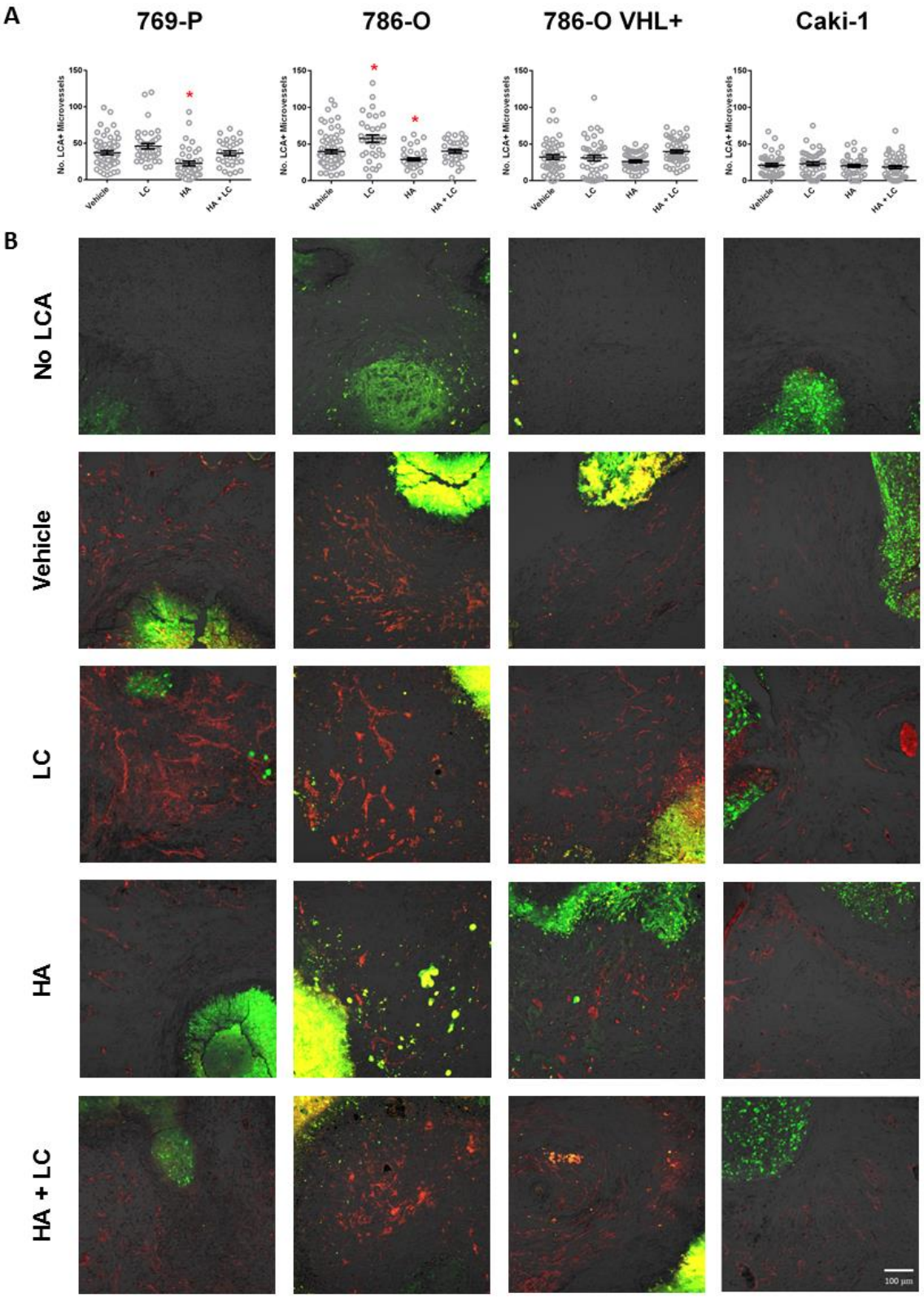
A
769-P
786-O
786-O VHL+
Caki-1
No. LCA+ Microvessels
Vehicle
LC
HA
HA + LC
B
No LCA
Vehicle
LC
HA
HA + LC
100 µm

Figure 13. Systemic inhibition of endogenous H_2S production with hydroxylamine (HA) reduces the vascularization of VHL-deficient ccRCC xenografts. ccRCC cell lines were xenografted into the CAM of 9-day old chicken embryos and given 2 days to establish themselves within the surrounding tissue. Embryos were then systemically treated once a day for 4 days with 50 μL of 20 mM hydroxylamine (HA), 10 mM L-cysteine (LC) or a combination of both (HA + LC) through intravascular microinjection. Prior to harvest, embryos were systemically injected with rhodamine-conjugated *lens culinaris agglutinin* (rhodamine-LCA) to label all chick vasculature. **(A)** The number of rhodamine-LCA-positive blood vessels present in each field of view shot was counted manually following confocal imaging at 200X total magnification. Error bars represent standard error of the mean ($n \geq 30$ per treatment). One-way ANOVA with Dunnet's multiple comparisons test was used to assess statistical significance of treatments compared to PBS vehicle control (*; $p < 0.05$). **(B)** Representative images of data depicted in (A). Rhodamine-LCA-positive blood vessels (red) are seen in close proximity to EGFP-expressing RCC cells (green). Scale bar represents 100 μm.

3.3.2 Inhibition of endogenous H_2S production restricts the growth of ccRCC xenografts

Similar trends were observed when analyzing the effect of H_2S production on tumour growth as measured by cross-sectional area of whole tumours prior to harvest (Figure 14). HA treatment was able to significantly ($p < 0.05$) decrease the size of 769-P xenografts, but not the size of 786-O xenografts (Figure 14). Conversely, HA treatment had no effect on the cross-sectional area of VHL WT Caki-1 and 786-O VHL+ xenografts (Figure 14). As with vascularization, treatment with HA and LC simultaneously was able to attenuate the decrease in size in 786-O and 769-P xenografts (Figure 14). Qualitative inspection of tumours revealed that HA treatment also resulted in necrotic and dysmorphic tumours (Figure 14B).

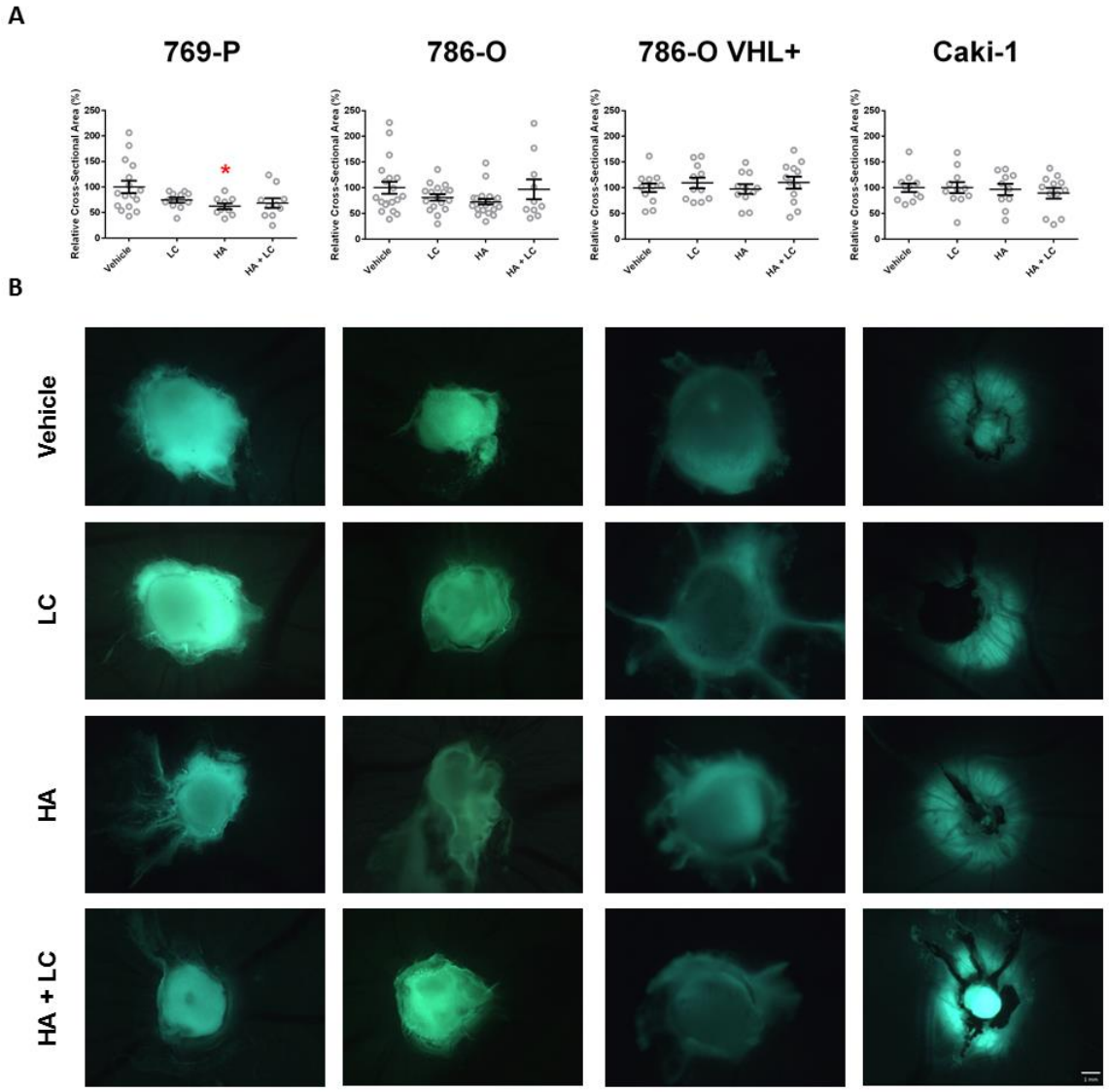

Figure 14. Systemic inhibition of endogenous H_2S production with hydroxylamine (HA) restricts the growth of VHL-deficient ccRCC xenografts. ccRCC cell lines were xenografted into the CAM of 9-day old chicken embryos and given 2 days to establish themselves within the surrounding tissue. Embryos were then systemically treated once a day for 4 days with 50 µL of 20 mM hydroxylamine (HA), 10 mM L-cysteine (LC) or a combination of both (HA + LC) through intravascular microinjection. Prior to harvest, fluorescent stereoscope images were obtained for each tumour. **(A)** The cross-sectional area of stereoscope images (20X) of each tumour was measured using ImageJ software. Error bars represent standard error of the mean ($n \geq 10$ per treatment). One-way ANOVA with Dunnet's multiple comparisons test was used to asses statistical significance of treatments compared to PBS vehicle control (*; $p < 0.05$). **(B)** Representative images of data depicted in (A). zsGreen expression (green) was used to identify RCC cells. Scale bar represents 1 mm.

3.4 Objective IV – Is Endogenous H_2S Production Enhanced in Human ccRCC Tumours?

3.4.1 Expression of CBS or CSE is not upregulated in human ccRCC tumours

In an attempt to link increased endogenous H_2S production to the progression of actual ccRCC tumours, patient-matched renal biopsies of healthy and diseased tissue were probed for CBS and CSE. Antibody staining was scored on a scale of 0-3 for intensity of localized (punctate dots) and diffuse (hazy, non-specific) expression. When all tumours were analyzed together – without being sub-classified as benign, malignant, non-ccRCC or ccRCC – diseased tissue had significantly ($p < 0.0001$) lower diffuse expression of both CBS and CSE, whereas localized expression was maintained (Figure 15A). The same trend applied when tumour classes of benign (Figure 15B), malignant (Figure 15C) and ccRCC (Figure 15D, E) were analyzed individually.

3.4.2 Expression of CBS or CSE is not correlated with Fuhrman grade or tumour size

To determine whether expression of CBS and CSE were in some way correlated with prognostic factors of ccRCC, correlation analyses were performed for staining intensity/Fuhrman grade, as well as staining intensity/tumour size. When localized expression of CBS and CSE was plotted against Fuhrman grade, no significant correlation was apparent (CBS: $r = -0.044$; CSE: $r = 0.272$). Diffuse expression of CBS and CSE was also not correlated with Fuhrman grade (CBS: $r = 0.085$; CSE $r = -0.043$). There was also no correlation between tumour volume and diffuse/localized expression of CBS (diffuse: $r = -0.153$; localized: $r = -0.135$) and CSE (diffuse: $r = 0.008$; localized: $r = 0.171$). Clinical details of patient samples are available in Appendix A.

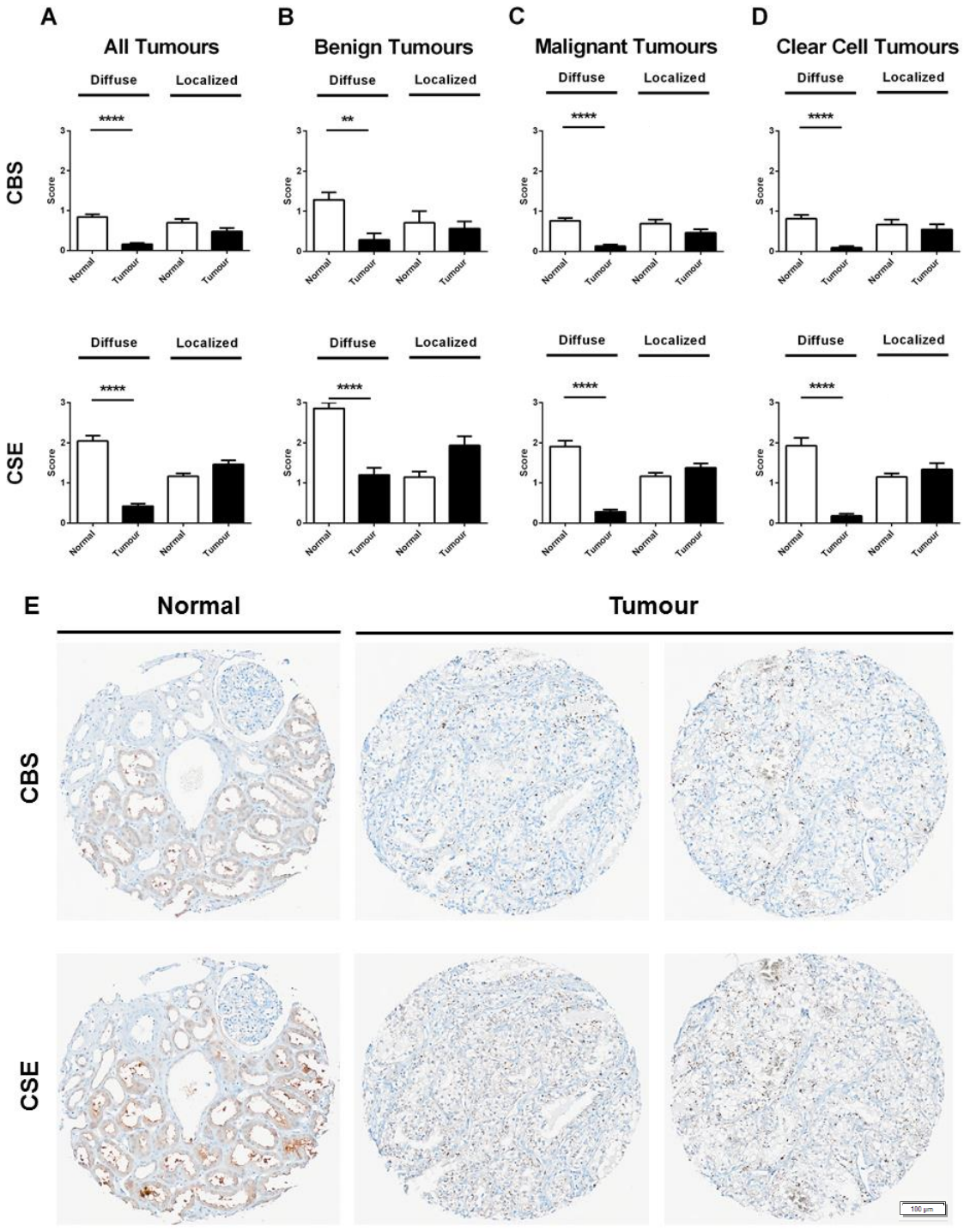
A
All Tumours
B
Benign Tumours
C
Malignant Tumours
D
Clear Cell Tumours
Diffuse
Localized
CBS
CSE
Score
Normal
Tumour
E
Normal
Tumour
100 µm

Figure 15. Diffuse and localized expression patterns of CBS and CSE in human renal tumour samples. Patient-matched biopsies from healthy (normal, n = 1 per patient) and diseased (tumour, n = 2 per patient) renal tissue were fixed, paraffin embedded into tissue microarray blocks, sectioned and immunohistochemically probed for both CBS and CSE. Images of stained sections were scored for both intensity of diffuse expression (diffuse) and intensity of localized expression (localized) on a scale of 0-3 in a blinded fashion. Error bars represent standard error of the mean (SEM). One-way ANOVA with Tukey's multiple comparisons test was used to asses statistically significant differences between groups (** $p < 0.01$; *** $p < 0.001$; **** $p < 0.0001$). Data were categorized by tumour type: **(A)** All tumours, n = 49 normal sections, n = 98 tumour sections; **(B)** Benign tumours, n = 7 normal sections, n = 14 tumour sections; **(C)** Malignant tumours, n = 42 normal sections, n = 84 tumour sections; **(D)** Clear-cell tumours, n = 27 normal sections, n = 54 tumour sections. **(E)** Representative expression patterns of CBS and CSE in normal and ccRCC tissue samples. Note in ccRCC samples the loss of diffuse CBS and CSE expression but maintenance of intensely staining puncta. Scale bar represents 100 μm.

4. Discussion

4.1 Relation to Initial Hypothesis

In order for something to accumulate, the rate of its production must exceed the rate of its removal. Our understanding of endogenous H_2S production by CBS, CSE and MPST is in its infancy, and our understanding of H_2S removal via mitochondrial oxidation is even less well-developed. It was originally hypothesized that endogenous production of H_2S would be increased in ccRCC cell lines lacking a functional copy of the VHL tumour suppressor, as a result of HIF-1/2α-mediated upregulation of H_2S-producing enzymes. While levels of H_2S were elevated in VHL-deficient ccRCC cell lines, it was not due to increased expression of the enzymes responsible for H_2S production – CBS, CSE and MPST. The most likely explanation for this result is that loss of VHL function and HIF-1/2α accumulation results in decreased mitochondrial biogenesis and respiration (55), thus eliminating the primary mechanism of H_2S removal – mitochondrial oxidation. Therefore, while VHL inactivation and HIF-1/2α accumulation does not influence H_2S *production* by inducing expression of CBS, CSE and MPST, VHL inactivation and HIF-1/2α accumulation likely influence H_2S *removal* by decreasing overall mitochondrial activity.

The efficacy of targeted therapies for cancer treatment lies in the cancer possessing some trait that non-malignant cells do not possess. Targeted therapies that have been developed for treatment of ccRCC are clinically effective due to their ability to specifically target these traits with relatively mild adverse effects (42). However, while specificity of action is desired with any treatment, it inherently limits the range of cellular processes that are subject to inhibition. In the case of ccRCC, today's clinical therapies are unable to concurrently target tumour cell growth/survival and the tumour's angiogenic potential (11). While the targeted approach has been shown to be a sound one, the identification of new targets that may be mediating multiple aspects of disease should continue to be pursued.

Here it has been shown that targeting the endogenous production of H_2S can reduce the proliferation, survival, metabolic output, and angiogenic potential of ccRCC cell lines, with minimal effects on non-malignant cells treated *in vitro* and *in vivo*. This presents endogenous H_2S-production as a valuable target in ccRCC, which when inhibited restricts multiple facets of cancer progression.

4.2 VHL, H_2S and Oxygen Sensing

The VHL tumour suppressor is a key component of the cellular response to hypoxic growth conditions. Since O_2 is essential for ATP production through oxidative phosphorylation, cells must rely on glycolysis for ATP production under hypoxic or anaerobic conditions. Through evolution, eukaryotic cells have also come to realize that a drop in O_2 concentration is usually due to disruption of blood supply, so hypoxic cells secrete factors to stimulate the growth and attraction of new blood vessels. The shift in metabolism and angiogenic response under hypoxia are both mediated by VHL, and unintentional triggering of these responses occurs in the majority of ccRCC tumours as a result of complete loss of VHL function (16). The perceived hypoxia, or *pseudohypoxia* of ccRCC tumours has been well-documented (14), however loss of VHL function alone does not lead to the formation of ccRCC tumours and holds no value as a prognostic indicator of disease (22,23).

There is much evidence to support that endogenous H_2S acts as an oxygen sensor in many eukaryotes, including humans, and as such it has many things in common with the VHL/HIF-1/2α pathway (62). H_2S is constantly being produced by cells throughout the body (64), and in turn it is removed by mitochondria in an oxygen-dependent fashion (122). Thus under normoxia, mitochondrial oxidation of H_2S is high and levels of H_2S remain low, ensuring that oxidative phosphorylation can continue without being inhibited by H_2S at Complex IV of the ETC (63,121). However under hypoxia, mitochondrial oxidation of H_2S is impaired and H_2S accumulates within the cell where it can directly influence cell signaling through post-translational modification of proteins through cysteine (S)-sulfhydration (102). S-sulfhydration of GAPDH increases its glycolytic activity by 700%, thus ensuring that the cell can satisfy its demand for ATP in the absence of oxidative phosphorylation (102). H_2S accumulation under hypoxia also

affects endothelial cells through paracrine S-sulfhydration of PDE5 and K_{ATP} channels which are necessary events in vasodilatory and angiogenic signalling pathways that aim to restore blood supply (107,108).

If both the VHL/HIF-1/2α pathway and H_2S production/oxidation pathway are mechanisms of sensing and responding to hypoxia, then surely ccRCC tumours can become pseudohypoxic when either pathway, or both pathways, become dysfunctional. In fact, loss of VHL function and HIF-1/2α accumulation in ccRCC may also be responsible for the loss of mitochondrial oxidation of H_2S, which provides a link between these two oxygen-sensing pathways in ccRCC. Baseline measurements of H_2S were shown to be higher in VHL-deficient ccRCC cell lines than in VHL WT ccRCC cell lines. This would suggest that these two pathways are linked. Decreased mitochondrial biogenesis, respiration and overall O_2 consumption has been reported in ccRCC through various mechanisms involving HIF-1/2α accumulation, which further supports this link (55,56).

4.3 Crosstalk between HIF-1/2α and H_2S

There has been evidence to suggest that in addition to decreased mitochondrial oxidation of H_2S under hypoxia, levels of H_2S also increase under hypoxia as a result of HIF-1/2α-mediated induction of CBS (99). While there did not appear to be aberrant upregulation of CBS, CSE, nor MPST in VHL-deficient ccRCC cell lines, there was a slight (though not significant) decrease in CBS and CSE expression when VHL function was restored to 786-O cells. It is unlikely that such drastic differences in endogenous levels of H_2S observed between VHL WT and VHL-deficient cell lines can be explained by this modest change in CBS and CSE expression. However, it is possible that HIF-1/2α-mediated control over CBS and CSE is contributing in some small way to increased production of H_2S. Perhaps hypoxic induction of CBS and CSE is of greater use in cells that display relatively low baseline normoxic expression of these enzymes, when compared to renal epithelial cells that display high baseline normoxic expression (86).

HIF-1/2α transcription factors may not play an important role in regulating the expression of CBS, CSE and MPST, however that is not to say that HIF-1/2α doesn't regulate the

activity of CBS, CSE and MPST. Measurement of enzyme activity in cell lines with different HIF-1α and HIF-2α expression profiles was not undertaken here due to a lack of equipment required for such biochemical assays. However, differences in relative expression of the upper and lower bands of CSE and MPST were observed in western blot analysis of 786-O cells with and without functional VHL. While the changes that these bands represent in terms of protein structure and function have not been investigated, it is possible that they may represent differences in enzyme activity, or even differences in enzyme localization. CSE has been shown to translocate to mitochondria in response to various stressors, and others have shown that this translocation/stress is associated with slight changes in the appearance of the band in western blots (123). In contrast, there is also evidence to suggest that H_2S being produced by CBS, CSE and MPST may reciprocally alter HIF-1/2α activity (143), which could have implications on how ccRCC progresses.

As stated previously, loss of VHL function can result in tumours that overexpress HIF-1α and HIF-2α to varying degrees, leading to H1H2 and H2 tumours (24,26). These two subsets of VHL-deficient ccRCC tumours have been shown to be unique with regards to their preferred metabolic and proliferative pathways due to the differences in how HIF-1α and HIF-2α interact with other oncogenes like c-MYC and MXI1 (24,55). It is well accepted that one of the key steps in ccRCC progression is loss of VHL function, which results in VHL-deficient tumours with the H1H2 phenotype (24). Recent evidence suggests that loss of HIF-1α – resulting in the more aggressive H2 phenotype – may be another key event in ccRCC progression, although the mechanism by which HIF-1α is lost is unknown (9,18,30). Exogenous H_2S has been shown to reduce both the translational expression, and the activity of HIF-1α (143), however this effect has been shown to be dependent on VHL function and mitochondrial activity (144). Interestingly, H_2S-mediated HIF-1α degradation also only occur under true hypoxic conditions – not in response to hypoxia-mimetics, nor in pseudohypoxic RCC cell lines (144). There is also evidence that a reducing environment can enhance the stability of HIF-2α, although the effects of a reducing environment on HIF-1α stability were not investigated (145). Further investigation into whether increased levels of endogenous H_2S plays a role in loss of HIF-1α in ccRCC is required.

4.4 H_2S in ccRCC Proliferation, Metabolism and Survival

There are dynamic relationships that exist between cell growth, proliferation, metabolism and survival. On the surface these relationships may seem obvious – through metabolism, cells generate energy and molecules that are needed to grow in size, proliferate and survive in general (53). It is only after considering the various trade-offs that exist between these variables that one realizes the complex decisions that cells make on a minute-to-minute basis. For example, different growth factors stimulate different proliferative and metabolic pathways, which generate variable levels of ROS. The degree of ROS production in turn affects the activity of these proliferative pathways and, if excessive, can induce a cell to undergo apoptosis. These relationships become even more counter-intuitive in the context of cancer, where due to mutations, the cancer cell can no longer recognize the value on either side of the trade-off, and does not react the way a normal cell would (53).

Here we showed that H_2S production contributes to the enhanced proliferation observed in ccRCC cell lines, and targeting its production can slow, and even stop, proliferation. Exogenous H_2S has been shown to play a role in the cell cycle entry and proliferation of colonocytes through increased production of NADPH, activation of mitogen-activated protein kinase and Akt signalling pathways, and inactivation of the cell-cycle inhibitor p21 (130,146). Likewise, inhibition of endogenous H_2S synthesis can slow the proliferation of ovarian cancer and colon cancer cell lines (131,133). It was observed here that the range of concentrations, as well as treatment time, at which the CBS/CSE inhibitor halted proliferation before becoming cytotoxic was small. As the length of treatment time and/or concentration of the inhibitor increased, loss of H_2S production resulted in decreased metabolic activity, decreased ATP production, and ultimately apoptosis and necrosis. Seeing as loss of H_2S production was ultimately cytotoxic in ccRCC cell lines and not simply cytostatic, one is led to believe that it plays an important role in energy production. As observed here, a slight decrease in H_2S production results in a small deficit in energy production and influences the cell to stop dividing in order to maintain essential survival processes. However, a greater decrease in H_2S production

results in a significant deficit in energy production to the point where the cell can no longer maintain essential processes and dies.

In this study, energy production – metabolism – was measured using two different assays – the XTT assay and total ATP quantitation. The XTT assay measures metabolic activity by quantifying the turnover of electron carriers that donate electrons to coenzyme Q. This would include NADH, flavin adenine dinucleotide, and, in the context of H_2S, SQR (122). Here it was found that the VHL-deficient ccRCC cell lines not only produced higher levels of H_2S than their VHL WT counterparts, but were also more susceptible to metabolic inhibition with HA. Given the lack of mitochondrial respiration in VHL-deficient ccRCC cell lines, it is likely that inhibiting H_2S production resulted in a decrease in glycolytic activity, and decreased NADH production by LDH. This is supported by results of the ATP assay, in which loss of H_2S production drastically reduced both hypoxic and normoxic ATP levels. Others have reported that H_2S mediates its metabolic effects in cancer by donating electrons to the ETC through mitochondrial oxidation (131,133). However if this was the case in ccRCC, one would have expected that metabolic inhibition would only have been achieved under normoxic conditions, seeing as mitochondrial oxidation requires oxygen (122). This isolated decline in normoxic metabolism was not observed in the VHL-deficient cell lines, but was observed when VHL was reconstituted into 786-O cells.

Results of the ATP assay did not entirely agree with results of the XTT assay. HK-2 ATP levels were significantly reduced upon HA treatment, however no significant difference was apparent in the XTT assay. This could be due to the fact that the ATP assays were 6 hours in length whereas the XTT assays were 48 hours in length. Also, H_2S has been shown to reverse the flow of electrons through Complex I of the ETC, forcing Complex I to take electrons from coenzyme Q and reduce NAD^+ into NADH (122). This allows the cell to oxidize H_2S before it becomes toxic, while at the same time keeping the pool of available NADH high. In this way, H_2S could still be contributing to ATP production in nonmalignant renal epithelial cells – as was seen here and elsewhere (122). However, loss of H_2S oxidation would not be apparent in an XTT assay since loss

of Complex I reversion would not change the level of coenzyme Q activation – coenzyme Q would just be oxidized by NADH instead of SQR.

The XTT assay also showed that decreased metabolism upon HA treatment could be rescued in VHL-deficient cell lines when LC was also present in growth media. This rescuing effect was not seen in the ATP assay, however it was observed in the flow cytometry viability assays. In addition to its role in the ETC and metabolism, coenzyme Q also serves antioxidative functions within the plasma membrane, playing a role in the oxidative stress response (147). Therefore, a positive signal in the XTT assay can also indicate increased antioxidative activity, increased resistance to oxidative stress, and improvement in survival. It is known that the metabolic reprogramming in VHL-deficient ccRCC helps to keep oxidative stress in check by rerouting certain glycolytic intermediates towards the production of NADPH (53). NAD^+ levels must also remain high in order for aerobic glycolysis to function (137), which is thought to be largely accomplished by LDH in ccRCC (55). Recent evidence has shown that production of H_2S in other cancers is a crucial component of the aerobic glycolysis energy circuit that reduces oxidative stress and contributes to ATP production by maintaining production of NAD^+ (138,139). Therefore, in helping to maintain the supply of NAD^+ that fuels aerobic glycolysis in ccRCC, H_2S may also ensure that production of the antioxidant NADPH also remains high.

As has been seen in studies of ovarian cancer (133) and colon cancer (131), increasing concentration of inhibitors of CBS and CSE results in a steep drop off in ccRCC cell viability. Interestingly, most of the cell lines investigated here were not susceptible to inhibition with PAG – which specifically inhibits CSE – despite the fact that all cell lines expressed similar levels of CSE. Cell lines were much more susceptible to inhibition with HA – a dual inhibitor of CBS and CSE – and cell survival was observed to drop steeply around 4 mM (140). Analysis of the flow cytometry plots displaying the proportions of apoptotic and necrotic cells reveals that the majority of cell death is due to necrosis that occurs following 24 hour treatment with 2-4 mM HA. Such a sudden decline in viability suggests that at this concentration of the CBS/CSE dual inhibitor, levels of H_2S have declined to a point where the cell can no longer perform essential

processes and/or can no longer cope with the oxidative stress being applied. This is supported by the observation that in ccRCC cell lines viability was more severely impacted under normoxic conditions when levels of oxidative stress are higher. Similarly, others have shown that addition of the antioxidant glutathione can attenuate declines in viability seen following loss of H_2S production (133).

4.5 H_2S in ccRCC Angiogenesis

VHL-deficient ccRCC tumours are highly angiogenic as a result of high VEGF secretion that is driven by upregulation of both HIF-1α and HIF-2α (17,27). VEGF secretion has been shown to be positively correlated with the size, vascularization, stage and Fuhrman grade of ccRCC tumours and has great prognostic value (148). The efficacy of bevacizumab and various RTKIs in the clinical setting speaks to the importance of VEGF-mediated angiogenesis in ccRCC progression both prior to and following metastasis (11). Multiple sources of evidence suggest that VEGF-mediated angiogenesis is dependent upon tonic inhibition of PDE5 by H_2S in endothelial cells (107-109,149). Other mechanisms by which H_2S exerts its pro-angiogenic effects have also been suggested (71,149). ccRCC xenograft vascularization assays performed here support these lines of evidence.

It was found that the attraction of blood vessels towards VHL-deficient ccRCC xenografts could be reduced upon systemic inhibition of endogenous H_2S production. It could not be determined whether the intravascularly-injected inhibitor was targeting H_2S production in endothelial cells or in the cancer cells themselves. The VHL-deficient xenografts were observed to decrease in size following HA treatment which could indicate direct cytotoxicity of the treatment, and suggest that H_2S production was being targeted in the tumour. However, the decrease in xenograft size could also have been the effect of being starved of nutrients that aren't being supplied due to devascularization, which would suggest that treatments failed to reach the tumour are were acting on endothelial cells. Others have shown that chick endothelial cells are susceptible to inhibition of endogenous H_2S production within the CAM vasculature (71).

Interestingly, the vascularization of VHL WT xenografts was shown to not be susceptible to inhibition of H_2S production. These cell lines have been shown to secrete lower levels of VEGF and were, on average, less well vascularized than their VHL-deficient counterparts (26,27). The VEGF-mediated vascularization of these tumours plays less of a role and this is likely why the inhibitor was not effective. The fact that the inhibitor had no effect on the vascularization of xenografts secreting lower levels of VEGF lends credence to the role of H_2S in VEGF-mediated angiogenesis. Of further interest, systemic treatment with LC resulted in noticeable vessel vasodilation, but only when these vessels were in close proximity to VHL-deficient xenografts. This would suggest that the treatments are acting directly on the cancer cells, resulting in changes in tumour-derived H_2S that affects the surrounding vasculature through paracrine signalling.

4.6 Translational Applications

In this study, it has been shown that inhibition of endogenous H_2S production can target multiple aspects of ccRCC disease progression, making it a potentially promising treatment option of mRCC. Depending on the dosage of treatment, the dual CBS/CSE inhibitor preferentially targeted the proliferation, metabolism, and survival of ccRCC cell lines over non-malignant renal epithelial cells *in vitro*. Furthermore, systemic intravascular injection of the inhibitor was able to decrease the vascularization of ccRCC xenografts without impacting the survival of chick embryos. Some of these effects were observed in both VHL WT and VHL-deficient cell lines, and some were observed regardless of VHL status. When translating these findings to the clinical setting, it will be important to identify markers that are more predictive of therapeutic efficacy than VHL-deficiency seems to be (148). As was observed in ccRCC cell lines, human ccRCC tumours did not display increased expression of H_2S-producing enzymes when compared to normal tissue, therefore total expression of CBS, CSE and MPST may not be helpful in this regard. However, interesting localization patterns of CBS and CSE were observed in ccRCC which could be of prognostic value or provide insight into the role of H_2S in ccRCC progression.

While stage IV mRCC has often been the focus when developing new therapies against ccRCC, (neo)adjuvant therapies for treatment of stage II and stage III ccRCC have not

been a priority (36). Many of these diseases have a high risk of relapsing within 5 years of surgical resection and this contributes heavily to disease mortality (36). The cellular source of cancer relapse is currently unknown, although there is strong evidence to suggest that cancer stem cells may be responsible for this relapse in ccRCC and other cancers (150). Recent work has shown that the production of H_2S plays a key role in maintaining the stem-like phenotype of cancer cells through induction of stem cell factors OCT4 and NANOG, and through regulation of cellular energy production and oxidative stress (139). Endogenous H_2S production was also associated with the spheroid-forming and transdifferentiation potential of cells, which are thought to be important processes in disease relapse (139). Treatment with inhibitors of H_2S synthesis either before or after nephrectomy might limit the ability of any remaining cancer cells to form new tumours.

One of the challenges of treating mRCC is its resistance to well-established, cost-effective, readily-available systemic therapies such as chemotherapy and radiation therapy (8). It has been shown that chemopreventive agents – agents that limit the efficacy of chemotherapies – often increase the antioxidative potential of cancer cells through increased production of glutathione and NADPH and increased activity of Nrf2 (151,152). S-Sulfhydration of Keap1 – a protein that suppresses Nrf2 – has been shown to prevent the inhibitory effects that Keap1 has on Nrf2, thus increasing the antioxidative response (96). Additional antioxidative properties of H_2S include increased production of reduced glutathione and polysulfides (67,115), which may be involved in conferring chemoresistance in ovarian cancer (133). Also, hypoxia-induced radioresistance may be mediated by the cytoprotective effects of H_2S accumulation under hypoxic conditions (134,135). Together, there is much evidence to support that inhibition of endogenous H_2S production may enhance conventional forms of systemic therapy and should be investigated further.

While targeted therapies have been shown to improve PFS and ORR of patients afflicted with mRCC, durable complete responses remain elusive and therapy resistance remains an issue (41,42). Cancer therapies apply a selective pressure on tumours which may or may not affect all cells within a tumour. Those cells that are more resistant to the applied pressure are more likely to survive and proliferate, whereas the cells that are affected by

the treatment are removed. With successive rounds of therapy, the composition of the tumour changes such that most of the cells are resistant to the applied pressure, and the therapy becomes ineffective. This process called tumour progression applies to various selective pressures – such as hypoxia, nutrient deprivation and oxidative stress – that occur naturally as the tumour grows in size and composition (136). Endogenous production of H_2S seems to facilitate recovery from these selective pressures that arise throughout the course of tumour progression (137,138). It would be interesting to determine whether cells that develop resistance to targeted therapies also produce higher levels of H_2S. If so, combining inhibitors of endogenous H_2S production with recently developed targeted therapies could delay the onset of resistance in mRCC. Similar reasoning suggests that inhibition of endogenous H_2S production might be a form of therapy that ccRCC tumours are less inclined to develop resistance to, although export of the inhibitors by P-glycoprotein remains a possibility (8).

4.7 Recommendations

The results of this study have exposed multiple avenues for future research. First and foremost, while the use of a dual CBS/CSE inhibitor has provided valuable information regarding the adverse effects of such a drug when used *in vitro* and *in vivo*, siRNA- or shRNA-mediated knockdown of CBS, CSE and MPST would be more valuable in determining the importance of each of these three enzymes. There are currently no bona fide MPST inhibitors, and the dual CBS/CSE inhibitor used here has its limitations (140). Generation of cell lines with each of CBS, CSE and MPST knocked out using shRNA would be ideal in that it would allow for longer experiments both *in vitro* and *in vivo*, although knocking out each enzyme in all cell lines investigated here would be quite time-consuming. However, it may be the only way to determine if one of these H_2S-producing enzymes is more important than the others, which can then drive the development of specific inhibitors.

In this study, the elevated level of H_2S in VHL-deficient ccRCC cell lines was explained by decreased mitochondrial biogenesis and activity. While reduced mitochondrial activity and biogenesis has been observed in ccRCC (153), and it is known that the majority of ccRCC tumours are VHL-deficient (1), the mechanisms linking

mitochondrial metabolism, loss of VHL function and accumulation of HIF-1/2α are still being investigated (55). Moreover, ccRCC cell lines may exhibit higher levels of oxidative phosphorylation than primary ccRCC cells (153). Establishing a more concrete relationship between loss of mitochondrial oxidation, VHL deficiency and accumulation of H_2S is a priority. Measurement of H_2S in primary ccRCC cells using the intracellular fluorescent probe and live-cell imaging would be ideal given the high throughput nature of the assay. DNA, RNA and protein analysis of these primary cells would then allow for determination of VHL mutation status, HIF-1/2α expression profiling and metabolic profiling, each of which could be correlated against the level of H_2S in each sample. Treatment of these primary cells with inhibitors of endogenous H_2S production and subsequent viability, proliferation, and metabolic assays would provide a more translational approach than the one used here.

The CAM angiogenesis assay used here provided good evidence that inhibition of endogenous H_2S production can reduce microvascular density of ccRCC tumours. The logical next step in investigating the role of H_2S in ccRCC vascularization is xenografting human cell lines into immune-deficient mice and determining whether similar effects are observed. Furthermore, this more complex mammalian system will provide insight into the true adverse effects that systemic inhibition of H_2S production has on the host. Inhibitors of H_2S production have been used to treat subcutaneously-xenografted colon cancer tumours in mice, although inhibitors were injected subcutaneously and not intravascularly (131). Given the immunogenic nature of ccRCC (40), and the prominent role of H_2S in immunology and renal inflammation (78), it would be interesting to evaluate how this treatment changes the interaction between the tumour and the host immune system. There are commercially available, mouse-derived renal cancer cell lines that would make this possible.

Mouse models have also been developed to evaluate spontaneous metastasis of renal cancer cells after orthotopic implantation within the kidney, which would facilitate investigation of the role that H_2S plays in metastasis (154). Prior to investigating the involvement of H_2S in metastatic progression *in vivo*, it would be best to first investigate the involvement of H_2S in ccRCC migration and expression of epithelial-mesenchymal

transition (EMT) markers. H_2S has been shown to increase the migration of endothelial cells (108) and colon cancer cells (131), and has also been shown to induce expression of EMT markers COX-2 and MMP2 in liver cancer cells (155). Addition of 'anti-metastatic' to the list of anti-tumourigenic properties that this therapy has shown to possess would increase the likelihood of its clinical efficacy.

5. Conclusions

From this body of work, the following conclusions can be drawn:

1. Levels of H_2S are increased in ccRCC cell lines lacking a functional copy of the VHL tumour suppressor.
2. Increased levels of H_2S in ccRCC cell lines are not due to increased expression of the H_2S-producing enzymes CBS, CSE and MPST. Furthermore, these enzymes are not upregulated in human ccRCC tumours.
3. Targeting endogenous H_2S production in ccRCC cell lines using inhibitors results in decreased cell proliferation, metabolism and survival when compared to non-malignant renal epithelial cells.
4. Systemic inhibition of endogenous H_2S production in chick embryos can reduce the vascularization of VHL-deficient ccRCC xenografts.

References

(1) Audenet F, Yates DR, Cancel-Tassin G, Cussenot O, Roupret M. Genetic pathways involved in carcinogenesis of clear cell renal cell carcinoma: genomics towards personalized medicine. BJU Int 2012 Jun;109(12):1864-1870.

(2) Bhatt JR, Finelli A. Landmarks in the diagnosis and treatment of renal cell carcinoma. Nat Rev Urol 2014 Sep;11(9):517-525.

(3) Habib SL, Prihoda TJ, Luna M, Werner SA. Diabetes and risk of renal cell carcinoma. J Cancer 2012;3:42-48.

(4) Lindblad P, Chow WH, Chan J, Bergstrom A, Wolk A, Gridley G, et al. The role of diabetes mellitus in the aetiology of renal cell cancer. Diabetologia 1999 Jan;42(1):107-112.

(5) Setiawan VW, Stram DO, Nomura AM, Kolonel LN, Henderson BE. Risk factors for renal cell cancer: the multiethnic cohort. Am J Epidemiol 2007 Oct 15;166(8):932-940.

(6) Weikert S, Boeing H, Pischon T, Weikert C, Olsen A, Tjonneland A, et al. Blood pressure and risk of renal cell carcinoma in the European prospective investigation into cancer and nutrition. Am J Epidemiol 2008 Feb 15;167(4):438-446.

(7) Zhu Y, Wang HK, Zhang HL, Yao XD, Zhang SL, Dai B, et al. Visceral obesity and risk of high grade disease in clinical t1a renal cell carcinoma. J Urol 2013 Feb;189(2):447-453.

(8) Motzer RJ, Russo P. Systemic therapy for renal cell carcinoma. J Urol 2000 Feb;163(2):408-417.

(9) Oosterwijk E, Rathmell WK, Junker K, Brannon AR, Pouliot F, Finley DS, et al. Basic research in kidney cancer. Eur Urol 2011 Oct;60(4):622-633.

(10) Linehan WM, Ricketts CJ. The metabolic basis of kidney cancer. Semin Cancer Biol 2013 Feb;23(1):46-55.

(11) Monzon JG, Heng DY. Management of metastatic kidney cancer in the era of personalized medicine. Crit Rev Clin Lab Sci 2014 Apr;51(2):85-97.

(12) Singer EA, Gupta GN, Marchalik D, Srinivasan R. Evolving therapeutic targets in renal cell carcinoma. Curr Opin Oncol 2013 May;25(3):273-280.

(13) Drabkin HA, Gemmill RM. Cholesterol and the development of clear-cell renal carcinoma. Curr Opin Pharmacol 2012 Dec;12(6):742-750.

(14) Haase VH. Renal cancer: oxygen meets metabolism. Exp Cell Res 2012 May 15;318(9):1057-1067.

(15) Clifford SC, Prowse AH, Affara NA, Buys CH, Maher ER. Inactivation of the von Hippel-Lindau (VHL) tumour suppressor gene and allelic losses at chromosome arm 3p in primary renal cell carcinoma: evidence for a VHL-independent pathway in clear cell renal tumourigenesis. Genes Chromosomes Cancer 1998 Jul;22(3):200-209.

(16) Gossage L, Eisen T, Maher ER. VHL, the story of a tumour suppressor gene. Nat Rev Cancer 2015 Jan;15(1):55-64.

(17) Maxwell PH, Wiesener MS, Chang GW, Clifford SC, Vaux EC, Cockman ME, et al. The tumour suppressor protein VHL targets hypoxia-inducible factors for oxygen-dependent proteolysis. Nature 1999 May 20;399(6733):271-275.

(18) Baldewijns MM, van Vlodrop IJ, Vermeulen PB, Soetekouw PM, van Engeland M, de Bruine AP. VHL and HIF signalling in renal cell carcinogenesis. J Pathol 2010 Jun;221(2):125-138.

(19) Ahluwalia A, Tarnawski AS. Critical role of hypoxia sensor--HIF-1alpha in VEGF gene activation. Implications for angiogenesis and tissue injury healing. Curr Med Chem 2012;19(1):90-97.

(20) Tory K, Brauch H, Linehan M, Barba D, Oldfield E, Filling-Katz M, et al. Specific genetic change in tumors associated with von Hippel-Lindau disease. J Natl Cancer Inst 1989 Jul 19;81(14):1097-1101.

(21) Whaley JM, Naglich J, Gelbert L, Hsia YE, Lamiell JM, Green JS, et al. Germ-line mutations in the von Hippel-Lindau tumor-suppressor gene are similar to somatic von Hippel-Lindau aberrations in sporadic renal cell carcinoma. Am J Hum Genet 1994 Dec;55(6):1092-1102.

(22) Mandriota SJ, Turner KJ, Davies DR, Murray PG, Morgan NV, Sowter HM, et al. HIF activation identifies early lesions in VHL kidneys: evidence for site-specific tumor suppressor function in the nephron. Cancer Cell 2002 Jun;1(5):459-468.

(23) Kapitsinou PP, Haase VH. The VHL tumor suppressor and HIF: insights from genetic studies in mice. Cell Death Differ 2008 Apr;15(4):650-659.

(24) Gordan JD, Lal P, Dondeti VR, Letrero R, Parekh KN, Oquendo CE, et al. HIF-alpha effects on c-Myc distinguish two subtypes of sporadic VHL-deficient clear cell renal carcinoma. Cancer Cell 2008 Dec 9;14(6):435-446.

(25) Krieg M, Haas R, Brauch H, Acker T, Flamme I, Plate KH. Up-regulation of hypoxia-inducible factors HIF-1alpha and HIF-2alpha under normoxic conditions in renal carcinoma cells by von Hippel-Lindau tumor suppressor gene loss of function. Oncogene 2000 Nov 16;19(48):5435-5443.

(26) Raval RR, Lau KW, Tran MG, Sowter HM, Mandriota SJ, Li JL, et al. Contrasting properties of hypoxia-inducible factor 1 (HIF-1) and HIF-2 in von Hippel-Lindau-associated renal cell carcinoma. Mol Cell Biol 2005 Jul;25(13):5675-5686.

(27) Shinojima T, Oya M, Takayanagi A, Mizuno R, Shimizu N, Murai M. Renal cancer cells lacking hypoxia inducible factor (HIF)-1alpha expression maintain vascular endothelial growth factor expression through HIF-2alpha. Carcinogenesis 2007 Mar;28(3):529-536.

(28) Gunaratnam L, Morley M, Franovic A, de Paulsen N, Mekhail K, Parolin DA, et al. Hypoxia inducible factor activates the transforming growth factor-alpha/epidermal growth factor receptor growth stimulatory pathway in VHL(-/-) renal cell carcinoma cells. J Biol Chem 2003 Nov 7;278(45):44966-44974.

(29) Smith K, Gunaratnam L, Morley M, Franovic A, Mekhail K, Lee S. Silencing of epidermal growth factor receptor suppresses hypoxia-inducible factor-2-driven VHL-/- renal cancer. Cancer Res 2005 Jun 15;65(12):5221-5230.

(30) Dalgliesh GL, Furge K, Greenman C, Chen L, Bignell G, Butler A, et al. Systematic sequencing of renal carcinoma reveals inactivation of histone modifying genes. Nature 2010 Jan 21;463(7279):360-363.

(31) Motzer RJ, Hutson TE, Tomczak P, Michaelson MD, Bukowski RM, Oudard S, et al. Overall survival and updated results for sunitinib compared with interferon alfa in patients with metastatic renal cell carcinoma. J Clin Oncol 2009 Aug 1;27(22):3584-3590.

(32) Ljungberg B, Cowan NC, Hanbury DC, Hora M, Kuczyk MA, Merseburger AS, et al. EAU guidelines on renal cell carcinoma: the 2010 update. Eur Urol 2010 Sep;58(3):398-406.

(33) Campbell SC, Novick AC, Belldegrun A, Blute ML, Chow GK, Derweesh IH, et al. Guideline for management of the clinical T1 renal mass. J Urol 2009 Oct;182(4):1271-1279.

(34) Escudier B, Eisen T, Porta C, Patard JJ, Khoo V, Algaba F, et al. Renal cell carcinoma: ESMO Clinical Practice Guidelines for diagnosis, treatment and follow-up. Ann Oncol 2012 Oct;23 Suppl 7:vii65-71.

(35) Pal SK, Haas NB. Adjuvant therapy for renal cell carcinoma: past, present, and future. Oncologist 2014 Aug;19(8):851-859.

(36) Janowitz T, Welsh SJ, Zaki K, Mulders P, Eisen T. Adjuvant therapy in renal cell carcinoma-past, present, and future. Semin Oncol 2013 Aug;40(4):482-491.

(37) van der Poel HG, Roukema JA, Horenblas S, van Geel AN, Debruyne FM. Metastasectomy in renal cell carcinoma: A multicenter retrospective analysis. Eur Urol 1999;35(3):197-203.

(38) Bhatt RS, Landis DM, Zimmer M, Torregrossa J, Chen S, Sukhatme VP, et al. Hypoxia-inducible factor-2alpha: effect on radiation sensitivity and differential regulation by an mTOR inhibitor. BJU Int 2008 Aug;102(3):358-363.

(39) Lei Y, Geng Z, Guo-Jun W, He W, Jian-Lin Y. Prognostic significance of survivin expression in renal cell cancer and its correlation with radioresistance. Mol Cell Biochem 2010 Nov;344(1-2):23-31.

(40) Gouttefangeas C, Stenzl A, Stevanovic S, Rammensee HG. Immunotherapy of renal cell carcinoma. Cancer Immunol Immunother 2007 Jan;56(1):117-128.

(41) Autorino R, Di Lorenzo G. An evolving role for immunotherapy in metastatic RCC. Nat Rev Urol 2010 Jun;7(6):305-307.

(42) Amin A, White RL,Jr. High-dose interleukin-2: is it still indicated for melanoma and RCC in an era of targeted therapies? Oncology (Williston Park) 2013 Jul;27(7):680-691.

(43) Huang D, Ding Y, Li Y, Luo WM, Zhang ZF, Snider J, et al. Sunitinib acts primarily on tumor endothelium rather than tumor cells to inhibit the growth of renal cell carcinoma. Cancer Res 2010 Feb 1;70(3):1053-1062.

(44) Yuen JS, Sim MY, Siml HG, Chong TW, Lau WK, Cheng CW, et al. Inhibition of angiogenic and non-angiogenic targets by sorafenib in renal cell carcinoma (RCC) in a RCC xenograft model. Br J Cancer 2011 Mar 15;104(6):941-947.

(45) Xin H, Zhang C, Herrmann A, Du Y, Figlin R, Yu H. Sunitinib inhibition of Stat3 induces renal cell carcinoma tumor cell apoptosis and reduces immunosuppressive cells. Cancer Res 2009 Mar 15;69(6):2506-2513.

(46) Zoncu R, Efeyan A, Sabatini DM. mTOR: from growth signal integration to cancer, diabetes and ageing. Nat Rev Mol Cell Biol 2011 Jan;12(1):21-35.

(47) Toschi A, Lee E, Gadir N, Ohh M, Foster DA. Differential dependence of hypoxia-inducible factors 1 alpha and 2 alpha on mTORC1 and mTORC2. J Biol Chem 2008 Dec 12;283(50):34495-34499.

(48) Cho DC, Cohen MB, Panka DJ, Collins M, Ghebremichael M, Atkins MB, et al. The efficacy of the novel dual PI3-kinase/mTOR inhibitor NVP-BEZ235 compared with rapamycin in renal cell carcinoma. Clin Cancer Res 2010 Jul 15;16(14):3628-3638.

(49) WARBURG O. On the origin of cancer cells. Science 1956 Feb 24;123(3191):309-314.

(50) Unwin RD, Craven RA, Harnden P, Hanrahan S, Totty N, Knowles M, et al. Proteomic changes in renal cancer and co-ordinate demonstration of both the glycolytic and mitochondrial aspects of the Warburg effect. Proteomics 2003 Aug;3(8):1620-1632.

(51) Kim JW, Tchernyshyov I, Semenza GL, Dang CV. HIF-1-mediated expression of pyruvate dehydrogenase kinase: a metabolic switch required for cellular adaptation to hypoxia. Cell Metab 2006 Mar;3(3):177-185.

(52) Fantin VR, St-Pierre J, Leder P. Attenuation of LDH-A expression uncovers a link between glycolysis, mitochondrial physiology, and tumor maintenance. Cancer Cell 2006 Jun;9(6):425-434.

(53) Chen X, Qian Y, Wu S. The Warburg effect: Evolving interpretations of an established concept. Free Radic Biol Med 2015 Feb;79C:253-263.

(54) David CJ, Chen M, Assanah M, Canoll P, Manley JL. HnRNP proteins controlled by c-Myc deregulate pyruvate kinase mRNA splicing in cancer. Nature 2010 Jan 21;463(7279):364-368.

(55) Zhang H, Gao P, Fukuda R, Kumar G, Krishnamachary B, Zeller KI, et al. HIF-1 inhibits mitochondrial biogenesis and cellular respiration in VHL-deficient renal cell carcinoma by repression of C-MYC activity. Cancer Cell 2007 May;11(5):407-420.

(56) Tsao CC, Teh BT, Jonasch E, Shreiber-Agus N, Efstathiou E, Hoang A, et al. Inhibition of Mxi1 suppresses HIF-2alpha-dependent renal cancer tumorigenesis. Cancer Biol Ther 2008 Oct;7(10):1619-1627.

(57) Bernards R, Weinberg RA. A progression puzzle. Nature 2002 Aug 22;418(6900):823.

(58) Chen CQ, Xin H, Zhu YZ. Hydrogen sulfide: third gaseous transmitter, but with great pharmacological potential. Acta Pharmacol Sin 2007 Nov;28(11):1709-1716.

(59) Furchgott RF, Zawadzki JV. The obligatory role of endothelial cells in the relaxation of arterial smooth muscle by acetylcholine. Nature 1980 Nov 27;288(5789):373-376.

(60) Tenhunen R, Marver HS, Schmid R. The enzymatic conversion of heme to bilirubin by microsomal heme oxygenase. Proc Natl Acad Sci U S A 1968 Oct;61(2):748-755.

(61) Hancock JT, Whiteman M. Hydrogen sulfide and cell signaling: team player or referee? Plant Physiol Biochem 2014 May;78:37-42.

(62) Olson KR. Hydrogen sulfide as an oxygen sensor. Clin Chem Lab Med 2013 Mar 1;51(3):623-632.

(63) Petersen LC. The effect of inhibitors on the oxygen kinetics of cytochrome c oxidase. Biochim Biophys Acta 1977 May 11;460(2):299-307.

(64) Stipanuk MH, Beck PW. Characterization of the enzymic capacity for cysteine desulphhydration in liver and kidney of the rat. Biochem J 1982 Aug 15;206(2):267-277.

(65) Abe K, Kimura H. The possible role of hydrogen sulfide as an endogenous neuromodulator. J Neurosci 1996 Feb 1;16(3):1066-1071.

(66) Hosoki R, Matsuki N, Kimura H. The possible role of hydrogen sulfide as an endogenous smooth muscle relaxant in synergy with nitric oxide. Biochem Biophys Res Commun 1997 Aug 28;237(3):527-531.

(67) Kimura H. Physiological role of hydrogen sulfide and polysulfide in the central nervous system. Neurochem Int 2013 Nov;63(5):492-497.

(68) Chen WL, Niu YY, Jiang WZ, Tang HL, Zhang C, Xia QM, et al. Neuroprotective effects of hydrogen sulfide and the underlying signaling pathways. Rev Neurosci 2014 Dec 22.

(69) Wang R. Signaling pathways for the vascular effects of hydrogen sulfide. Curr Opin Nephrol Hypertens 2011 Mar;20(2):107-112.

(70) Liu YH, Yan CD, Bian JS. Hydrogen sulfide: a novel signaling molecule in the vascular system. J Cardiovasc Pharmacol 2011 Dec;58(6):560-569.

(71) Szabo C, Papapetropoulos A. Hydrogen sulphide and angiogenesis: mechanisms and applications. Br J Pharmacol 2011 Oct;164(3):853-865.

(72) Farrugia G, Szurszewski JH. Carbon monoxide, hydrogen sulfide, and nitric oxide as signaling molecules in the gastrointestinal tract. Gastroenterology 2014 Aug;147(2):303-313.

(73) Linden DR. Hydrogen sulfide signaling in the gastrointestinal tract. Antioxid Redox Signal 2014 Feb 10;20(5):818-830.

(74) Veeranki S, Tyagi SC. Role of hydrogen sulfide in skeletal muscle biology and metabolism. Nitric Oxide 2015 Apr 30;46:66-71.

(75) Okamoto M, Yamaoka M, Kimura T. Hydrogen sulfide and its effect on pancreatic beta-cells. Nihon Rinsho 2013 Jan;71(1):175-180.

(76) Ruginsk SG, Mecawi AS, da Silva MP, Reis WL, Coletti R, Lima JB, et al. Gaseous Modulators in the Control of the Hypothalamic Neurohypophyseal System. Physiology (Bethesda) 2015 Mar;30(2):127-138.

(77) Taniguchi S, Niki I. Significance of hydrogen sulfide production in the pancreatic beta-cell. J Pharmacol Sci 2011;116(1):1-5.

(78) Lobb I, Sonke E, Aboalsamh G, Sener A. Hydrogen sulphide and the kidney: Important roles in renal physiology and pathogenesis and treatment of kidney injury and disease. Nitric Oxide 2015 Apr 30;46:55-65.

(79) Mani S, Cao W, Wu L, Wang R. Hydrogen sulfide and the liver. Nitric Oxide 2014 Sep 15;41:62-71.

(80) Gai JW, Wahafu W, Guo H, Liu M, Wang XC, Xiao YX, et al. Further evidence of endogenous hydrogen sulphide as a mediator of relaxation in human and rat bladder. Asian J Androl 2013 Sep;15(5):692-696.

(81) Olson KR, Whitfield NL, Bearden SE, St Leger J, Nilson E, Gao Y, et al. Hypoxic pulmonary vasodilation: a paradigm shift with a hydrogen sulfide mechanism. Am J Physiol Regul Integr Comp Physiol 2010 Jan;298(1):R51-60.

(82) Wei HL, Zhang CY, Jin HF, Tang CS, Du JB. Hydrogen sulfide regulates lung tissue-oxidized glutathione and total antioxidant capacity in hypoxic pulmonary hypertensive rats. Acta Pharmacol Sin 2008 Jun;29(6):670-679.

(83) Srilatha B, Adaikan PG, Li L, Moore PK. Hydrogen sulphide: a novel endogenous gasotransmitter facilitates erectile function. J Sex Med 2007 Sep;4(5):1304-1311.

(84) Whiteman M, Le Trionnaire S, Chopra M, Fox B, Whatmore J. Emerging role of hydrogen sulfide in health and disease: critical appraisal of biomarkers and pharmacological tools. Clin Sci (Lond) 2011 Dec;121(11):459-488.

(85) Szabo C. Hydrogen sulphide and its therapeutic potential. Nat Rev Drug Discov 2007 Nov;6(11):917-935.

(86) House JD, Brosnan ME, Brosnan JT. Characterization of homocysteine metabolism in the rat kidney. Biochem J 1997 Nov 15;328 (Pt 1)(Pt 1):287-292.

(87) Bostom A, Brosnan JT, Hall B, Nadeau MR, Selhub J. Net uptake of plasma homocysteine by the rat kidney in vivo. Atherosclerosis 1995 Jul;116(1):59-62.

(88) Xia M, Chen L, Muh RW, Li PL, Li N. Production and actions of hydrogen sulfide, a novel gaseous bioactive substance, in the kidneys. J Pharmacol Exp Ther 2009 Jun;329(3):1056-1062.

(89) Xue H, Yuan P, Ni J, Li C, Shao D, Liu J, et al. H(2)S inhibits hyperglycemia-induced intrarenal renin-angiotensin system activation via attenuation of reactive oxygen species generation. PLoS One 2013 Sep 13;8(9):e74366.

(90) Lu M, Liu YH, Goh HS, Wang JJ, Yong QC, Wang R, et al. Hydrogen sulfide inhibits plasma renin activity. J Am Soc Nephrol 2010 Jun;21(6):993-1002.

(91) Yamamoto J, Sato W, Kosugi T, Yamamoto T, Kimura T, Taniguchi S, et al. Distribution of hydrogen sulfide (H(2)S)-producing enzymes and the roles of the H(2)S donor sodium hydrosulfide in diabetic nephropathy. Clin Exp Nephrol 2013 Feb;17(1):32-40.

(92) Ishii I, Akahoshi N, Yu XN, Kobayashi Y, Namekata K, Komaki G, et al. Murine cystathionine gamma-lyase: complete cDNA and genomic sequences, promoter activity, tissue distribution and developmental expression. Biochem J 2004 Jul 1;381(Pt 1):113-123.

(93) Li N, Chen L, Muh RW, Li PL. Hyperhomocysteinemia associated with decreased renal transsulfuration activity in Dahl S rats. Hypertension 2006 Jun;47(6):1094-1100.

(94) Beltowski J. Hypoxia in the renal medulla: implications for hydrogen sulfide signaling. J Pharmacol Exp Ther 2010 Aug;334(2):358-363.

(95) Taabazuing CY, Hangasky JA, Knapp MJ. Oxygen sensing strategies in mammals and bacteria. J Inorg Biochem 2014 Apr;133:63-72.

(96) Paul BD, Snyder SH. H(2)S signalling through protein sulfhydration and beyond. Nat Rev Mol Cell Biol 2012 Jul 11;13(8):499-507.

(97) Kabil O, Banerjee R. Redox biochemistry of hydrogen sulfide. J Biol Chem 2010 Jul 16;285(29):21903-21907.

(98) Renga B. Hydrogen sulfide generation in mammals: the molecular biology of cystathionine-beta- synthase (CBS) and cystathionine-gamma-lyase (CSE). Inflamm Allergy Drug Targets 2011 Apr;10(2):85-91.

(99) Takano N, Peng YJ, Kumar GK, Luo W, Hu H, Shimoda LA, et al. Hypoxia-inducible factors regulate human and rat cystathionine beta-synthase gene expression. Biochem J 2014 Mar 1;458(2):203-211.

(100) Kabil O, Banerjee R. Enzymology of H2S biogenesis, decay and signaling. Antioxid Redox Signal 2014 Feb 10;20(5):770-782.

(101) Modis K, Asimakopoulou A, Coletta C, Papapetropoulos A, Szabo C. Oxidative stress suppresses the cellular bioenergetic effect of the 3-mercaptopyruvate sulfurtransferase/hydrogen sulfide pathway. Biochem Biophys Res Commun 2013 Apr 19;433(4):401-407.

(102) Mustafa AK, Gadalla MM, Sen N, Kim S, Mu W, Gazi SK, et al. H2S signals through protein S-sulfhydration. Sci Signal 2009 Nov 10;2(96):ra72.

(103) Jaffrey SR, Snyder SH. The biotin switch method for the detection of S-nitrosylated proteins. Sci STKE 2001 Jun 12;2001(86):pl1.

(104) Li L, Rose P, Moore PK. Hydrogen sulfide and cell signaling. Annu Rev Pharmacol Toxicol 2011;51:169-187.

(105) Mustafa AK, Sikka G, Gazi SK, Steppan J, Jung SM, Bhunia AK, et al. Hydrogen sulfide as endothelium-derived hyperpolarizing factor sulfhydrates potassium channels. Circ Res 2011 Nov 11;109(11):1259-1268.

(106) Sen N, Paul BD, Gadalla MM, Mustafa AK, Sen T, Xu R, et al. Hydrogen sulfide-linked sulfhydration of NF-kappaB mediates its antiapoptotic actions. Mol Cell 2012 Jan 13;45(1):13-24.

(107) Coletta C, Papapetropoulos A, Erdelyi K, Olah G, Modis K, Panopoulos P, et al. Hydrogen sulfide and nitric oxide are mutually dependent in the regulation of angiogenesis and endothelium-dependent vasorelaxation. Proc Natl Acad Sci U S A 2012 Jun 5;109(23):9161-9166.

(108) Papapetropoulos A, Pyriochou A, Altaany Z, Yang G, Marazioti A, Zhou Z, et al. Hydrogen sulfide is an endogenous stimulator of angiogenesis. Proc Natl Acad Sci U S A 2009 Dec 22;106(51):21972-21977.

(109) Cai WJ, Wang MJ, Moore PK, Jin HM, Yao T, Zhu YC. The novel proangiogenic effect of hydrogen sulfide is dependent on Akt phosphorylation. Cardiovasc Res 2007 Oct 1;76(1):29-40.

(110) Phaniendra A, Jestadi DB, Periyasamy L. Free radicals: properties, sources, targets, and their implication in various diseases. Indian J Clin Biochem 2015 Jan;30(1):11-26.

(111) Kabil O, Motl N, Banerjee R. H2S and its role in redox signaling. Biochim Biophys Acta 2014 Aug;1844(8):1355-1366.

(112) Luo Y, Yang X, Zhao S, Wei C, Yin Y, Liu T, et al. Hydrogen sulfide prevents OGD/R-induced apoptosis via improving mitochondrial dysfunction and suppressing an ROS-mediated caspase-3 pathway in cortical neurons. Neurochem Int 2013 Dec;63(8):826-831.

(113) Bos EM, Wang R, Snijder PM, Boersema M, Damman J, Fu M, et al. Cystathionine gamma-lyase protects against renal ischemia/reperfusion by modulating oxidative stress. J Am Soc Nephrol 2013 Apr;24(5):759-770.

(114) Zhang Y, Tang ZH, Ren Z, Qu SL, Liu MH, Liu LS, et al. Hydrogen sulfide, the next potent preventive and therapeutic agent in aging and age-associated diseases. Mol Cell Biol 2013 Mar;33(6):1104-1113.

(115) Kimura Y, Kimura H. Hydrogen sulfide protects neurons from oxidative stress. FASEB J 2004 Jul;18(10):1165-1167.

(116) Elrod JW, Calvert JW, Morrison J, Doeller JE, Kraus DW, Tao L, et al. Hydrogen sulfide attenuates myocardial ischemia-reperfusion injury by preservation of mitochondrial function. Proc Natl Acad Sci U S A 2007 Sep 25;104(39):15560-15565.

(117) Nishida M, Sawa T, Kitajima N, Ono K, Inoue H, Ihara H, et al. Hydrogen sulfide anion regulates redox signaling via electrophile sulfhydration. Nat Chem Biol 2012 Aug;8(8):714-724.

(118) Hourihan JM, Kenna JG, Hayes JD. The gasotransmitter hydrogen sulfide induces nrf2-target genes by inactivating the keap1 ubiquitin ligase substrate adaptor through formation of a disulfide bond between cys-226 and cys-613. Antioxid Redox Signal 2013 Aug 10;19(5):465-481.

(119) Peake BF, Nicholson CK, Lambert JP, Hood RL, Amin H, Amin S, et al. Hydrogen sulfide preconditions the db/db diabetic mouse heart against ischemia-reperfusion injury by activating Nrf2 signaling in an Erk-dependent manner. Am J Physiol Heart Circ Physiol 2013 May;304(9):H1215-24.

(120) Szabo C, Ransy C, Modis K, Andriamihaja M, Murghes B, Coletta C, et al. Regulation of mitochondrial bioenergetic function by hydrogen sulfide. Part I. Biochemical and physiological mechanisms. Br J Pharmacol 2014 Apr;171(8):2099-2122.

(121) Goubern M, Andriamihaja M, Nubel T, Blachier F, Bouillaud F. Sulfide, the first inorganic substrate for human cells. FASEB J 2007 Jun;21(8):1699-1706.

(122) Lagoutte E, Mimoun S, Andriamihaja M, Chaumontet C, Blachier F, Bouillaud F. Oxidation of hydrogen sulfide remains a priority in mammalian cells and causes reverse electron transfer in colonocytes. Biochim Biophys Acta 2010 Aug;1797(8):1500-1511.

(123) Fu M, Zhang W, Wu L, Yang G, Li H, Wang R. Hydrogen sulfide (H2S) metabolism in mitochondria and its regulatory role in energy production. Proc Natl Acad Sci U S A 2012 Feb 21;109(8):2943-2948.

(124) Teng H, Wu B, Zhao K, Yang G, Wu L, Wang R. Oxygen-sensitive mitochondrial accumulation of cystathionine beta-synthase mediated by Lon protease. Proc Natl Acad Sci U S A 2013 Jul 30;110(31):12679-12684.

(125) Modis K, Coletta C, Erdelyi K, Papapetropoulos A, Szabo C. Intramitochondrial hydrogen sulfide production by 3-mercaptopyruvate sulfurtransferase maintains mitochondrial electron flow and supports cellular bioenergetics. FASEB J 2013 Feb;27(2):601-611.

(126) Ma K, Liu Y, Zhu Q, Liu CH, Duan JL, Tan BK, et al. H2S donor, S-propargyl-cysteine, increases CSE in SGC-7901 and cancer-induced mice: evidence for a novel anti-cancer effect of endogenous H2S? PLoS One 2011;6(6):e20525.

(127) Lee ZW, Teo XY, Tay EY, Tan CH, Hagen T, Moore PK, et al. Utilizing hydrogen sulfide as a novel anti-cancer agent by targeting cancer glycolysis and pH imbalance. Br J Pharmacol 2014 Sep;171(18):4322-4336.

(128) Murata T, Sato T, Kamoda T, Moriyama H, Kumazawa Y, Hanada N. Differential susceptibility to hydrogen sulfide-induced apoptosis between PHLDA1-overexpressing oral cancer cell lines and oral keratinocytes: role of PHLDA1 as an apoptosis suppressor. Exp Cell Res 2014 Jan 15;320(2):247-257.

(129) Zhao K, Li S, Wu L, Lai C, Yang G. Hydrogen sulfide represses androgen receptor transactivation by targeting at the second zinc finger module. J Biol Chem 2014 Jul 25;289(30):20824-20835.

(130) Cai WJ, Wang MJ, Ju LH, Wang C, Zhu YC. Hydrogen sulfide induces human colon cancer cell proliferation: role of Akt, ERK and p21. Cell Biol Int 2010 Apr 14;34(6):565-572.

(131) Szabo C, Coletta C, Chao C, Modis K, Szczesny B, Papapetropoulos A, et al. Tumor-derived hydrogen sulfide, produced by cystathionine-beta-synthase, stimulates bioenergetics, cell proliferation, and angiogenesis in colon cancer. Proc Natl Acad Sci U S A 2013 Jul 23;110(30):12474-12479.

(132) Fan K, Li N, Qi J, Yin P, Zhao C, Wang L, et al. Wnt/beta-catenin signaling induces the transcription of cystathionine-gamma-lyase, a stimulator of tumor in colon cancer. Cell Signal 2014 Dec;26(12):2801-2808.

(133) Bhattacharyya S, Saha S, Giri K, Lanza IR, Nair KS, Jennings NB, et al. Cystathionine beta-synthase (CBS) contributes to advanced ovarian cancer progression and drug resistance. PLoS One 2013 Nov 13;8(11):e79167.

(134) Zhang J, Xie Y, Xu Y, Pan Y, Shao C. Hydrogen sulfide contributes to hypoxia-induced radioresistance on hepatoma cells. J Radiat Res 2011;52(5):622-628.

(135) Zhang J, Xie Y, Xu Y, Shao C. Suppression of endogenous hydrogen sulfide contributes to the radiation-induced bystander effects on hypoxic HepG2 cells. Radiat Res 2012 Nov;178(5):395-402.

(136) Jamal-Hanjani M, Quezada SA, Larkin J, Swanton C. Translational Implications of Tumor Heterogeneity. Clin Cancer Res 2015 Mar 15;21(6):1258-1266.

(137) Akakura S, Ostrakhovitch E, Sanokawa-Akakura R, Tabibzadeh S. Cancer cells recovering from damage exhibit mitochondrial restructuring and increased aerobic glycolysis. Biochem Biophys Res Commun 2014 Jun 13;448(4):461-466.

(138) Sanokawa-Akakura R, Ostrakhovitch EA, Akakura S, Goodwin S, Tabibzadeh S. A H2S-Nampt dependent energetic circuit is critical to survival and cytoprotection from damage in cancer cells. PLoS One 2014 Sep 23;9(9):e108537.

(139) Ostrakhovitch EA, Akakura S, Sanokawa-Akakura R, Goodwin S, Tabibzadeh S. Dedifferentiation of cancer cells following recovery from a potentially lethal damage is mediated by H2S-Nampt. Exp Cell Res 2015 Jan 1;330(1):135-150.

(140) Asimakopoulou A, Panopoulos P, Chasapis CT, Coletta C, Zhou Z, Cirino G, et al. Selectivity of commonly used pharmacological inhibitors for cystathionine beta synthase (CBS) and cystathionine gamma lyase (CSE). Br J Pharmacol 2013 Jun;169(4):922-932.

(141) Fergelot P, Bernhard JC, Soulet F, Kilarski WW, Leon C, Courtois N, et al. The experimental renal cell carcinoma model in the chick embryo. Angiogenesis 2013 Jan;16(1):181-194.

(142) Montoya LA, Pluth MD. Selective turn-on fluorescent probes for imaging hydrogen sulfide in living cells. Chem Commun (Camb) 2012 May 16;48(39):4767-4769.

(143) Wu B, Teng H, Yang G, Wu L, Wang R. Hydrogen sulfide inhibits the translational expression of hypoxia-inducible factor-1alpha. Br J Pharmacol 2012 Dec;167(7):1492-1505.

(144) Kai S, Tanaka T, Daijo H, Harada H, Kishimoto S, Suzuki K, et al. Hydrogen sulfide inhibits hypoxia- but not anoxia-induced hypoxia-inducible factor 1 activation in a von hippel-lindau- and mitochondria-dependent manner. Antioxid Redox Signal 2012 Feb 1;16(3):203-216.

(145) Chen H, Shi H. A reducing environment stabilizes HIF-2alpha in SH-SY5Y cells under hypoxic conditions. FEBS Lett 2008 Nov 26;582(28):3899-3902.

(146) Deplancke B, Gaskins HR. Hydrogen sulfide induces serum-independent cell cycle entry in nontransformed rat intestinal epithelial cells. FASEB J 2003 Jul;17(10):1310-1312.

(147) Navas P, Villalba JM, de Cabo R. The importance of plasma membrane coenzyme Q in aging and stress responses. Mitochondrion 2007 Jun;7 Suppl:S34-40.

(148) Sun M, Shariat SF, Cheng C, Ficarra V, Murai M, Oudard S, et al. Prognostic factors and predictive models in renal cell carcinoma: a contemporary review. Eur Urol 2011 Oct;60(4):644-661.

(149) Bibli SI, Yang G, Zhou Z, Wang R, Topouzis S, Papapetropoulos A. Role of cGMP in hydrogen sulfide signaling. Nitric Oxide 2015 Apr 30;46:7-13.

(150) Matak D, Szymanski L, Szczylik C, Sledziewski R, Lian F, Bartnik E, et al. Biology of renal tumour cancer stem cells applied in medicine. Contemp Oncol (Pozn) 2015;19(1A):A44-51.

(151) Hayes JD, McMahon M, Chowdhry S, Dinkova-Kostova AT. Cancer chemoprevention mechanisms mediated through the Keap1-Nrf2 pathway. Antioxid Redox Signal 2010 Dec 1;13(11):1713-1748.

(152) Jaramillo MC, Zhang DD. The emerging role of the Nrf2-Keap1 signaling pathway in cancer. Genes Dev 2013 Oct 15;27(20):2179-2191.

(153) Nilsson H, Lindgren D, Mandahl Forsberg A, Mulder H, Axelson H, Johansson ME. Primary clear cell renal carcinoma cells display minimal mitochondrial respiratory capacity resulting in pronounced sensitivity to glycolytic inhibition by 3-Bromopyruvate. Cell Death Dis 2015 Jan 8;6:e1585.

(154) Tracz A, Mastri M, Lee CR, Pili R, Ebos JM. Modeling spontaneous metastatic renal cell carcinoma (mRCC) in mice following nephrectomy. J Vis Exp 2014 Apr 29;(86). doi(86):10.3791/51485.

(155) Zhen Y, Pan W, Hu F, Wu H, Feng J, Zhang Y, et al. Exogenous hydrogen sulfide exerts proliferation/anti-apoptosis/angiogenesis/migration effects via amplifying the activation of NF-kappaB pathway in PLC/PRF/5 hepatoma cells. Int J Oncol 2015 May;46(5):2194-2204.

Appendices

Appendix A: Human RCC Clinical Data

Patient #	Sex	Age at surgery	Histological subtype*	Fuhrman Grade	Tumor necrosis	Tumor Dimensions	T stage**	N stage	M stage
1	F	75	1	2	N	6*5.5*5	5	-	0
2	M	58	3	2	Y	6*5,5*5	2	-	0
3	F	59	1	4	Y	12*8*7	5	0	0
4	M	47	1	3	N	7,5*7*5	5	0	0
5	F	65	4	3	Y	5*7,8*6	3	-	0
6	M	79	6	-	Y	2.4*2.1*1.9	1	-	0
7	M	53	1	2	Y	3,3*2,6*2,6	1	-	0
8	M	69	1	2	N	2,5*2*1,8	1	-	0
9	M	58	1	2	N	3,7*3,5*3	1	-	0
10	F	54	9	-	-	3,5*2,5	4	-	0
11	M	61	1	2	Y	3*2,5*2,2	1	-	0
12	M	63	2	3	N	1,4*1,2*1,2	1	-	0
13	M	50	2	3	N	3,5*3*3	1	-	0
14	M	64	7	4	Y	14*12*12	4	-	1
15	M	61	1	3	N	5,5*5*5,5	4	-	1
16	M	50	1	3	Y	5*4*3	2	-	0
17	M	77	1	3	N	7,5*6.5*6	5	-	0

Patient #	Sex	Age at surgery	Histological subtype*	Fuhrman Grade	Tumor necrosis	Tumor Dimensions	T stage**	N stage	M stage
18	M	67	3	4	N	4*2,5*2,5	1	-	0
19	M	63	3	3	Y	1,4*1,2*1,1	1	-	0
20	F	63	8	1	N	1,4*1,3*0,9	1	-	0
21	M	80	1	3	Y	4*3,8*3,5	1	-	0
22	M	66	4	-	N	5*4*3,3	2	-	0
23	M	69	1	3	N	5*4*4	4	-	0
24	F	68	1	3	N	3*2.5*2	1	-	0
25	F	38	3	3	N	6.5*4*4	2	-	0
26	M	66	3	3	N	5*4*3.3	2	-	0
27	M	50	10	2	N	3*2,5*2	1	-	0
28	M	78	3	3	Y	8,5*8*8	4	1	0
29	M	70	6	-	N	3,5*3*3	1	-	0
30	M	77	1	2	N	5*5*4	2	-	0
31	F	57	1	4	Y	10*10*9	5	-	1
32	F	70	1	4	Y	7,2*7*5,5	3	-	0
33	F	63	7	2	N	2,5*2,5*2,3	1	-	0
34	M	50	4	-	N	7,5*7*6	3	-	0
35	M	69	1	3	N	1,7*1,6*1,4	1	-	0
36	M	62	1	3	Y	9.5*9*5	4	-	0

Patient #	Sex	Age at surgery	Histological subtype*	Fuhrman Grade	Tumor necrosis	Tumor Dimensions	T stage**	N stage	M stage
37	F	49	1	4	Y	8*8*5	5	-	1
38	M	63	3	4	Y	3.5*3*3 & 4*4*3.5	5	-	0
39	M	57	2	3	N	6,5*5*4	2	-	0
40	F	62	1	4	N	8*5,5*5	5	0	1
41	F	58	1	4	N	9*8*7,5	4	-	1
42	F	50	1	3	N	6*5*5	4	-	0
43	M	44	4	2	N	8*5,5*6	3	-	0
44	F	47	5	1	Y	2,5*2,2*1,5	1	-	0
45	M	59	3	-	-	-99	-	-	0
46	M	54	1	1	Y	2,5*2,2*1,1	1	-	0
47	F	45	1	-	-	5	2	-	0
48	M	55	1	3	Y	8,8*8,5*7,8	4	-	0
49	M	49	1	2	N	2,5*2*2	1	0	0
50	M	54	1	3	Y	4,5*3,3*4,5	2	-	0

* 1=Clear Cell, 2=Papillary type I, 3=Papillary typeII, 4=Chromophobe, 5=Collecting duct, 6=Oncocytoma, 7=unclassified, 8=thyroid-like RCC, 9=Angiomyolipoma, 10=multilocular cystic RCC

** 1=T1a, 2=T1b, 3=T2, 4=T3a, 5=T3b, 6=T3c, 7=T4

Curriculum Vitae

Name:	Eric Sonke
Post-secondary Education and Degrees:	Western University London, Ontario, Canada 2008-2013 B.M.Sc. Western University London, Ontario, Canada 2013-2015 M.A.
Honours and Awards:	Province of Ontario Graduate Scholarship 2013-2014, 2014-2015
Related Work Experience	Teaching Assistant The University of Western Ontario 2013-2015

Publications:

Sonke E, Verrydt M, Postenka CO, Pardhan S, Willie CJ, Mazzola CR, Hammers MD; Pluth MD, Lobb I, Power NE, Chambers AF, Leong HS, Sener A. (Accepted). Inhibition of endogenous hydrogen sulfide production in clear-cell renal cell carcinoma cell lines and xenografts restricts their growth, survival and angiogenic potential. Nitric Oxide.

Lobb I, Sonke E, Aboalsamh G, Sener A. (2015). Hydrogen sulphide and the kidney: Important roles in renal physiology and pathogenesis and treatment of kidney injury and disease. Nitric Oxide, 46, 55-65

Sonke E, Verrydt M, Lobb I, Mazzola CR, Chambers AF, Leong HS, Sener A. (2014). Endogenous hydrogen sulfide production plays a role in the survival, growth and neovascularization of renal cell carcinoma tumours. Nitric Oxide, 39, S26

Sonke E, Yang Y, Lobb I, Sener A. (2013). Inhibition of endogenous hydrogen sulphide production reduces hypoxia-induced proliferation in renal cell carcinoma cell lines. Journal of the Canadian Urological Association, 7, 5-6-S2